

**Incorporation of Biomechanical Child Cadaver Neck  
Behaviour in a Child Model and Injury Prediction in Vehicle  
Frontal Crash**

by

Wencheng Zhang

A Thesis  
submitted to the Faculty of Graduate Studies  
through Mechanical Engineering  
in partial fulfillment of the requirements for  
the degree of Master of Applied Science at the  
University of Windsor

Windsor, Ontario, Canada

2008

© 2008 Wencheng Zhang



Library and  
Archives Canada

Bibliothèque et  
Archives Canada

Published Heritage  
Branch

Direction du  
Patrimoine de l'édition

395 Wellington Street  
Ottawa ON K1A 0N4  
Canada

395, rue Wellington  
Ottawa ON K1A 0N4  
Canada

*Your file* *Votre référence*  
*ISBN: 978-0-494-47047-3*  
*Our file* *Notre référence*  
*ISBN: 978-0-494-47047-3*

**NOTICE:**

The author has granted a non-exclusive license allowing Library and Archives Canada to reproduce, publish, archive, preserve, conserve, communicate to the public by telecommunication or on the Internet, loan, distribute and sell theses worldwide, for commercial or non-commercial purposes, in microform, paper, electronic and/or any other formats.

The author retains copyright ownership and moral rights in this thesis. Neither the thesis nor substantial extracts from it may be printed or otherwise reproduced without the author's permission.

**AVIS:**

L'auteur a accordé une licence non exclusive permettant à la Bibliothèque et Archives Canada de reproduire, publier, archiver, sauvegarder, conserver, transmettre au public par télécommunication ou par l'Internet, prêter, distribuer et vendre des thèses partout dans le monde, à des fins commerciales ou autres, sur support microforme, papier, électronique et/ou autres formats.

L'auteur conserve la propriété du droit d'auteur et des droits moraux qui protègent cette thèse. Ni la thèse ni des extraits substantiels de celle-ci ne doivent être imprimés ou autrement reproduits sans son autorisation.

---

In compliance with the Canadian Privacy Act some supporting forms may have been removed from this thesis.

Conformément à la loi canadienne sur la protection de la vie privée, quelques formulaires secondaires ont été enlevés de cette thèse.

While these forms may be included in the document page count, their removal does not represent any loss of content from the thesis.

Bien que ces formulaires aient inclus dans la pagination, il n'y aura aucun contenu manquant.

  
**Canada**

## **AUTHOR'S DECLARATION OF ORIGINALITY**

I hereby certify that I am the sole author of this thesis and that no part of this thesis has been published or submitted for publication.

I certify that, to the best of my knowledge, my thesis does not infringe upon anyone's copyright nor violate any proprietary rights and that any ideas, techniques, quotations, or any other material from the work of other people included in my thesis, published or otherwise, are fully acknowledged in accordance with the standard referencing practices. Furthermore, to the extent that I have included copyrighted material that surpasses the bounds of fair dealing within the meaning of the Canada Copyright Act, I certify that I have obtained a written permission from the copyright owner(s) to include such material(s) in my thesis and have included copies of such copyright clearances to my appendix.

I declare that this is a true copy of my thesis, including any final revisions, as approved by my thesis committee and the Graduate Studies office, and that this thesis has not been submitted for a higher degree to any other University or Institution.

## **ABSTRACT**

This research was completed in an effort to improve the biofidelity of a finite element child model and the accuracy of injury predictions in forward facing child restraint seats during numerical simulations of frontal crashes.

After material alterations to the child model, neck tensile force was found to be within the range of cadaver tests and the rotation-moment curves were in good agreement with the corridor of the pediatric cadaver head/neck complex tests.

The altered child model has illustrated more accurate biomechanical responses and kinematics; its biofidelity has been improved. The upper and lower neck tensile forces of the child model were reduced by approximately 35% and 41%, respectively. Tensile deformation of the child neck was increased by 2.75 times while rotational deformation increased by 37%. The percentage error of the maximum displacements of the child head was reduced from approximately 16% to 13.5%.

## **DEDICATION**

To my loving wife Xiaoying, who has offered inspiration, encouragement and unconditional support throughout the course of this research and to my daughters Simone, Melissa and Keri for their love and patience.

## **ACKNOWLEDGEMENTS**

The author is indebted to his academic advisor, Dr. William Altenhof, for his exceptional support and guidance throughout the duration of this research as well as his invaluable knowledge of vehicle crashworthiness and FE numerical simulations. The author would like to thank Dr. K. Mizuno for providing the THUMS adult and child models and related information of the development. The author would also like to thank the research team led by Dr. W. Altenhof for their support in the research.

## TABLE OF CONTENTS

AUTHOR'S DECLARATION OF ORIGINALITY	iii
ABSTRACT	iv
DEDICATION	v
ACKNOWLEDGEMENTS	vi
LIST OF TABLES	x
LIST OF FIGURES	xi
LIST OF ABBREVIATIONS	xvi
LIST OF NOMENCLATURE	xvii
1. INTRODUCTION	1
2. LITERATURE REVIEW	4
2.1 Child safety in motor vehicle crashes	4
2.1.1 Children fatalities and injuries in motor vehicle crashes and its Impacts	4
2.1.2 Children Seating Positions, Restrains and Injury patterns	6
2.1.2.1. Restraint use and their effectiveness	7
2.1.2.2. Seating positions	10
2.1.2.3. Injury pattern in vehicle crashes	11
2.1.3 Preventions of children injury in motor vehicle crash	13
2.1.3.1 Current safety standards for children	13
2.1.3.1.1 Federal Motor Vehicle Safety Standard 208	13
2.1.3.1.2 Federal Motor Vehicle Safety Standard 213	13
2.1.3.1.3 Federal Motor Vehicle Safety Standard 225	15
2.1.3.1.4 Federal Motor Vehicle Safety Standard 217, 220, 222	16
2.1.3.2 Child restraint system (CRS)	17
2.2 Child anatomy	21
2.2.1 Children head development	22
2.2.2 Comparison of adult and child cervical spine anatomies	22
2.2.2.1 Adult cervical spine	22
2.2.2.2 Child cervical spine	25
2.3 Injury mechanisms for child occupants in motor vehicle accidents	27
2.3.1 Child head injuries	27
2.3.2 Pediatric cervical spine injuries	28

2.4 Children injury cases studies	30
2.5 Predictions of children injury in motor vehicle crashes	33
2.5.1 Experimental tests and real world crashes	33
2.5.2 Numerical simulations with human models in children injury studies	41
3. FOCUS OF RESEARCH	50
4. CHILD HEAD/NECK COMPONENT MODEL DEVELOPMENT	52
4.1 Head/neck cadaver test	52
4.2 Head/neck component model development	54
4.2.1 From child model to head/neck component model	54
4.2.2 Loading and boundary conditions	56
4.2.2.1 Extension/flexion bending conditions	57
4.2.2.2 Tensile loading condition	57
4.2.3 Basic model simulation setup	57
4.3 Data extraction of the head/neck simulation model	59
5. COMPARISONS OF HEAD/NECK MODEL WITH PEDIATRIC DATA	61
5.1 Comparison of base model and the cadaver head/neck complex test	61
5.1.1 Tensile loading condition	61
5.1.2 Extension/flexion bending condition	63
5.2 Parametric Study	64
5.2.1 Energy absorption in the cervical spine	64
5.2.2 Altering the material properties	65
5.3 Comparison of altered model with cadaver head/neck complex tests	69
5.3.1 Tensile loading condition	69
5.3.2 Extension/flexion bending condition	70
6. IMPLEMENTATION OF CHILD BIOMECHANICAL NECK BEHAVIOUR INTO THE CHILD MODEL	72
6.1 FMVSS 213 sled simulation with the child model	72
6.1.1 Child model	73
6.1.2 Child restraint system (CRS) and FMVSS 213 bench seat	75
6.1.3 Numerical simulation setup under FMVSS 213 sled test condition	78
6.1.4 Implement neck data from the altered head/neck component model	80



6.2 Child model simulating a cadaver frontal impact sled test	81
6.2.1 Cadaver frontal impact sled test	81
6.2.2 Simulation setup under cadaver sled test condition	82
6.3 Data extraction from the child model	82
6.4 Injury parameters	83
6.4.1 Head injury criteria	84
6.4.2 Neck injury criteria	84
<b>7. COMPARISON OF CHILD MODEL BEFORE/AFTER NECK ALTERATION</b>	<b>85</b>
7.1 Qualitative Comparison	85
7.2 Quantitative Comparison of Kinematical and Biomechanical Responses	91
7.2.1 Head response	91
7.2.1.1 Head accelerations and head injury criteria (HIC)	91
7.2.1.2 Head rotation	94
7.2.1.3 Head displacement and trajectory	95
7.2.2 Neck response	97
7.2.2.1 Upper neck forces	97
7.2.2.2 Lower neck forces	98
7.2.2.3 Neck deflection	99
7.2.2.4 Neck Rotation	100
7.2.3 Chest response	100
7.2.3.1 Chest accelerations	100
7.2.3.2 Chest deflection	102
7.3 Discussions	103
<b>8. CONCLUSIONS, LIMITATION AND FUTURE WORK</b>	<b>108</b>
8.1 Conclusions	108
8.2 Limitations	109
8.3 Future Work	110
<b>REFERENCES</b>	<b>111</b>
APPENDIX A – Comparison between FE Child Model Version 1 and Version 2	116
APPENDIX B – The Abbreviated Injury Scale	125
APPENDIX C – Strain Energy Distribution of Neck Soft Tissues in the Child Head/Neck Component Model	126
APPENDIX D – Copyright Permission	127
<b>VITA AUCTORIS</b>	<b>136</b>

## LIST OF TABLES

Table		Page
2.1	Comparison of children age 0 children age 0-3 killed or injured, by role in year 2005 and 2006 (NHTSA 2007)	5
2.2	Restraint uses by passenger vehicle Occupants involved in fatal crashes by age group, 2005.	9
2.3	Sled test matrix.	36
4.1	Matrix of head/neck component models under different loading conditions.	59
5.1	Cervical spine material property alternations.	68
6.1	SAE J211 filters for child occupant injury data.	83
7.1	Values of the Head Injury Criteria (HIC)	94

## LIST OF FIGURES

Figure		Page
2.1	Percent of passengers injured, age 0 – 15, by vehicle body type, restraint use, among single vehicle crashes.	8
2.2	Total traffic fatalities among children age 14 and under by age group, 1995-2005.	9
2.3	Predicted risk of serious injury for each restraint/seating position group.	11
2.4	Body region distribution of child occupants and adult drivers.	12
2.5	FMVSS 213 sled test pulse upper and lower limits and a pulse used from a real sled test.	15
2.6	Child Restraint Systems (CRS) (NHTSA): A. Rearward facing child safety seat; B. Forward facing child safety seat; C. High back booster seat; D. Backless booster seat.	18
2.7	Child convertible seat with 5-point harness (NHTSA).	18
2.8	Comparison of children fatality rates in car crashes in Sweden and in France (Children in Cars by Volvo 2002).	19
2.9	Comparison of children injury rates in car crashes in Sweden and in Germany (Children in Cars by Volvo 2002).	19
2.10	Lower Anchors and Tethers for Children (LATCH) (NHTSA DOT HS 809 489 August 2002).	20
2.11	Development of human being (Children in Cars by Volvo 2004).	21
2.12	Skull profiles showing changes in size and shape	22
2.13	Human adult spinal column and the soft tissues: A. Spinal column; B. Vertebrae and intervertebral disc; C. Ligaments.	23
2.14	Human adult cervical spine: A. anterior view; B. side view	24
2.15	(a) Schematic of the one-, three, and six-year-old, and adult human cervical spine vertebra. (b) Schematic of the one-, three-, and six-year-old and adult human cervical spine functional spinal unit.	26

Figure	Page
2.16 (A) Occipitocervical dislocation in a 23 month old male involved in a frontal collision; (B) C2 fracture through the base of the odontoid process in a 35 month old child involved in a frontal collision.	31
2.17 (A) MRI of tectorial membrane hemorrhage and (B) Synovial Capsule Hemorrhage in 3 year-old.	33
2.18 Test setup in ECE R44 CRS tests with Hybrid III 3-year-old child dummy and CRS (a) 5-point harness; (b) tray shield.	35
2.19 CRS sled acceleration with ECE R44 corridor.	35
2.20 Child dummy positions and restraint systems: 3-year-old (a) 5-point harness child seat, (b) backless booster and (c) shoulder/lab seatbelt; 6year-old (d) backless booster, (e) high back booster and (f) shoulder/lab seatbelt.	37
2.21 Total Human Total Human Model for Safety (THUMS) developed by Toyota research laboratory.	43
2.22 Pediatric cadaver cervical extension at C2, unfiltered data.	45
2.23 Pediatric cadaver cervical load deflection curve, unfiltered data.	46
2.24 Q3 dummy head/neck component sled test.	47
2.25 (a) Physical model of the cervical spine based on CT scan of a three-year-old child including skull base (C0) and (b) Complete finite element model of the head and neck complex.	47
2.26 Different views of finite element mesh of ligamentous of adult C4–C5–C6 spine.	48
4.1 Figure 4.1 Pediatric cadaver test and CAE simulation set-ups under bending load condition: (a) Cadaver bending test and (b) FE simulation set-up.	53
4.2 Pediatric cadaver test and CAE simulation set-ups under tensile load condition: (a) Cadaver Tensile test and (b) FE simulation set-up.	53
4.3 Head/Neck component model developments: (A) child model, (B) and (C) isolated head/neck component model.	54

Figure		Page
4.4	Enlarged view of cervical spine (C1-C7) and partial thoracic spine (T1 to T2).	55
4.5	Regions of soft tissue components in terms of different material properties.	56
4.6	Adjustment for the head/neck component model: (A) before tilted and (B) after tilted.	58
4.7	Upper and lower neck cross section definitions.	59
5.1	Load Deflection Curve Comparison of Head/Neck Base Model CAE Simulation and Pediatric Cadaver Tests of 8 specimens aged 2 to 7.5 years.	62
5.2	Neck's moment-rotation range (T2) comparison of head/neck base model simulation and pediatric cadaver head/neck complex tests of 9 specimens aged 2 to 7.5 years.	63
5.3	Energy-time curves of the most effective ligaments for energy absorption in the vicinities of C2-C3 and C6-C7 of the cervical spine under tensile loading condition.	65
5.4	Groups of soft tissue components with different material properties.	66
5.5	Force-deflection curve comparison of some head/neck altered model simulations and pediatric cadaver tests of 8 specimens aged 2 to 7.5 years.	67
5.6	Moment-flexion/extension curve comparison of some head/neck altered model simulations and pediatric cadaver tests of specimens aged 2 to 7.5 years.	68
5.7	Force-deflection curve comparison of final head/neck altered model simulation and pediatric cadaver tests of 8 specimens aged 2 to 7.5 years.	69
5.8	Moment-flexion/extension curve comparison of final head/neck altered model simulation and pediatric cadaver tests of specimens aged 2 to 7.5 years.	71
6.1	FMVSS 213 standard input acceleration versus time curve.	73
6.2	Three-year-old child model.	74

Figure	Page
6.3 (A) Sectional comparison of the behaviour of the Hybrid III 3-year-old dummy model and the child model and (B) Comparison of the head rotation about Y-axis.	75
6.4 (A) Front isometric view of the deformable CRS, (A) Rear isometric views of the deformable CRS.	76
6.5 The seatbelt, LATCH, top tether, and the five point restraint system.	77
6.6 The model of the foam pad.	77
6.7 Complete FE model of the deformable CRS and FMVSS 213 bench seat.	78
6.8 Combination of child model with CRS and FMVSS 213 bench seat.	79
6.9 Child cadaver testing acceleration pulse.	82
7.1 Child model simulating FMVSS 213 frontal crash side view: before neck altered on left and after neck altered on the right.	86
7.2 Child model simulating FMVSS 213 frontal crash cross sectional view: before neck altered on left and after neck altered on the right	88
7.3 Detail of neck deformation of the child model at 92.5 ms in cross sectional view: the shear deformation of C1-C2 of the child model after neck altered as indicated in the area with an arrow.	90
7.4 Head acceleration in X direction.	92
7.5 Head acceleration in Z direction.	93
7.6 Head resultant acceleration.	93
7.7 Chin to chest contact force.	94
7.8 Head rotations in the sagittal plane.	95
7.9 Head trajectories under FMVSS 213 frontal impact sled test condition.	96
7.10 Head trajectory under cadaver frontal impact sled test condition.	96
7.11 Upper neck tensile forces.	97
7.12 Lower neck tensile forces.	98

Figure	Page
7.13 Measurement of Neck Deflection (C1-T1): (A) without neck alterations and (B) with neck alterations.	99
7.14 Neck Rotation in sagittal plane.	100
7.15 Chest Acceleration in X direction.	101
7.16 Chest acceleration in Z direction.	102
7.17 Chest resultant accelerations.	102
7.18 Chest deflections.	103
A.1 Child model and its modifications from version 1 to version 2.	117
A.2 FMVSS 213 sled test at Graco Corporation's sled testing facilities.	118
A.3 FMVSS 213 sled test acceleration (with the upper/lower limits) versus time curve.	118
A.4 Sled test with test subject and CRS.	119
A.5 Child cadaver testing acceleration pulse.	119
A.6 Kinematic response comparison of FMVSS 213 simulations of the child model version 1 and version2.	120
A.7 Sectional view of kinematic response comparison of FMVSS 213 simulations of the child model version 1 and version 2.	121
A.8 Head acceleration comparison of FMVSS 213 and cadaver sled test simulations of the child model version 1 and version2.	122
A.9 Chest acceleration comparison of FMVSS 213 and cadaver sled test simulations of the child model version 1 and version2.	123
A.10 Lower neck section force comparison of FMVSS 213 and cadaver sled test simulations of the child model version 1 and version2.	124
A-11 Strain energy distribution of neck soft tissues in the child head/neck component model under tensile loading condition.	126

## LIST OF ABBREVIATIONS

AIS	Abbreviated Injury Scale
ASCII	American Standard Cord for Information Interchange
ATD	Anthropomorphic Test Device
CAD	Computer Aided Design
CSI	Cervical Spine Injury
CMVSS	Canadian Motor Vehicle Safety Standards
CRABI	Child Restraint Air Bag Interaction Dummy
CRS	Child Restraint System
ECE	Economic Commission for Europe
FARS	Fatality Analysis Reporting System
FEMB	Finite Element Model Builder
FMVSS	Federal Motor Vehicle Safety Standards
FTSS	First Technology Safety Systems
ISO	International Standards Organization
LATCH	Lower Anchors and Tethers for Children
MAIS	Maximum Abbreviated Injury Scale
NASS	National Accident Sampling System
NCAP	New Car Assessment Program
NEXUS	National Emergency X-Radiography Utilization Study
NHTSA	National Highway Traffic Safety Administration
NOPUS	National Occupant Protection Use Survey
OOP	Out Of Position
SAE	Society of Automotive Engineers
SUV	Sport Utility Vehicle
THUMS	Total Human Model for Safety
WHO	World Health Organization



## LIST OF NOMENCLATURE

$a$	Acceleration
$a_x$	Acceleration in the $x$ direction
$a_y$	Acceleration in the $y$ direction
$a_z$	Acceleration in the $z$ direction
$a_{\text{resultant}}$	Resultant Acceleration
$E$	Elastic modulus
$F_{\text{resultant}}$	Resultant Force
$F_x$	Force in the $x$ direction
$F_y$	Force in the $y$ direction
$F_z$	Force in the $z$ direction/Axial Force
$F_{zc}$	Critical Axial Force
HIC	Head Injury Criteria
HIC <sub>15</sub>	Head Injury Criteria over 15 ms time duration
HIC <sub>36</sub>	Head Injury Criteria over 36 ms time duration
$M_{\text{resultant}}$	Resultant Moment
$M_x$	Moment in the $x$ direction
$M_y$	Moment in the $y$ direction/Bending Moment
$M_{yc}$	Critical Bending Moment
$M_z$	Moment in the $z$ direction
$N_{ij}$	Neck injury criteria
$\rho$	Density
$\nu$	Poisson's Ratio
$x, y, z$	Local coordinate system axes
$X, Y, Z$	Global coordinate system axes

## 1. INTRODUCTION

Each year motor vehicle collisions cause death and injuries to thousands of people in North America and throughout the whole world. According to the 2007 report of the World Health Organization (WHO), Youth and Road Safety [1], the annual costs of road crashes in low-income and middle-income countries was estimated to be between US\$ 65 billion and US\$ 100 billion which is more than the total annual amount received in development aid. Road traffic crashes and their consequences cost governments approximately 2% of their Gross National Product.

Traffic accidents are one of the leading causes of injuries and fatalities to children and young people. More than 1000 young people under the age of 25 years are killed every day in road traffic crashes around the world [1]. Fatal injuries for children include head and neck injuries.

Statistics of child fatalities due to vehicle accidents from the year 1995 to 2000 in New South Wales [2] showed that children in the 3 to 4 year age group accounted for a greater number of passenger fatalities (45.5 percent) than any other age group. Based on the 2006 National Highway Traffic Safety Administration (NHTSA) report [3], motor vehicle accidents are the leading cause of death for children three years of age.

To prevent child injuries or fatalities in vehicle crash, one needs to understand the kinematic and biomechanical responses of children and predict the risks of injuries when they ride as passengers. Anthropomorphic test devices (ATD's) have been used extensively in experimental and numerical analyses to understand child kinematics during simulated laboratory crash testing. The Hybrid III dummy family, including male, female and child dummies, has been officially used as ATD in vehicle development and in research on occupant protection.

The Hybrid III 3-year-old child dummy is one of the child dummy series from the Hybrid III family. According to recent studies, Kang et al [4], and Arbogast et al. [5] indicated that the Hybrid III 3-year-old child dummy had limitations in kinematic and biomechanical responses in frontal crash, especially as a result of the rigidity of the cervical and thoracic spine. Unfortunately there is no easy approach to quickly improve the biofidelity of physical test dummies. Human-like models developed for simulating

human performance in vehicle crash events and predicting injuries hold advantages over test dummies. Detailed human anatomic geometries, material properties, and information from the latest experimental tests and clinical findings can be more easily implemented in a human model than in a test dummy. With a human model, parametric and multiple case studies can be performed.

One such human model is the Total Human Model for Safety (THUMS), which was developed by a Toyota research laboratory. The model contains detailed body parts, organs, and soft tissues based on the anatomic and geometric data of a 50<sup>th</sup> percentile American male. In 2005 and 2006, Mizuno [6] [7] presented a 3-year-old child model which was scaled down from the THUMS using a model-based approach. Anatomic, geometric, and material data of a 3 year old were partially incorporated into this child model. It was validated with the Hybrid III 3-year-old child dummy corridor tests and compared with limited available data.

Child neck injury occurs rarely. However, this injury is fatal. The biofidelity of the cervical spine in the child model is critical, not only for the kinematic and biomechanical responses of the child neck, but also for the prediction of head injury potentials. Since the cervical spine in the child model was scaled from the THUMS model, it does not accurately reflect the anatomic geometry and the material properties of 3-year-olds. In 2005 Ouyang et al. [8] performed a series of pediatric cadaver tests with subjects of 10 head/neck complexes of children aged from 2 to 12 years. These specimens were subjected to tensile distraction and extension/flexion bending under an appropriate combination of non-destructive and destructive loading conditions. This pediatric data is the only currently available data for understanding child neck tolerance and injury potentials. To the best of the author's knowledge, this pediatric data has not been applied to any child models except in an attempt made recently by Tot in 2007 [9]. The outcome was limited because of the current level of biofidelity of the Hybrid III 3-year-old child dummy.

There exist a small number of child cervical spine and head/neck finite element (FE) models. One of them was created by Dupuis et al. in 2005 [10], using the anatomic geometric data from the neck of a three-year-old through CT scan and validated against a Q3 dummy head/neck component sled tests. Soft tissues, such as ligament and

intervertebral discs, used adopted or scaled down material properties from the data in available literature. Another study presented by Kumaresan et al. in 2000 [11], in which child cervical spine models were developed using three different approaches, investigated the child neck biomechanical responses under various loading conditions. Scaling down geometrically from an adult human model was considered as Approach 1. Incorporating the local anatomic geometry and material properties of a three-year-old into the adult human model was considered as Approach 2. Geometrically scaling down from an adult human model and incorporating the local anatomic geometry and material properties of three-year-olds became Approach 3. It was found that Approach 2 produced significantly greater changes in flexibility under all loading modes than the other two approaches. The conclusion drawn from this research was that the flexibility of the cervical spine of a child was predominantly controlled by local anatomic geometry and material properties.

However, the material properties of these models were not based on data from pediatric cadavers. It is difficult to judge the accuracy of the biomechanical responses of these models in reflecting a real life child of the same age.

It is necessary to utilize first-hand pediatric data and clinical findings to improve the kinematics and biofidelity of 3-year-old child models. For this resean, the objective of the proposed research is to correlate biomechanical response of the cervical spine of the child model with pediatric cadaver data. Head kinematics and neck injury potentials will be compared with a 3-year-old cadaver sled test in a frontal impact event and real cases of car crash accidents. It is expected that the biofidelity of the child model can be improved after the incorporation of the pediatric cadaver test data. This would be helpful for increasing confidence in child injury predictions as well as vehicle and CRS designs for child safety.

## **2. LITERATURE REVIEW**

### **2.1 Child safety in motor vehicle crashes**

#### **2.1.1 Children fatalities and injuries in motor vehicle crashes and its impact**

Motor vehicles are major transportation tools in most of developed and developing countries. In 2007, the World Health Organization (WHO) published a report entitled Youth and Road Safety [1] indicating that more than 1000 young people under the age of 25 years killed every day in road traffic crashes around the world and that motor vehicle crash is one of the leading causes of death for children and young people.

The report indicates that the nature and severity of the injuries that children and youth sustain in traffic collisions are influenced by age and the type of road use. Traumatic brain injuries are the leading cause of traffic-related deaths and injuries in all countries regardless of income.

Motor vehicle crashes significantly impact economies of countries all around the world. It has been estimated that the annual costs of road crashes in low-income and middle-income countries are around US\$ 65 billion to US\$ 100 billion, which is more than the total annual amount received in development aid. Road traffic crashes and their consequences have cost governments up to 2% of their Gross National Product. In many low-income and middle-income countries, a large proportion of road traffic casualties are from the younger wage-earning groups. Even in high-income countries, road traffic crashes among young people impose a huge economic burden on societies. In the United States of America, crashes involving 15–20-year-old drivers cost the country approximately US\$ 41 billion in 2002.

NHTSA [3] indicated that in 2004, traffic crashes were the leading cause of death in North America for children aged 3 to 14. During 2005, in the United States, an average of 5 children aged 14 and younger were killed and approximately 640 were injured every day in motor vehicle crashes. In the same year, 7,493 passenger vehicle occupants 14 and younger were involved in fatal crashes. The Canadian motor vehicle traffic collision statistics of 2005 [12] indicated 210,629 occupant injuries in vehicle crashes, including

17,529 serious injuries and 2,923 fatalities. Within the age range of birth to 4 years, 2,649 children were injured, 310 were seriously injured, and 24 fatal accidents occurred.

The recently published report 2006 Annual Assessment of Motor Vehicle Crashes [13] presents the latest comparison of data regarding killed and injured children aged birth to 3 years in 2005 and 2006 as shown in Table 2.1. This table indicates that most children of this group, either killed or injured, were vehicle occupants in the crash events. It was also found that in year 2006 the number of children aged 0 – 3 years, as vehicle occupants who were killed in vehicle crashes, decreased by 1.6% while the number of children injured increased by 5 %.

Thus it is very important to understand the causes of child injuries and fatalities and the relationship between injures and fatalities and child restraint usage and seating positions.

**Table 2.1 Comparison of children aged 0-3 killed or injured by role in year 2005 and 2006 [13]**

<i>Role</i>	<i>Year</i>		<i>% Change</i>
	<i>2005</i>	<i>2006</i>	
<b>Killed</b>	<b>476</b>	<b>459</b>	<b>-3.6%</b>
<b>Occupants</b>	<b>376</b>	<b>370</b>	<b>-1.6%</b>
<b>Nonoccupants</b>	<b>100</b>	<b>89</b>	<b>-11%</b>
<b>Injured*</b>	<b>43,000</b>	<b>43,000</b>	<b>0.0%</b>
<b>Occupants</b>	<b>40,000</b>	<b>42,000</b>	<b>+5.0%</b>
<b>Nonoccupants</b>	<b>2,000</b>	<b>1,000</b>	<b>-50%**</b>

*\*Totals may not add due to rounding. Percentages computed after rounding.*

*\*\*Change in nonoccupants injured is statistically significant at the 0.05 level (95% confidence intervals)*

*Sources: FARS, NASS GES*

In addition to restraint use and seating position, the crash mode is another major factor in child occupant safety. A research group from Toyota Motor Corporation of Japan [14] analyzed the National Police Agency data in 1999 and indicated that frontal impact accounted for 73% of the fatal accidents and was deemed the leading cause of death. A study from Arbogast et al. [5] also showed that in America frontal crashes were the most common vehicle accidents and accounted for 45% of the all crash modes in 2004.

Children aged 3 years have been one of the most concentrated group in the child occupant protection research as they are representative of a special development stage of human beings and are also in the transition stage of child restraint use from rearward facing position to forward facing position in some countries such as Sweden. Children in the 3 to 4 year age group account for a greater number of passenger fatalities (45.5 percent) than any other age group. This has been shown by statistics of child fatalities in vehicle accidents from 1995 to 2000 in New South Wales [2]

The following section will review the current studies regarding the effects of restraint use and seating position for different child groups including children aged 3, and the injury pattern in vehicle crashes.

### **2.1.2 Children seating positions, restrains and injury patterns**

Seating position and restraint use play very important roles in child injuries in vehicle crashes. Two groups of researchers conducted investigations and analyses on the relationships between seating position and restraint configurations and the risk of injury among children in passenger vehicle crashes in 2005 [15] [16]. Findings from these investigations are summarized in section 2.1.2.1 and brief details of the reports are provided in the two subsequent paragraphs.

The research group from NHTSA has published a technical report, *Child Passenger Fatalities and Injuries, Based on Restraint Use, Vehicle Type, Seat Position, and Number of Vehicles in the Crash* [15]. This report was based on the data regarding injuries resulting from motor vehicle crashes during the years 1998 to 2002 collected by the Fatality Analysis Reporting System (FARS), National and Automotive Sampling System (NASS) General Estimates System (GES) of the National Center for Statistics and Analysis (NCSA). The objective of this study was to analyze passenger vehicle crashes involving children aged birth to 15 years. This study is intended to provide a better understanding of where the focus should lie with future safety efforts that seek to improve highway transportation for children.

Another research group from the Children's Hospital of Philadelphia and University of Pennsylvania School of Medicine [16] collected data on vehicle crashes

that were insured by State Farm Insurance Company in 15 states. This was a cross-sectional study of children under the age of 16 who were involved in crashes of insured vehicles, with data collected through insurance claim records and a telephone survey. A probability sample of 17,980 children in 11,506 crashes was collected between December 1, 1998 and November 30, 2002.

Both of the studies divided the children birth to 15 year old into different age groups. There were three age groups in NHTSA's study, 0-3 years, 4-7 years and 8-15 years. Additionally, a group of youth aged 16 and older was considered for perspective purposes. The research group from Philadelphia grouped the children differently. They divided the children who were involved in vehicle accidents into four age groups in their study: 0-3 years, 4-8 years, 9-12 years and 13-15 years.

#### **2.1.2.1. Restraint use and their effectiveness**

The two studies mentioned above indicated that unrestrained children were more likely to be killed or injured, as compared to restrained children. The risk of injury for unrestrained children was more than 3 times higher than that for restrained children according to the study from the research group from Philadelphia, which included all types of passenger vehicles. The NHTSA study made more detailed investigations and found that unrestrained children in light trucks and vans (LTVs) in multi-vehicle fatal crashes were 2.5 to 5.4 times as likely to be fatally injured as children who were restrained, and children in passenger cars were 1.6 to 1.8 times as likely to be fatally injured if unrestrained. In fatal crashes, restrained children in passenger cars were more likely to be fatally injured than restrained children in LTVs. Figure 2.1 illustrates the percent of passengers injured, aged birth – 15 years, by vehicle body type, and restraint use among single vehicle crashes [15].



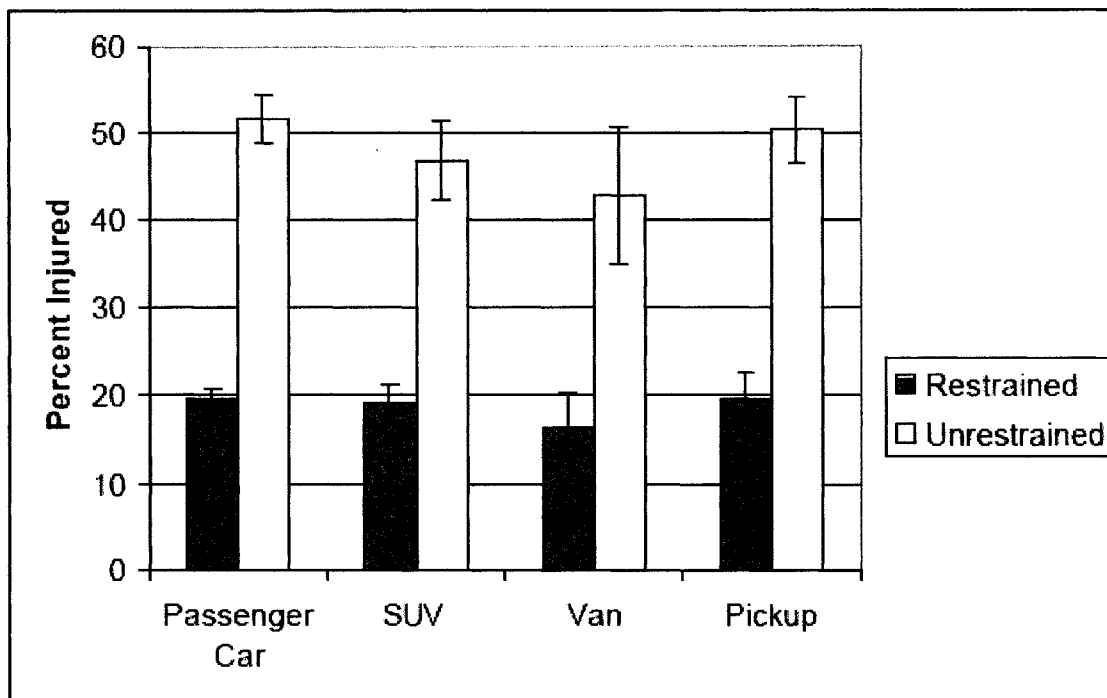


**Figure 2.1 Percent of passengers injured, aged birth – 15 years, by vehicle body Type, and restraint use among single vehicle crashes [15]**

Additionally, it is reported [17] that the traffic fatalities of children from 1995 to 2005 show the reduction as illustrated in Figure 2.2. This is due to increased child restraint system usage. Table 2.2 shows the statistics of CRS use by child occupants in 2005. During this year, 7,493 passenger vehicle occupants aged 14 and younger were involved in fatal crashes. For those children where restraint use was known, 27 percent were unrestrained; among those who were fatally injured, 46 percent were unrestrained.

Research has shown that lap/shoulder safety belts, when used, reduce the risk of fatal injury to front seat occupants (age 5 and older) of passenger cars by 45 percent and the risk of moderate-to-critical injury by 50 percent. For light-truck occupants, safety belts reduce the risk of fatal injury by 60 percent and the risk of moderate-to-critical injury by 65 percent.

Research on the effectiveness of child safety seats has found them to reduce fatal injury by 71 percent for infants (less than 1 year old) and by 54 percent for toddlers (1-4

years old) in passenger cars. For infants and toddlers in light trucks, the corresponding reductions are 58 percent and 59 percent, respectively. Over the period from 1975 through 2005, an estimated 7,896 lives were saved by child restraints.

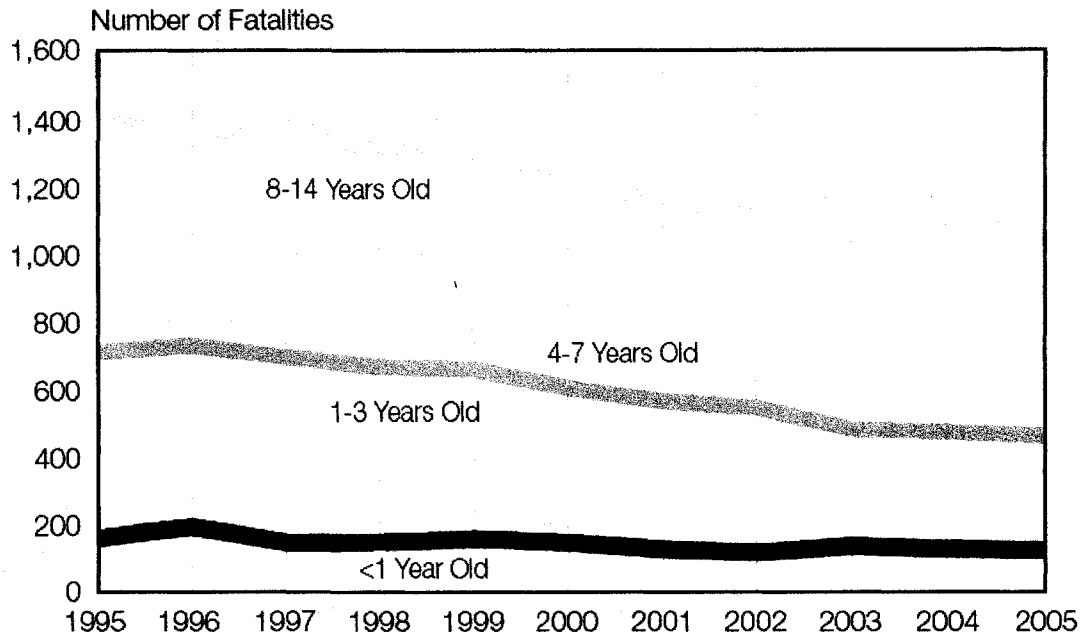


**Figure 2.2 Total traffic fatalities among children age 14 and under by age group, 1995-2005 [17]**

**Table 2.2 Restraint use by passenger vehicle occupants involved in fatal crashes by age group, 2005 [17].**

	Age Group (Years)						Total
	<1	1-3	4-7	8-13	14-19	All Other	
Restraint Used	86	83	73	67	56	65	<b>64</b>
Restraint Not Used	14	17	27	33	44	35	<b>36</b>

Note: Excluding unknown age and restraint use.

### **2.1.2.2. Seating positions**

In the previously identified studies child injuries and fatalities are also significantly influenced by seating positions. The data analysis from NHTSA's research group was independent of each condition of child restraint usage (restrained or unrestrained). In fatal vehicle crashes, the infants in the front seat had the highest fatality rate of 33% for restrained condition and 62% for unrestrained condition. When placed into the second row seats, infant fatality rates reduced to 20% for restrained condition and 54% for unrestrained condition. Similarly, children aged 1 – 3 years had a fatality rate of 18% for restrained condition and 41% for unrestrained condition when seated in the front seats compared with fatality rate 13% of infant for restrained condition and 23% for unrestrained condition when placed in second row seats. It can be stated that restrained children in the front seat were more likely to be fatally injured than restrained children in second row seats. It may be true that unrestrained children in the second row seat position can have a higher fatality rate than restrained children in front seat position. This is consistent with the findings of the research group from Philadelphia. Figure 2.3 [16] illustrates the cross sectional analysis results of restrained children in front seats versus the unrestrained children in the rear seats. From these findings, we understand that child restraint use has more effect on injury potential than seating positions.

Figure 2.3 presents the predictions of risk of serious injury for each seating position/restraint category for the overall study sample. For the total sample, it was found that injury risks were decreased when the children were appropriately restrained and sitting in the rear seat. Combining appropriate child restraint with rear seating position provides the best protection for children in vehicle crashes.

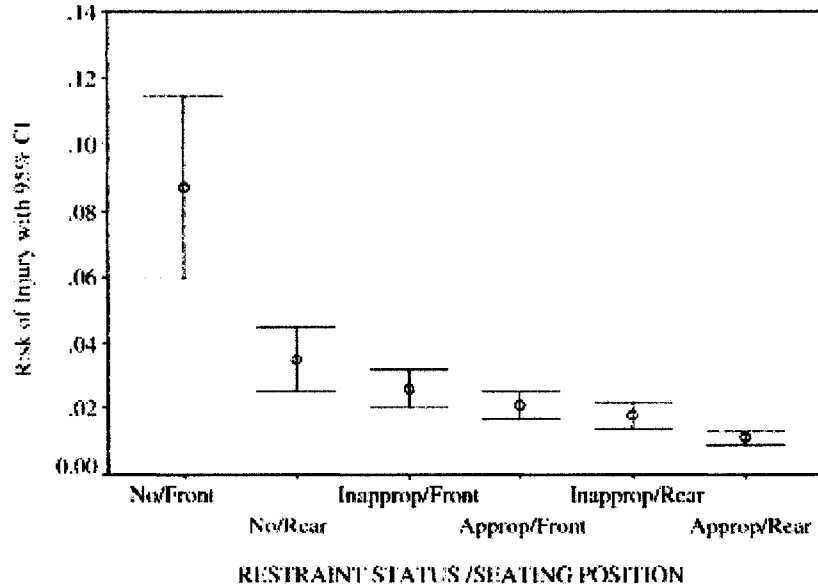


**Figure 2.3 Predicted risk of serious injury for each restraint/seating position group [16].**

**Note:** IC: confidence interval; Inapprop: inappropriate; Approp: appropriate

Reproduced with permission from *Pediatrics*, Vol. 115, Page(s) e305-e309, Copyright © 2005 by the AAP

### 2.1.2.3. Injury pattern in vehicle crashes

As the WHO reported in 2007 [1], the nature and severity of injuries that children and youth sustain in road traffic collisions are influenced by their age and the type of road user they are. Traumatic brain injuries are the leading cause of traffic-related deaths and injuries in both high-income countries as well as low-income and middle-income countries. As an example, a hospital study of children under 15 years in the United Arab Emirates found that head and neck injuries were responsible for 57% of fatalities. Common youth injuries in traffic crashes also include limb injuries, abrasions and contusions. Arbogast et al. [5] indicated similar results. As Figure 2.4 illustrates, head and face injuries were the most common injuries for child passengers while head, extremity, and thoracic injuries were the most common for drivers. The study shows that 35% of the crashes occurred near or at an intersection and frontal crashes were the most common (45%) followed by rear impacts (30%) and side impacts (22%). Rollovers represent 1.7% of the crashes in 2004.

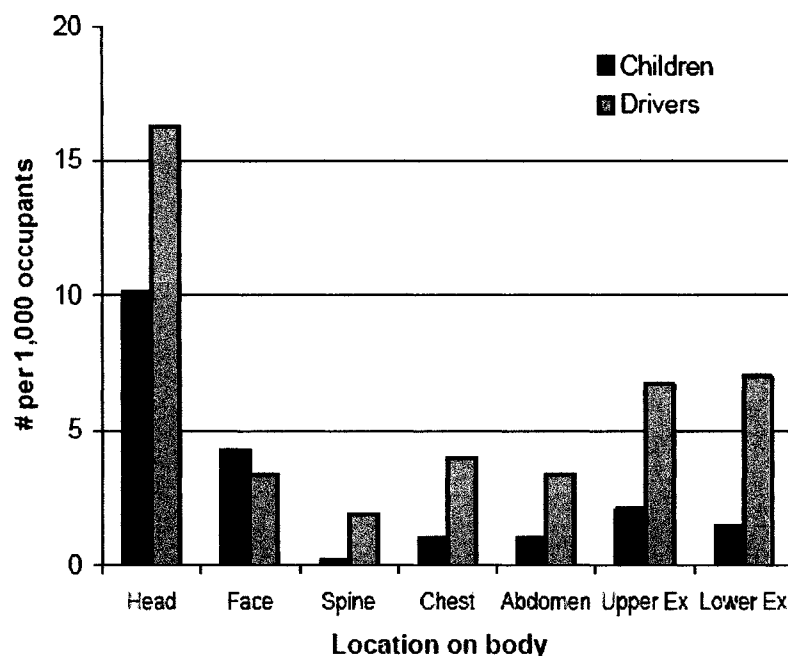


**Figure 2.4 Body region distributions of child occupants and adult drivers [5].**  
 Reprinted with permission from SAE Paper # 2006-21-0007 © 2006 Convergence Transportation Electronics Association and SAE International.

Parenteau et al. [18] found that rollover crashes involved the highest incidence of maximum Abbreviated Injury Scale (AIS) MAIS 3+ injury in children, followed by frontal and side impacts. Head and upper extremities were the body regions with most frequent serious injuries (AIS 3+). There are two types of injuries for children, contact injury and non-contact injury. The seatback, head restraint, B-pillar and interior surfaces were common injury sources for contact injuries.

The pattern and severity of child injuries are also related to the restraint type used. For example, during a frontal impact, the child restrained by a lap belt will continue to move forward more than an adult because of their increased flexibility, which increases the risk of injury to the brain and neck which may result from contact with the front seatbacks and other interior surfaces below the beltline.

Though pediatric cervical spine injury is rare, it is a devastating trauma outcome with fatal or life-long debilitating consequences [19]. Pediatric spinal column injuries to child occupants account for less than 15% of all spine injuries, and the injury and fatality rates caused by spinal cord injuries surpass those of adult passengers.

## **2.1.3 Preventions of children injury in motor vehicle crashes**

### **2.1.3.1 Current safety standards for children**

As Goldwitz and Van reported in 2006 [20], in the United States there were 60.8 million children aged 14 or younger, representing 20.7% of the US population base according to 2004 US Census estimates. As a result of the growing size and weight of a child body, keeping these children safe while riding in motor vehicles is a challenging task. Children have biomechanical characteristics that are unique from the rest of the population. To ensure the safety of child occupants, the safety requirements including restraint system use have been established in certain Federal Motor Vehicle Safety Standards (FMVSS).

The authors of the published paper [20] examined and summarized child occupant protection regulations in FMVSS, and also highlighted some child occupant safety issues. It can be found in the FMVSS a number of different standards and regulations that are specifically designed for or related to child occupants.

#### **2.1.3.1.1 Federal Motor Vehicle Safety Standard 208 [21]**

This standard is specifically designed for occupant protection in vehicle frontal crashes. It addresses the vehicle crashworthiness and occupant restraint system requirements. This standard requires that a rear-facing CRS should never be placed in a front seat. Two new requirements for advanced airbags will benefit child occupants:

- Suppression or low risk deployment of frontal passenger air bag with a 12-month old CRABI infant dummy,
- Suppression, dynamic out of position suppression or low risk frontal air bag deployment for a 3-year-old dummy (S21) and a 6-year-old dummy.
- Warnings from this standard are placed in vehicle for the child occupants as well.

#### **2.1.3.1.2 Federal Motor Vehicle Safety Standard 213**

This standard is directly applied to child occupant safety with requirements of specific CRS performance. FMVSS 213 has been significantly changed and expanded since it was first introduced in 1971 [22]. The requirements specified in the FMVSS 213

are applied to CRSs used in both motor vehicles and aircraft. Some of the major requirements include:

- A CRS is used to restrain children with weight up to 29 kg (65 lbs);
- For structural integrity requirements, complete separation of structural members or partial separation exposing features with a radius of less than 6.4 mm (0.25 in.) or protruding above adjacent surfaces more than 9.5 mm (0.375 in.) is not allowed;
- The head injury criteria (HIC) should be less than 1000 based on the calculation over a period of 36 ms or less and a limit of 60 g on chest accelerations with durations of 3 ms or more;
- For forward-facing CRS: excursion limits are 720 mm for the head and 915 mm for the knees;
- The angle between the back support surface and the seating surface must not be less than 45 degrees after the dynamic simulation test is completed;
- Buckles must have a release force between 40 and 62 N (9 and 14 lbs) before the CRS is tested dynamically (with 9 N (2 lbs) of applied tension), and no more than 71 N (16 lbs) after being tested dynamically (with an applied tension ranging from 50 N to 270 N, depending on the weight range of the CRS);
- CRSs must be permanently labeled with information specified in FMVSS 213, accompanied by printed instruction materials and come with a printed registration form;
- CRSs must be equipped with a means of anchoring the CRS to the lower anchorage points in motor vehicles. In addition, CRSs must be designed to allow installation in motor vehicles and aircraft with seat belts;
- Tethers are not required. However, CRSs equipped with tethers are tested both with tethers attached and detached;
- Dynamic sled test is conducted using a modified standard bench seat assembly, a modified pulse corridor as shown in Figure 2.5, the Hybrid III (3-year-old, 6-year-old, and weighted 6-year-old), CRABI (12-month-old), and newborn dummies.

It needs to be noted that the neck injury criteria that has been included in the FMVSS 208 does not appear in the FMVSS 213. This is due to the artifacts of the

Hybrid III dummy family used in the vehicle crash tests. The value of the neck injury criteria recorded from dummies during crash tests did not reflect child injury in the real world vehicle crashes.

Fidelity of Hybrid III dummies has been widely investigated by many researchers in recent years. One of the studies was conducted by Yannaccone et al. [23], simulating real-world crashes with a 3-year-old Hybrid-III dummy, which was used to analyze the dynamic response of a 3-year-old child in a real world crash and the neck injury based on the neck injury criteria, Nij. It was found in the study that injury prediction using either the neck load data or the Nij values from these tests would lead to a conclusion that many of the children exposed to the simulated crashes would have experienced cervical injuries, which is not supported by real-world observations.

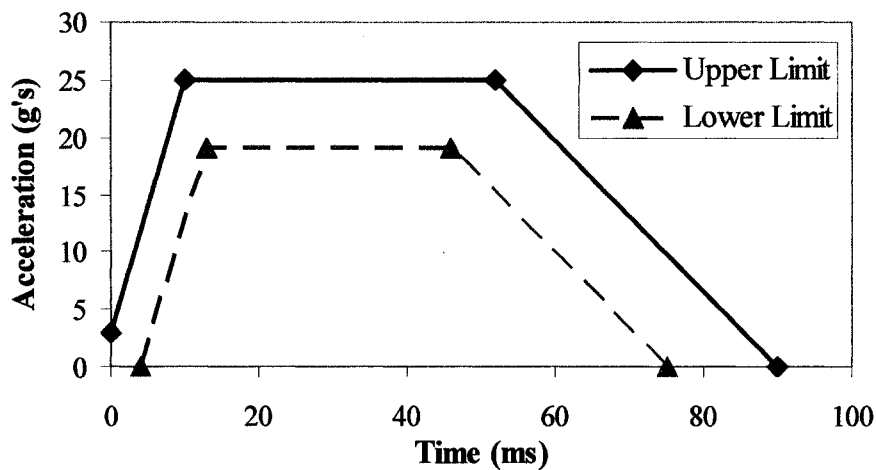


**Figure 2.5 FMVSS 213 sled test pulse upper and lower limits.**

### **2.1.3.1.3 Federal Motor Vehicle Safety Standard 225**

This standard was created for the design requirements of child restraint anchorages. The objective is to secure the effectiveness of the CRS through proper use. It requires a CRS anchorage system called Lower Anchors and Tethers for Children (LATCH). The standard requires two types of anchors for each equipped seating position: a tether strap anchor and a pair of lower anchorages. As a load requirement, the tether anchor must resist a 10,000 N (2,256 lbs) force for one second.



The lower anchorage requirements include: (1) the anchors themselves are transverse 6 mm diameter bars that must be rigidly fixed to the vehicle so that they will not deflect more than 5 mm under a 100 N (23 lbs) load; (2) a Child Restraint Fixture (CRF) essentially locates the lower anchorages in the vicinity of the seat light. The strength of the anchorages is specified with respect to the maximum permissible displacement of a reference point on a Static Force Application Device (SFAD) that is attached to the anchorages. A maximum 175 mm displacement is permitted when an 11,000 N (2,481 lbs) longitudinal force is applied and a maximum 150 mm when a 5,000N (1,128 lbs) lateral force is applied.

#### **2.1.3.1.4 Federal Motor Vehicle Safety Standard 217, 220 and 222**

These three standards are related to child occupants within school buses. FMVSS 217 deals with the emergency exit areas and window retention based on the types and capacities of different school buses specifically designed for child occupants. The purpose of FMVSS 220 is to reduce the number of deaths and the severity of injuries related to body deformation in a school bus rollover. It requires that the roof of a school bus should deform less than 130 mm and that emergency exits should still function when the school bus is subjected to a load 1.5 times the vehicle weight.

The requirements in FMVSS 222 are related the designs of seats and barriers, head impact protection and the anchorages of wheelchair positioning for a school bus. The required maximum loading is based on the number of occupants designed for the seat. The clearance between the seats or between the seat and barrier is 102 mm (4 inches) when the seat is subjected to a maximum loading 3,114 N for forward facing seating and 9,786 N for rearward facing seating, respectively. A barrier must be in place if there is no other seat within 610 mm (24 inches) in front of the seat. The barrier must meet the same force-deflection requirement as the seat.

There are also other standards, such as FMVSS 202 (head restraint), FMVSS 207/210 (seat pull test), FMVSS 209 (seatbelt assemblies) and FMVSS 401 (interior trunk release), which are not designed for children but may be applied to child occupants with considerations for pediatric anatomic characteristics.

### **2.1.3.2 Child Restraint System (CRS)**

Based on many years of statistics and research in real world vehicle crashes, observations clearly indicate that being restrained lowers a passenger's chance of being killed or injured, compared to when a passenger is unrestrained for all crash types [15]. The injury pattern and severity are influenced by restraint types [18] [24]. Use of an airbag increases the risk of injury and fatality for children. Using adult seatbelts could reduce the number of child fatalities but serious injuries may be instead caused by the seatbelt itself. Properly utilizing a CRS is the best way to protect child occupants in vehicle crashes.

Child restraint systems have been designed for children based on their age, weight and height [25]. Child safety seats are designed for children aged 4 and younger and weighing up to 18 kg (40 lbs). Children who weigh between 18 kg and (40 lbs) and 36 kg (80 lbs) and less than 145 cm (57 inches) of height should be restrained using low back or high back belt positioning booster seats until the vehicle's lap and shoulder belt fits correctly.

Figure 2.6A shows a rearward facing child safety seat applicable to children who are younger than 12 months and less than 9 kg (20 lbs) in North America. In Sweden, however, children are restrained in a rearward facing child safety seat until at least their third birthday. The benefits can be seen from the charts in Figure 2.7 and 2.8 which indicate that child fatality and injury rates are much lower in Sweden compared to France and Germany [26]. Figure 2.6 (B) and Figure 2.9 illustrate forward facing child seats. The 5-point harness convertible seat shown in Figure 2.9 can also be placed in the rearward facing position.

To ensure the effectiveness of the child restraint system and to make the installation easier, the LATCH system as shown in Figure 2.10 has been required by NHTSA for vehicles manufactured after September 1, 2002 [27].

As Howard et al. indicated in 2003 [28], the suggestion to keep children in a rearward facing position results from the heavy head and weak neck musculature which increase an infant and young child's risk of cervical spine injury in a frontal impact collision. The neck loads can be reduced and the cervical spine injuries of infant and young children can be prevented by turning young children to face the rear of the vehicle.

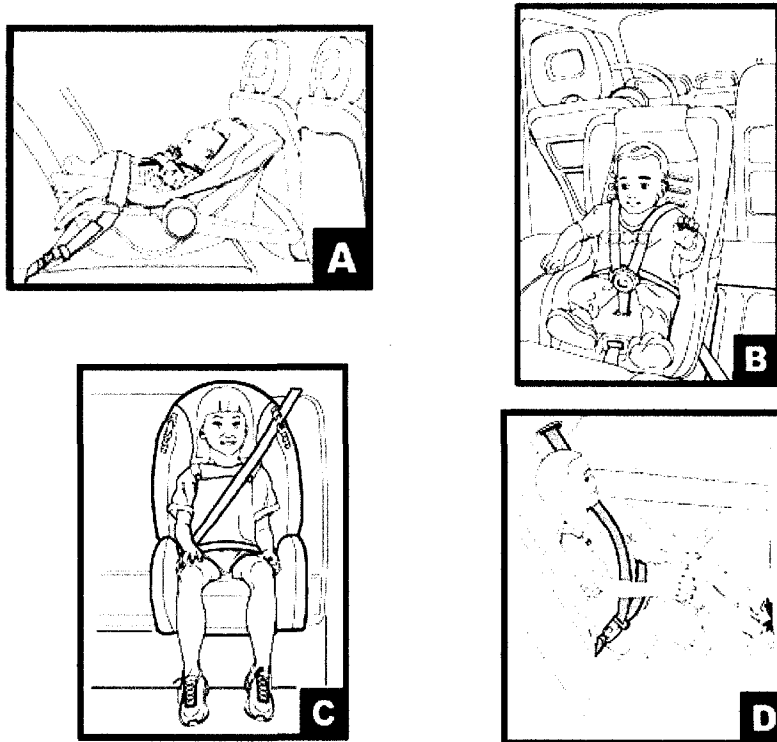
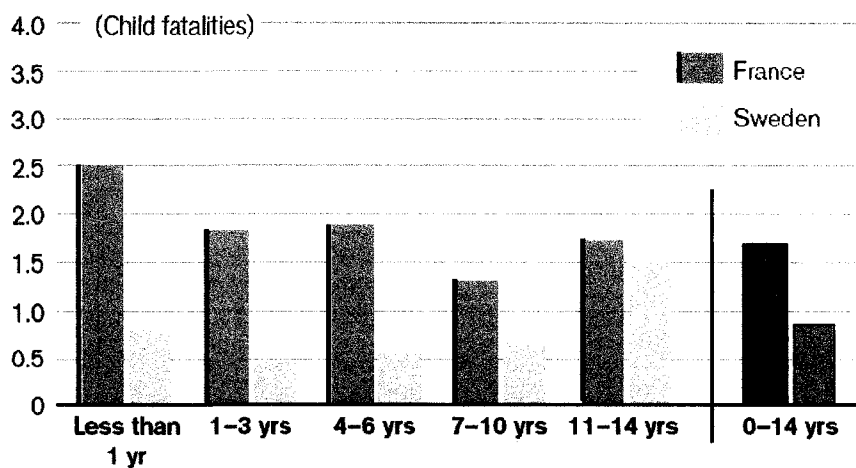


**Figure 2.6. Child Restraint Systems (CRS) [25]:**  
**A. Rearward facing child safety seat; B. Forward facing child safety seat;**  
**C. High back booster seat; D. Backless booster seat.**

### Fatality rates, children in cars, per 100,000 head of population



GRAPHICS: TOMAS ÖHRLING/INFC

**Figure 2.7 Comparison of child fatality rates in car crashes  
in Sweden and in France [26].**

## Injury rates, children in cars, 1999

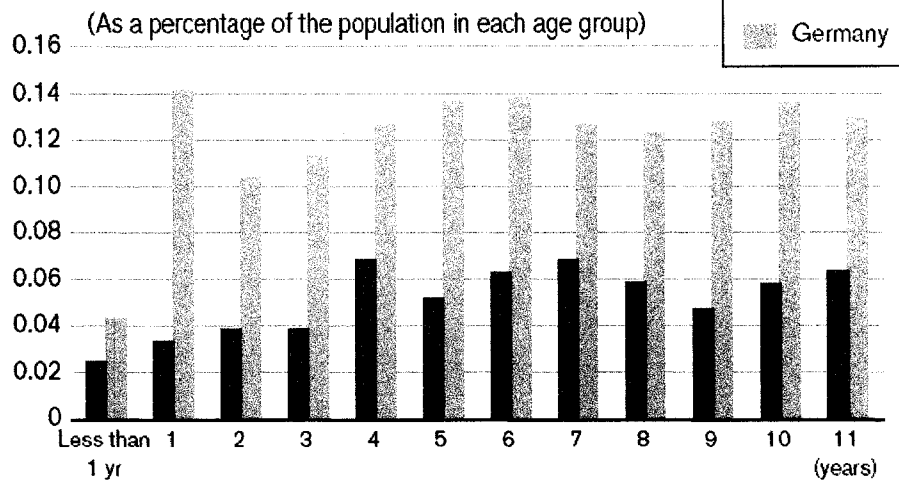


**Figure 2.8 Comparison of child injury rates in car crashes in Sweden and in Germany [26].**

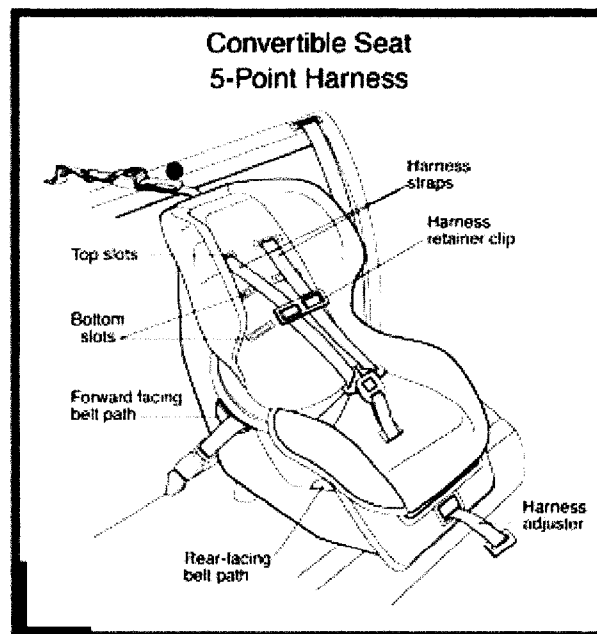


**Figure 2.9 Child convertible seat with 5-point harness [25].**

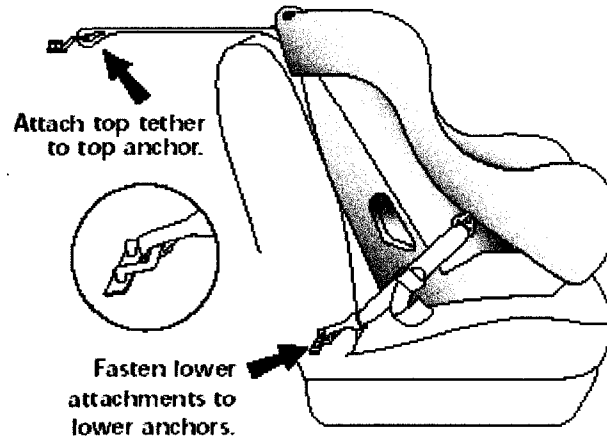


**Figure 2.10 Lower Anchors and Tethers for Children (LATCH) [27].**

In 2004, Menon et al. [24] evaluated the effectiveness of different restraint systems applied to children. For the evaluation, 18 sled tests were performed with three different speeds (24 kph, 40 kph and 56 kph) and four types of restraints (forward facing convertible seat, seatbelt positioning high back booster seat and backless booster seat, and adult's lap/shoulder belt). The tests were carried out using 3-year-old and 6-year-old Hybrid III dummies. The test results for the 3-year-old showed that forward facing convertible seats perform better than backless booster seats and adult's lap shoulder belts in terms of injury measurement. Since there is a problem of biofidelity for the 6-year-old Hybrid III dummy, some values of the injury criteria exceeded the threshold limits at 56 kph with high back or backless booster seats. The conclusion from this study is that the designs of the high back and backless booster seats need to be further investigated and improvements to the biomechanical response of Hybrid III dummies are necessary.

Due to reinforced regulations and child safety education campaigns, statistics of real world vehicle crashes have shown that approximately 70% of children aged birth-8 years are restrained in either a child safety seat or a belt-positioning booster seat [5]. Arbogast [5] also found in their study that the tendency of child fatality and injury is decreased with an increase of child restraint system use. To further improve child occupant safety, it is important to better understand the special anatomical characteristics of the child body in its development phase and the injury mechanisms. These topics will be discussed in the subsequent sections.

## 2.2 Child anatomy

Child anatomy differs significantly from adults. They have biomechanical characteristics that are unique and vary as a result of age. There is a challenge to keep child occupants safe because of the changes in body size and weight in their early development stage [20]. Knowledge about the differences in geometry and anthropometry between children and adults and the changes in biomechanical response and anatomical structure for children is critically important for improving child occupant protection. Figure 2.11 demonstrates the relative proportions of a human body from birth to adulthood [26]. Subsequent sections will discuss, in detail, growth variations and their implications for vehicle safety.

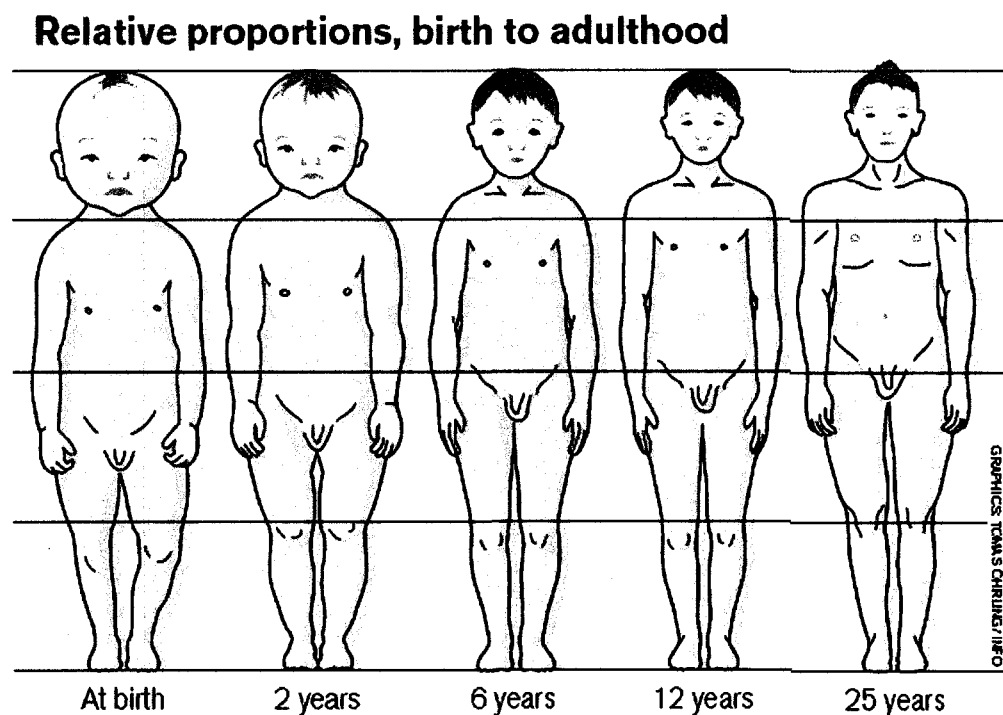


**Figure 2.11 Development of a human being [26].**

### 2.2.1 Children head development

A child's head is large and heavy in relation to the rest of the body. The proportion of head mass for a child (30% of the body weight at birth) is much higher than that of an adult (only 6% of body weight). The face of a child is also relatively small compared with the rest of its head and brain. Figure 2.12 illustrates skull profiles from a newborn to an adult. In addition to the differences in the weight and size of the head, the structure of a child's skull is also considerably different from that of adults. The shape of a child's head changes with age. Skulls of young children are thinner and more flexible. Direct geometrical skull scaling of an adult skull is not appropriate for biomechanical assessment of a child skull.

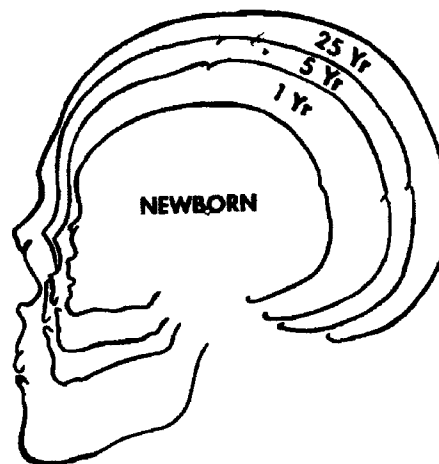


Figure 2.12 Skull profiles showing changes in size and shape [29].

### 2.2.2 Comparison of Adult and Child Cervical Spine Anatomies

#### 2.2.2.1 Adult cervical spine

Figure 2.13 (A) illustrates the human adult spinal column consisting of cervical spine (C1 to C7), thoracic spine (T1 to T12), lumbar spine (L1 to L5), sacral spine (S1 to S5) and coccyx (tailbone). The vertebrae are connected by soft tissues, such as intervertebral discs, facet joints and ligaments as shown in Figure 2.13 (B) and (C).

The cervical spine contains seven vertebrae C1 to C7 and there is an intervertebral disc between two vertebrae with the exception of the C1 and C2. Figure 2.14 (A) and (B) illustrates the anterior and axial views of the cervical spine. Figure 2.14 (B) also shows the intervertebral disc that consists of two parts, annulus fibrosus on the outside and nucleus pulposus at the centre. The soft tissues are responsible for not only maintaining the integrity of the cervical spine but also limiting the range of movement between the cervical vertebrae under normal conditions [30].

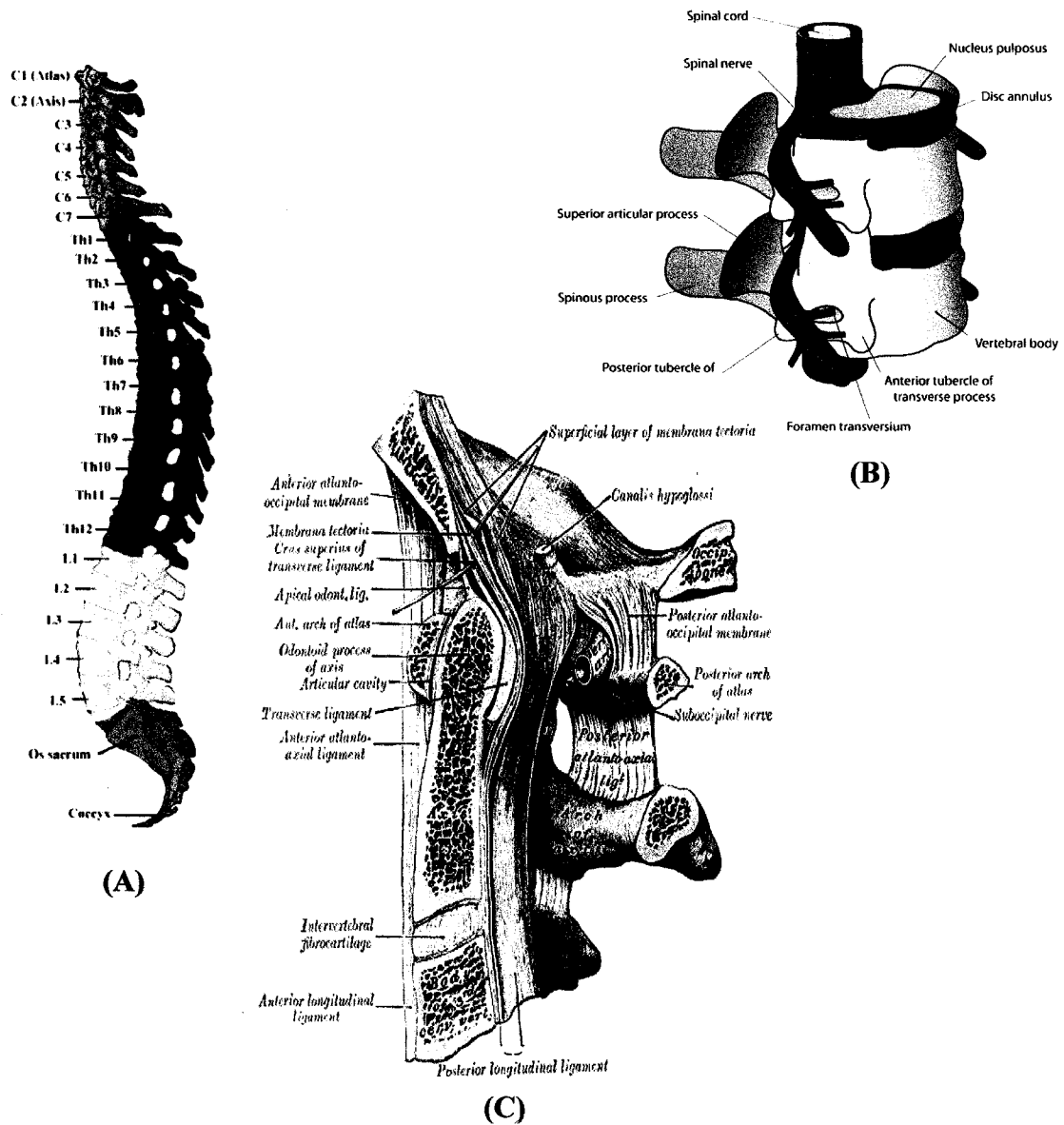


**Figure 2.13 Human adult spinal column and the soft tissues [31]: (A) Spinal column; (B) Vertebrae, intervertebral disc; (C) Ligaments.**



Ligaments usually resist only uniaxial tensile forces and some ligaments are capable of taking tensile forces in a range of directions because of their orientation. Cervical intervertebral discs respond to compression, bending, and tension loading conditions. Facet joints play a complementary role to the disc and serve as a major stabilizing structure for other tissues in the region of the neck. The normal and shear forces in the joint resist the external load due to the oblique orientation of the facet processes.

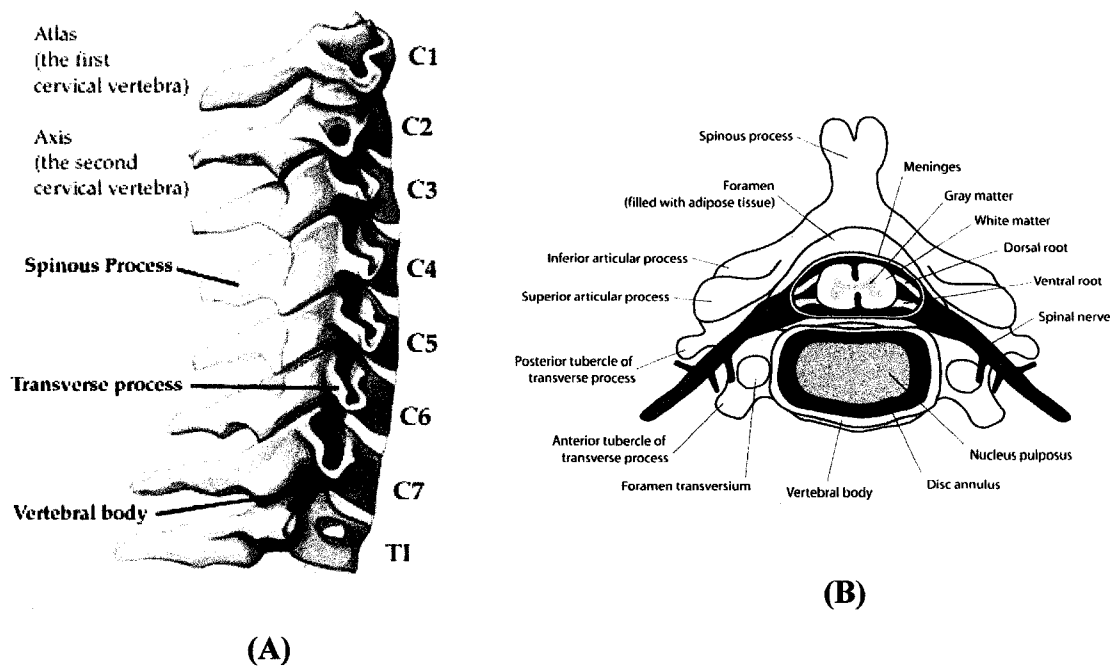


**Figure 2.14 Human adult cervical spine: (A) side view [59]; (B) axial view [31].**

### **2.2.2.2 Child cervical spine**

Many studies on pediatric cervical spines [5] [11] [26] [30] [32] indicate that the pediatric cervical spine is not a scaled-down version of an adult cervical spine. Anatomic differences between pediatric and adult cervical spines are prominent until approximately 8 years of age and persist to a lesser degree until approximately 12 years of age. Growth and developmental processes occur throughout the first two decades of human life to attain skeletal maturity. Child cervical vertebrae change shape progressively throughout the years when a child is growing, from the flat vertebrae of small children to the saddle-shaped vertebrae of adults. Figure 2.15 shows a comparison of the cervical vertebrae of children and adults. In the one-year-old vertebra, the ossification centers (centrum and neural arches) are loosely connected by cartilage materials (synchondroses). In the three-year-old vertebra, the neural arches fuse with each other posteriorly. In the six-year-old vertebra, the neural arches fuse with vertebral centrum anteriorly. In adult vertebra, primary ossification centers (centrum and neural arches) fuse completely and secondary ossification centers (uncinates and bifid spinous process) fuse with primary ossification centers. In the one-, three-, and six-year-old, the superior and inferior growth plates and the flat vertebral centrum without uncinates are seen. In the adult vertebra, saddle-shaped uncinates are seen [11]. By comparison with the adult, pediatric vertebrae have following characteristics:

- lack of the secondary ossification uncinata processes;
- the connection between vertebra and intervertebral discs of pediatric cervical spine are through the medium of growth plates;
- pediatric discs are characterized by a relatively larger size nucleus with a lack of clear demarcation between the loosely embedded fibers in the ground substance and nucleus pulposus.

These structural features indicate that the pediatric spine not only differs considerably from adult spines, but also varies among the different ages of the pediatric population.

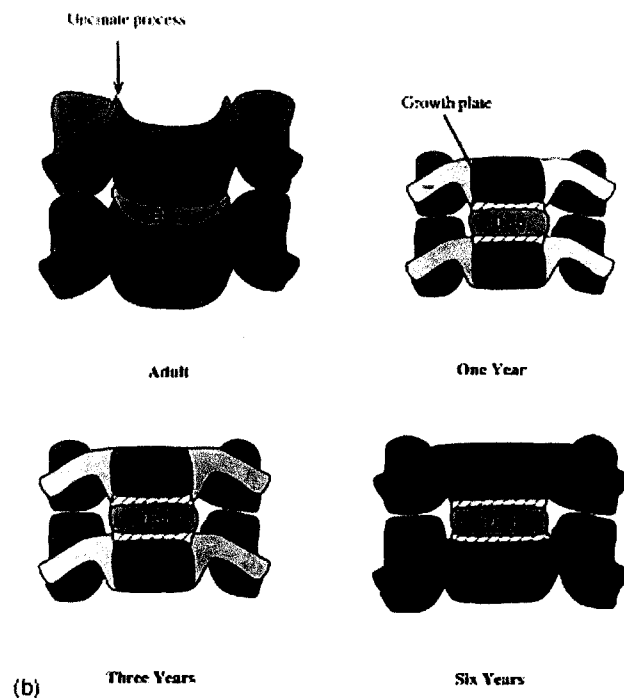
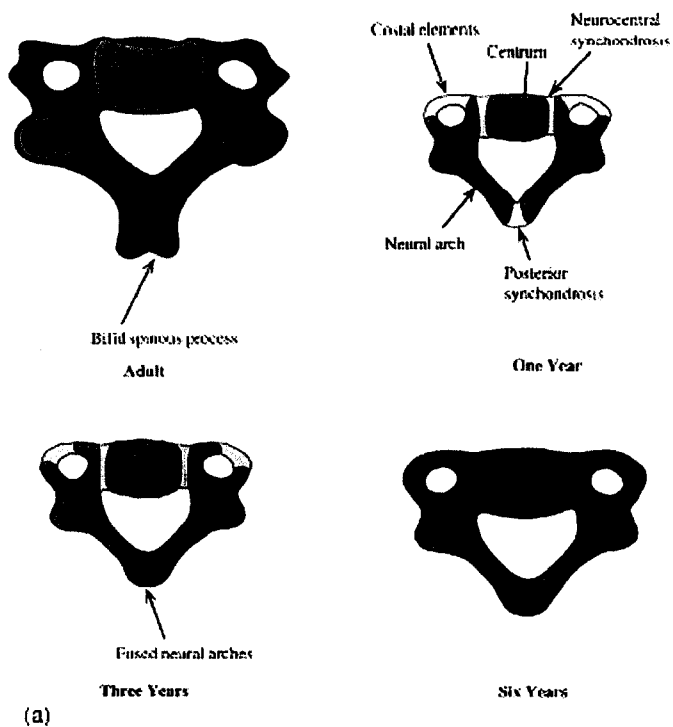


**Figure 2.15 (a) Schematic of the one-, three-, and six-year-old, and adult human cervical spine vertebra (superior view). (b) Schematic of the one-, three-, and six-year-old and adult human cervical spine functional spinal unit (anterior view) [11].**

Another factor which makes a child more vulnerable is its disproportionately slender and undeveloped neck. There is a similar gradual development of the muscles and ligaments in the neck. Human neck vertebrae also change shape progressively throughout growth, from a flat vertebra of a small child to the saddle-shaped vertebra of an adult. With a saddle-shaped geometry, vertebrae will hold together and support one another if the head is thrown forward. A young child lacks this extra protection [26]. It has been confirmed by the study of Viccellio et al [32] that the distribution of cervical spine injury (CSI) in children who are older than 12 years is similar to that of adults and the majority of CSI in younger children is in the area of C1-C2.

### **2.3 Injury mechanisms for child occupants in motor vehicle accidents**

The study performed by Arbogast and Winston in 2006 [5] shows that head and face injuries were the most common injuries for child passengers who were involved in crashes while head, extremity, and thoracic injuries were the most common for drivers. Figure 2.4 illustrates the distributions of body injury regions for child occupants and adult drivers.

#### **2.3.1 Child head injuries**

Babies and children are vulnerable when they ride in vehicles as passengers. Their heads are large and more massive in relation to the rest of their bodies. If a baby or child suffers head injuries, brain damage is often the result, which is generally much more serious than facial injuries. Head injuries in babies are frequently more severe because their skulls are thinner than adult skulls [26].

Statistics from 1991-1999 show that for all children who were between 4 and 12 years old and injured in vehicle crashes, the rate of head injuries was 50% if unrestrained and 30% if a lap-shoulder belt was used [18]. For the injured children who used forward facing child restraint system, 19% of them suffered head injuries [33].

The brain of a young child can experience large motion relative to its skull because the fontanelles allow volume changes in the skull. This relatively large motion may lead to shearing injuries of brain tissue. The fontanelles can also permit reduction in intracranial pressure [29].

Head injuries may be classified into contact and non-contact types. Contact injuries include skull fracture, epidural hematoma, and injuries to the frontal lobe. Head excursion and space reduction due to intrusion increase the chances of head impact with vehicle interior components, such as seats, pillars and doors. Inappropriate attachment to CRS, like a loose harness for example, is another factor that increases the chance of head contact due to the increased free head travelling distant during crashes. In either case, it increases the potential for head injuries.

It is believed that children in forward facing child restraint systems (FFCRS) also sustained inertial injuries to the head such as subdural hematomas [33]. If the restraint applied to the child is loose, it can also increase head acceleration thus contributing to this type of injury which is similar to head excursion. Non-contact head injuries, that is, inertial head injuries such as hematoma and concussion, result from significant head accelerations that a child cannot tolerate. During a vehicle frontal crash event, the head of a child moves relative to its torso. Though there is no contact outside the head, the contact force between the skull and the brain can result in significant distortion or damage.

Since the head injury criteria (HIC) was developed for adults based on the assumption of a rigid skull and research on the likelihood of brain injury due to skull fracture, it may inappropriate to apply the HIC to young children [29].

In addition, there is debate about non-contact head injuries. In some literature it has been indicated that the acceleration of the head is unlikely to reach a level which would be injurious to the brain for a car occupant in a crash. This is consistent with the findings as noted in the publication by McLean et al. [34] in 1995 and other studies, such as Meaney, Thibault and Gennarelli in 1994. The finding shows that there were no cases of brain injury without head impact in a series of more than 400 fatally injured road users.

### **2.3.2 Pediatric cervical spine injuries**

One of the major causes of pediatric cervical spine injury (PCSI) is vehicle crashes (30 to 40%) [28]. Head injuries may not be a result of an inertial loading during vehicle crash [34], but there is the potential for pediatric cervical spine injury as a result

of acceleration of the head with no direct impact during automotive crashes [35]. PCSI is rare in young children under the aged 8. It is usually fatal due to the underdeveloped cervical spine of children and soft tissues such as ligaments and musculatures in the area [36]. In the study of Lustrin [36], different types of pediatric cervical spine injuries and their mechanisms were presented. Child cervical spine injuries include spinal cord injury, occiput-C1 injury, fractures of the atlas, atlantoaxial injuries such as traumatic ligamentous disruption, rotatory subluxation, and odontoid in the level C1-C2 of the cervical spine, subaxial injuries (C3–C7), posterior ligamentous injuries, wedge compression fractures, and facet dislocations.

Studies have shown that cervical spine injuries in children occur at the middle or lower neck (C4-C7) as reported by Viccellio et al. [32] and Ouyang [8]. Most researchers, however, believe that upper level cervical spine injuries (C1-C3) constitute the majority of cases of pediatric neck injuries for young children based on real world vehicle crash cases and pediatric clinical findings [19] [28] [36] [37] [38]. The findings from Viccello et al. [32] and Ouyang et al. [8] that child cervical injuries occur at the middle and lower cervical vertebrae may not be appropriate as there were too few cases for young children aged 8 and younger in Viccellio's study. Additionally, the testing completed by Ouyang et al. [8] investigated only laboratory type pure tensile and bending loading conditions. While this study provides critical details associated with the biomechanical response of the cervical spine, it does not simulate loading behaviour in crash conditions. Furthermore, neck musculature was removed; limiting the appropriateness of the conclusions associated with the injury locations of the cervical spine.

Ivancic et al. [39] showed that in adults, the head/C1 joint were also significantly more flexible than all other spinal levels and does suffer from upper level cervical spine injuries. In general, CSIs are less common in children than in adults, but CSIs in the upper level neck in children are approximately two and a half times more common than in adults.

Instability of the pediatric cervical spine is the mechanism of upper cervical spine injuries in children. The hyper-mobility of a child's immature spine is a result of its relatively large head and weak neck muscles and also the incomplete ossification of the

odontoid process. The biomechanical and anatomical characteristics such as ligamentous laxity, shallow and angled facet joints, underdeveloped spinous processes, and physiologic anterior wedging of vertebral bodies contribute to high torque and shear forces acting on the C1-C2 region.

Among the upper CSIs, traumatic atlanto-occipital dislocation is often fatal and resulted from a sudden deceleration. As a result of the unstable atlanto-occipital articulation, young children are more vulnerable to cervical spine injury at the oriented atlanto-occipital joint area. An excessive deflection or rupture of the tectorial membrane and the alar ligaments results in the relative motion between the occiput and vertebrae. Bulas et al. [37] suggested that atlanto-occipital dislocation, as an upper neck injury, should be considered in all children involved in motor vehicle accidents.

Other upper cervical spine injuries may occur in the C1-C2 level with fractures of the atlas and atlantoaxial injuries such as ligamentous disruption, rotatory subluxation and odontoid separation between C1 and C2. The fracture of the ring of C1, a so-called Jefferson fracture, is caused by axial force and occurs through the anterior and posterior arches of C1. It will contribute to spinal cord injury when the fracture results in a reduction of the cervical spinal canal. Atlantoaxial injuries with the displacement of ligaments and relative rotation between two adjacent vertebrae exceeding their normal limits could also damage the spinal cord and the vertebral artery. If atlas fracture occurs without atlantoaxial injuries, the neck is considered to have a stable injury. Otherwise, it is considered to be an unstable neck injury.

## **2.4 Child injury cases studies**

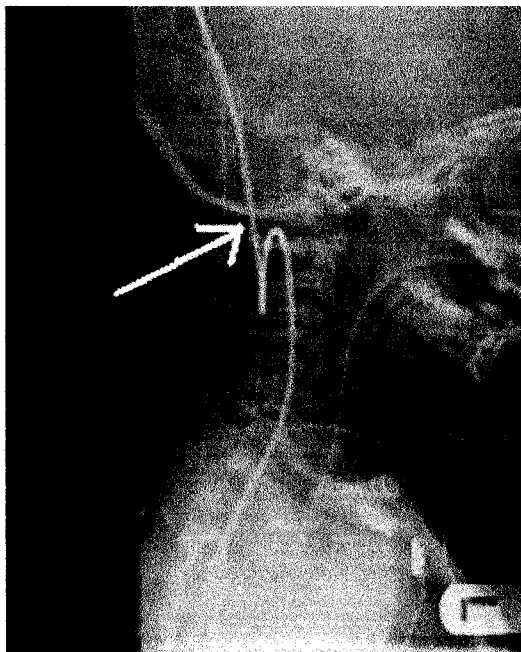
Investigations on pediatric cervical spine injuries in real world vehicle crashes can help one to better understand the injury mechanism and biomechanical responses of children. There have been crash cases in which children have sustained cervical spine injuries with contact or non-contact head impact.

Two cases studied by Howard et al. [28] were related to two young children who were properly restrained in a forward facing child restraint. Both children suffered upper

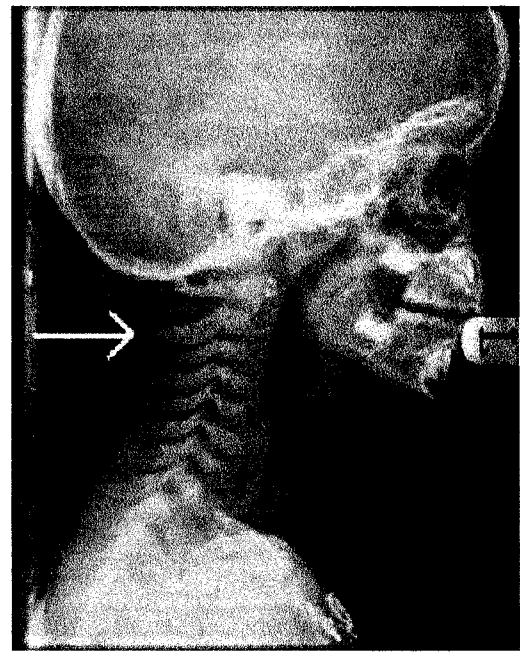
cervical spine injuries but there was no evidence of head contact during the frontal crash events.

In the first case, a child approximately two years old was sitting in a CRS in a 1994 Honda Accord when the car was directly struck in the left front at a speed of approximately 40 km/h (25 mph) by a minivan which lost control. The child sustained an occipitocervical dislocation as shown in Figure 2.16 (A) and died from this injury.

The second case involved a 3 year old child who was positioned in a forward facing five point harness child safety seat on the rear side seat of a Toyota 4Runner that lost control on a wet highway and hit a rock in a head-on collision at a speed of 60 km/h (37 mph). Two adults, one driver and one passenger in the front seat, in the vehicle suffered only minor hand or ankle injuries while the child sustained a C2 fracture through the base of the odontoid process as shown in Figure 2.16 (B). This child recovered from this injury.



(A)



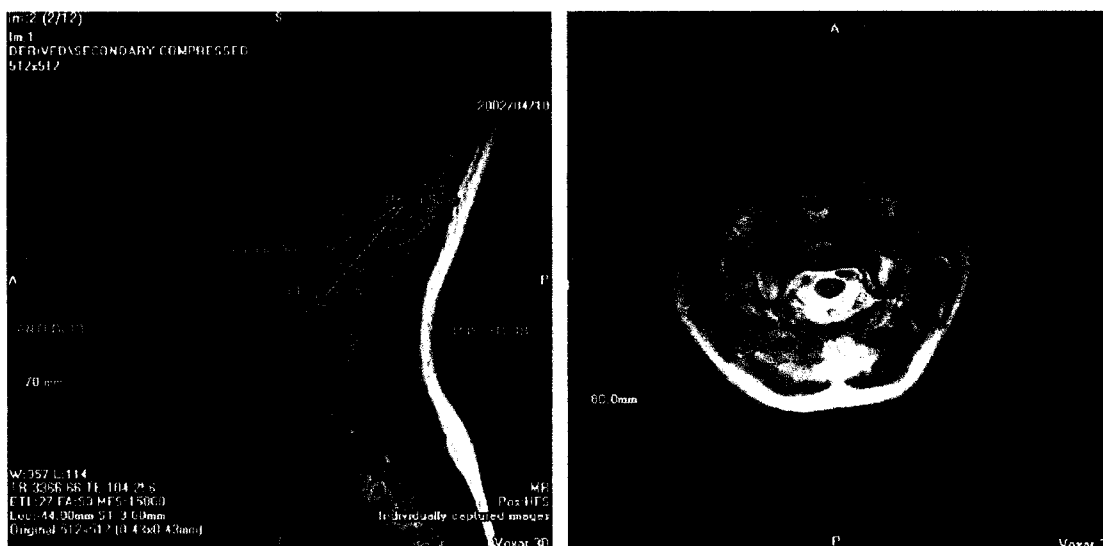
(B)

**Figure 2.16 (A) Occipitocervical dislocation in a 23 month old male involved in a frontal collision; (B) C2 fracture through the base of the odontoid process in a 35 month old child involved in a frontal collision [28].**



There was another case that involved 3 young children aged 3, 6 and 7 years who suffered different levels of upper cervical spine and head injuries and other injuries with evidence of head contact in a vehicle crash. For this case, it was reported by Sochor [38] that the vehicle with the three children experienced a full frontal crash with another car in a so called T-bone collision with a speed of approximately 45 km/h (28 mph). During the crash event all three children wore either an adult's shoulder/lap seatbelt or only a lap belt, both of which were considered as inappropriate restraints for young children. The 3-year-old who was seated in the rear with a lap belt only suffered synovial capsule with tectorial membrane hemorrhage (AIS = 2) as shown in Figure 2.17, and other injuries such as small bowel perforation (AIS = 3), bilateral iliac wing fractures (AIS = 2) and abdominal contusions (AIS = 1), which are typical for lap belt restraint injuries. The 6-year-old, who was also seated in the rear with lap belt only, experienced tectorial membrane hemorrhage with occipital condyle ligamentous injury (AIS = 2), right frontal bone depressed skull fracture with underlying subarachnoid hemorrhage (AIS = 3) which is considered as typical head contact injury. Other injuries included small bowel devascularization (AIS = 4), colon perforation (AIS = 3), L2-3 spinous process avulsion fractures (AIS = 2), L4 vertebral body fracture (AIS = 2) and abdominal contusion (AIS = 1). The third child who was 7 years old and restrained with an adult's shoulder/lap seatbelt in the front seat sustained cranial nerve palsy (AIS = 2) which was believed by the attending neurosurgeon to have resulted from stretching of the nerve by distracting the occiput from C1. Other injuries such as bilateral pulmonary contusions (AIS = 4), left # 2-6 rib fractures (AIS = 3) and lower abdominal contusions (AIS = 1) were also experienced by this child.

Tectorial membrane hemorrhage and occipital condyle hemorrhage are classified as threshold-type neck injuries and lower abdominal contusion is the typical lap belt injury suffered by young children. From all the cases above we understand the importance of appropriate child restraint systems. Even when children are properly restrained with CRS there could be an inertial injury to their neck.



(A)

(B)

**Figure 2.17 (A) MRI of tectorial membrane hemorrhage and (B) Synovial Capsule Hemorrhage in 3 year-old [38].**

Reprinted with permission from SAE Paper # 2006-01-0253 © 2006 SAE International.

## 2.5 Predictions of child injury in motor vehicle crashes

### 2.5.1 Experimental tests and real world crashes

For decades, different methodologies have been developed to improve child safety and to predict the kinematic response and injury risks of children in motor vehicle crashes. There are many different physical tests for improvement of vehicle design in occupant safety. Physical tests also serve as baselines for correlations with various numerical simulations that are conducted for predictions of occupant injury or fatality, kinematic response of the whole human body, risks of injuries to human organs and design iterations in different levels.

Current predictions of child injury risks from vehicle crashes mainly rely on the measurements of child ATD in experimental tests. The Hybrid III 3-year-old child dummy is used for predicting child injuries and assessing the performance of CRS in frontal impact tests.

There are several examples of such experimental tests. Following the guidelines of the Canadian Motor Vehicle Safety Standard 208 (CMVSS 208), similar to FMVSS 208 of the United States, a full vehicle frontal impact test was performed by Transport Canada using a 2004 four-door Mitsubishi Lancer sedan. The test setup and testing procedure were presented by Kapoor et al. in their study in 2006 [40] and by Wang et al in their SAE paper in 2006 [41]. The test dummy was a Hybrid III 3-year-old positioned in a forward facing convertible CRS with a 5-point harness. The test car impacted a stationary rigid barrier with a speed of 48 km/h (30 mph). To assess the potential injuries, acceleration pulses from the head, neck and chest and moments and forces from the neck of the child dummy were recorded during the test.

FMVSS 213 frontal dynamic sled test is specially designed for assessments of CRS performance and child injury potential in a simulated frontal crash. Sled tests were completed at Graco Corporation's sled testing facilities and a Hybrid III 3-year-old child dummy was also used. The same position and restraint system as the FMVSS 208 frontal crash test were applied to the child dummy. The acceleration pulse was within the corridor outlined in FMVSS 213. This is equivalent to an impact speed of 41.7 km/h (25.9 mph). The kinematic and biomechanical responses of the child dummy were recorded through accelerometers and high speed cameras. More details about this test will be discussed in chapter 6 or can be found in the literatures of Wang 2006 [41] and Turchi 2004 [42].

The test results mentioned above were used in comparisons with the numerical simulations. The comparisons of simulation results with tests will be discussed in the next section.

A similar frontal impact sled test with a Hybrid III 3-year-old child dummy was presented by Mizuno et al. [6] and [7]. This sled test was conducted under the sled test conditions of the United Nations Economic Commission for Europe Regulation 44 (UNECE R44). In these studies, sled tests were performed with two different CRS configurations, namely a 5-point restraint system and a tray shield form restraint system as shown in Figure 2.18. The effectiveness of the two types of restraints for protecting children from injuries was compared in this study. The acceleration pulse applied to the sled was in the corridor specified in the ECER44 requirement as shown in Figure 2.19.

The maximum acceleration and the initial velocity were 25g and 50 km/h, respectively. It was found in their research that the behaviour of a child in impacts may be difficult to predict by using the Hybrid III dummy with its stiff thorax spine box and that there were major differences in behaviour of the Hybrid III and child FE models in terms of thorax spine flexibility.

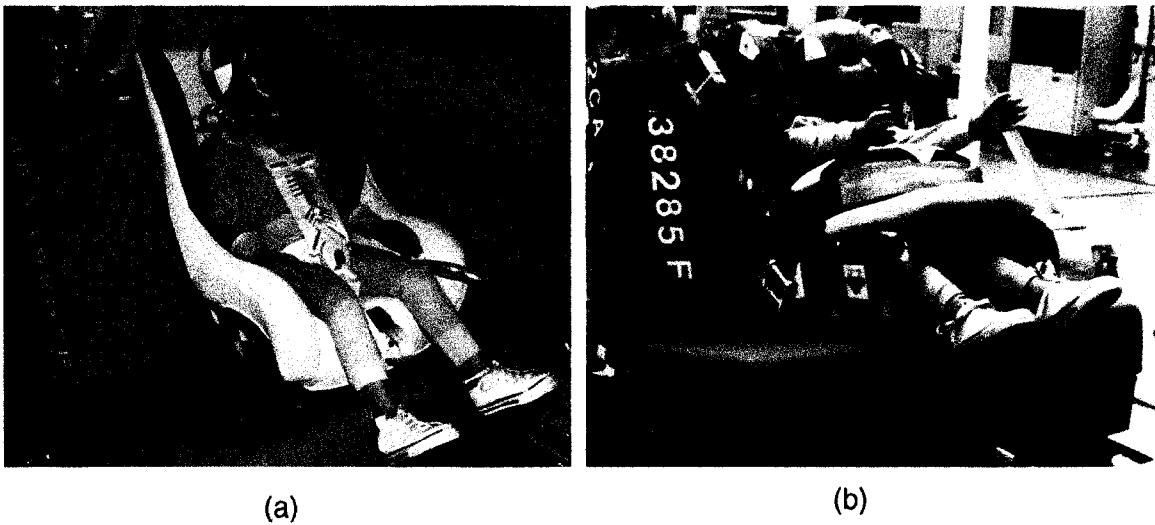


**Figure 2.18 Test setup in ECE R44 CRS tests with Hybrid III 3-year-old child dummy and CRS (a) 5-point harness; (b) tray shield [6].**

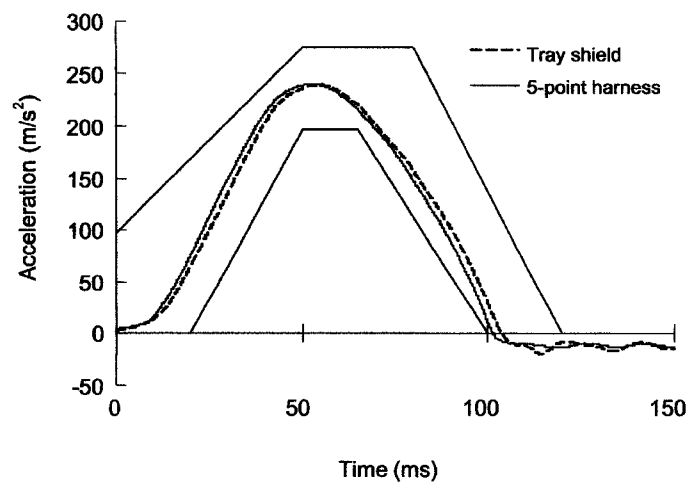


**Figure 2.19 CRS sled acceleration with ECE R44 corridor [6].**

Menon et al. [24] carried out a series of 18 sled tests performed on a HyGe accelerator sled. In these tests 3 and 6-year-old Hybrid III child dummies were used and positioned on either side of a standard FMVSS 213 bench seat. Table 3 shows the test matrix which includes the 18 tests at three speeds 24 kph, 40 kph and 56 kph and under four different restraint conditions: forward facing convertible child restraint (FFC), backless belt-positioning booster (NBB), high back belt-positioning booster (HBB) and lap shoulder belt (L/S). Figure 2.20 (a), (b) and (c) illustrate the positioning and restraint use of the Hybrid III 3-year-old child dummy and Figure 2.20 (d), (e) and (f) illustrate the positioning and restraint use of the Hybrid III 6-year-old child dummy. It was found that the lowest injury measurements were obtained for the 3-year old in a forward-facing convertible child restraint. The 6-year-old demonstrated maximal differential performance in the 56 kph test in a belt-positioning booster seat. It was also observed that the 6-year-old Hybrid III dummy in the high back booster seat showed extreme cervical flexion and chin-face contact with the chest.

Researchers and engineers usually use the data measured or recorded from the child dummies in the experimental tests to predict the levels of injuries and the effectiveness of restraint systems applied to child occupants in vehicle crashes. Although the Hybrid III dummy family, including the 3-year-old, are considered as state of the art ATDs and are required officially by NHTSA for the frontal impact tests, there are increasing concerns in recent years about the biofidelity or artifacts of Hybrid III child dummies especially in the area of the neck and upper torso.

**Table 2.3 Sled test matrix [24]**

	3-year-old HIII			6-year-old HIII		
24 kph	FFC	NBB	L/S	HBB	NBB	L/S
40 kph	FFC	NBB	L/S	HBB	NBB	L/S
56 kph	FFC	NBB	L/S	HBB	NBB	L/S

Reprinted with permission from SAE Paper # 2004-01-0319 © 2004 SAE International.

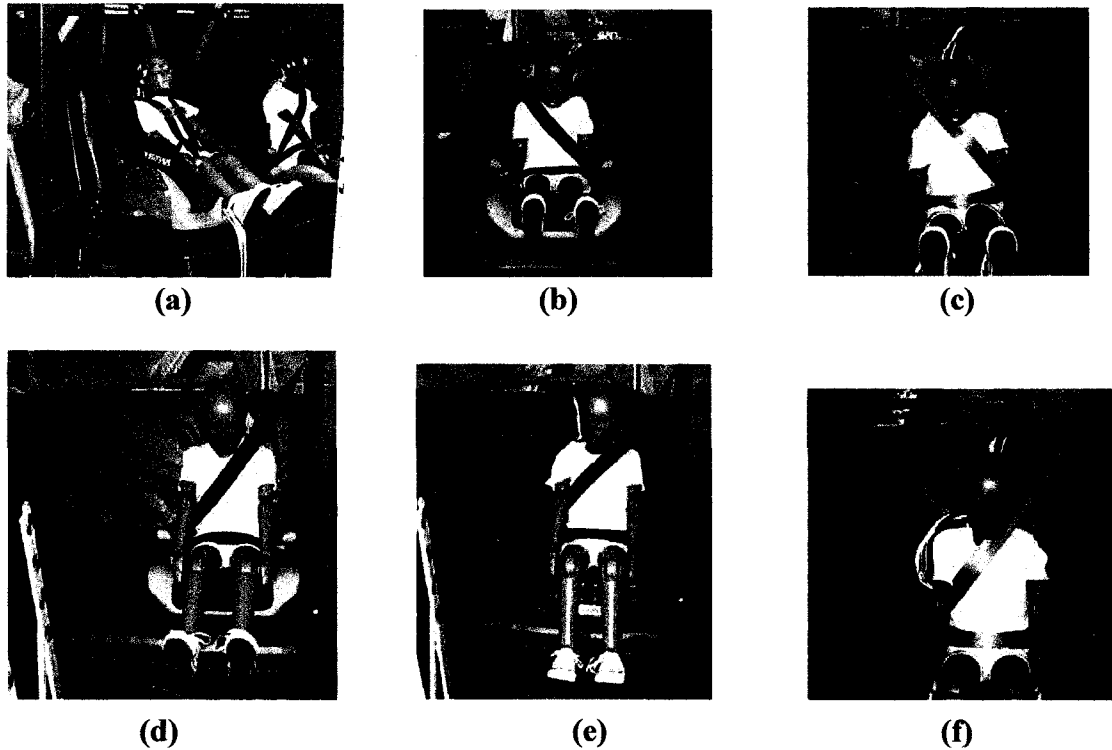


**Figure 2.20 Child dummy positions and restraint systems: 3-year-old (a) 5-point harness child seat, (b) backless booster and (c) shoulder/lap seatbelt; 6 year-old (d) backless booster, (e) high back booster and (f) shoulder/lap seatbelt [24].**

Reprinted with permission from SAE Paper # 2004-01-0319 © 2004 SAE International.

In 2006 Arbogast [5] pointed out that there are critical differences between the responses of the actual human body and predictions from ATDs due to the growing pediatric body. This brings the case that pediatric ATDs and their associated injury criteria are used as primary tools of assessment for child occupant protection in motor vehicles. One of the causes of the differences is the mobility of the human spine and the rigidity of current ATD. The head trajectory of the dummy can be significantly different when compared to that of a human, which is a result of significant spinal variations between the dummy and child. Kang et al. [4] analyzed the neck assessment values of Hybrid III ATD, including the 3- year-old child dummy in out-of-position (OOP) tests and observed that the 3-year-old child ATD predicted a moderate likelihood of severe neck injury while no injury was observed in a comparable cadaver test. They believe that the response of the head/neck system of the Hybrid III ATD is an artifact of the ATD and therefore may not be representative of a human. They also concluded that the thoracic

spine of the Hybrid III 6-year-old ATD was not biofidelic in restrained frontal crash tests, and the high neck forces and moments resulted from the stiff thoracic spine of the ATD are not representative of the true injury potential.

In the above-mentioned sled tests with 3 and 6 year old Hybrid III child dummies, Menon et al. [24] identified typical child injury mechanisms by analyzing real world crash data, and conducted the 18 sled tests with 3 and 6-year old Hybrid III ATDs to simulate the crash scenarios which had happened or may possibility happen in the real world. By comparing with the real world data, they suggested that the neck is lacking in biofidelity due to the current ATD's neck showing a higher degree of injury.

Yannaccone et al [23] simulated real-world crashes with a 3-year-old Hybrid-III dummy, which was used to analyze the dynamic response of a 3-year-old child in a real world crash and the neck injury based on the neck injury criteria, Nij. In the study, the biofidelity and kinematic response of the Hybrid III child dummy and the performance of the child restraint system with various configurations were investigated. The study considered two real cases of children, who experienced severe cervical spine injuries, who were similar in size as the 3-year-old Hybrid III dummy. Additionally, in the two frontal impacts there was no intrusion into the child position and no improper CRS use. In the study, each crash was simulated with the child ATD restrained in three different configurations:

- *Configuration 1.* ATD restrained as the child was in the actual crash, namely booster-with-shield (BWS) child restraint system (CRS) for Case 1 and lap-belt-only (LBO) restraint system for Case 2.
- *Configuration 2.* ATD restrained by a forward-facing, 5-point CRS.
- *Configuration 3.* ATD restrained by a tethered, forward facing, 5-point CRS.

Configuration 1 simulated the actual crash with the ATD restrained as the child had been in the crash. Configuration 2 and 3 simulated the manner in which children from 9 to 18 kg (20–40 lb) were typically restrained in the United States and in Australia, respectively.

It was found that some of the child injuries predicted in simulated crashes were consistent with the findings in documented real world cases. Some others, however, were inconsistent. The consistency resulted in the kinematic and dynamic responses observed

in experimental tests. Inconsistencies were associated with the use of unity as the limit for the neck injury criteria (Nij). A child injury prediction with child Hybrid III child dummy using the Nij value from tests would lead to a conclusion that many of the children exposed to simulated crashes would experience cervical spine injuries, which is not supported by real-world experience. This means that the necks of the current Hybrid III child dummies may not be representative of the necks of real children. As a result of the real-world results and the lack of knowledge regarding pediatric neck trauma, NHTSA decided not to incorporate any neck injury criteria into FMVSS 213 for now, but suggest further research into this area.

Due to the biofidelic limitations of the ATDs used in experimental crash tests, real world experience is important in the development of occupant safety [5]. However, it would be difficult to understand what really happened to the occupants, especially in cases with young children who have been injured or killed in a real world vehicle crash. To gain knowledge about pediatric kinematical and biomechanical response, to make more accurate injury prediction and also to improve the biofidelity of current child ATDs, living subjects or human cadaver tests and component tests such as the head impact test, the cervical spine test, and the head/neck complex test are critical. Even human surrogate tests can give valuable observations.

An investigation on the effect of age and gender on 3-D kinematics of the pediatric cervical spine was conducted by Greaves et al. in 2007 [43] through measurements from 60 child volunteers who were divided into four groups based on age and gender: young girls and young boys (4-10 years) and old girls and old boys (11-17 years). From the study, the research team determined for the first time the reference values of the helical axis of motion (HAM) of the pediatric cervical spine in flexion-extension, axial rotation and lateral bending and explained the relatively high incidence of upper cervical spine injuries in young children due to their high HAM location compared to adults. Similar volunteer tests, such as sled tests with volunteer subjects seated and belted on a rigid seat performed by the National Biodynamics Laboratory of France, provided results that were used for the validation of biomechanical models of the cervical spine [44]. The force-displacement corridors from volunteer tests were also used for correlations of numerical simulations models [6] [7].



Kinematic and biomechanical responses from volunteer tests are a more accurate reflection of human body response than ATDs. However, results are specific to loading conditions which have to be within the limit of the human body's tolerance for injury. Experimental human cadaver tests would be the best approach to evaluate the human body's tolerance for external loading and the severity of injuries from vehicle crashes. Laboratory testing provides the controlled input environment. However, on-going assessment of technology's impact on child injuries in the field is critical [5]. Compared to the tests done on adult cadavers, very few pediatric cadaver tests have been reported so far and few have been used for studies on children occupant protection and child dummy development.

The first study on pediatric cadaver tests was presented in Twentieth STAPP Car Crash Conference in 1976 by Kallieris et al. [45] from the University of Heidelberg. Comparisons of the cadaver test results with testing child dummies were performed in the research and later in the study of Cassan et al. in 1993 [46]. In [45] four pediatric cadaver sled tests were carried out with subjects aged 2.5, 5, 6 and 11 years old in child restraint systems to simulate frontal impacts. The test speeds were 30 km/h and 40 km/h. Two additional sled tests were conducted with child dummy Alderson VIP-6C under the same testing conditions as cadaver tests. Numerous muscular hemorrhages and hemorrhages of discs and ligaments were found in the cadaver tests. Though the child cadaver and child dummy had similar kinematics in the frontal impact sled tests, the child cadavers showed greater deformability and much longer rebound time for the head movement from forward to backward in comparison to the child dummy. This child cadaver test data was used for the evaluations of other child dummies, namely TNO P3 and CRABI 3-year-old and different child restraint systems by Cassan [46].

The second child cadaver test was conducted in 1976 at the Highway Safety Research Institute of the University of Michigan using a 6-year-old child cadaver. At the same time, a similar test using a 3-year-old child dummy was carried out for comparison. The results of the tests and the comparisons were reported by Wismans et al. in the Twenty-Third STAPP Car Crash Conference in 1979 [47]. The 6-year-old child cadaver was similar to a 4-year-old in height and weight and 11-12% greater than the 3-year-old child dummy. A Stroelee Wee Care child restraint was used and the FMVSS 213 sled test

procedure was followed. The tests showed that the child cadaver had a larger forward head excursion (370 mm) than the child dummy (300 mm) and higher chest acceleration ( $412 \text{ m/sec}^2$  at 48 ms for cadaver and  $340 \text{ m/sec}^2$  at 53 ms for dummy). Again the tests indicated that child cadavers had higher mobility of the neck and upper torso with much larger downward motion at maximum head forward excursion compared to the child dummy. These and all other known pediatric cadaver tests were summarized by Cassan in 1993 [46].

The above-mentioned child cadaver test data has great value for the development of child occupant protection methods, child restraint systems, and child dummies. In addition to the child cadaver tests, component tests such as head impact, cervical spine test, and head/neck complex test, are crucial to understanding the biomechanical characteristics of human beings in depth and detail. Such test data is commonly seen for adults yet very rarely seen for children. To the best of the author's knowledge, there is only one set of pediatric cadaver component test data available. This pediatric cadaver component test data was presented by Ouyang et al. in 2005 [8]. Tests used head/neck complexes from pediatric donors aged 2-12 years, and non-destructive flexion-extension bending, non-destructive tensile step-and-hold tests and tensile distraction loading was completed on the cervical vertebra. The head/neck specimen consists of head, cervical spine C1-C7 and thoracic spine T1-T2 with the mandible and neck musculature removed for the purpose of improving the visualization of the cervical vertebrae. The T1 and T2 vertebrae were potted in polymethylmethacrylate during the tests. The study characterized the response and tolerance of the pediatric cervical spine. This test data gives first-hand information about the biomechanical response of pediatric cervical spines and the tolerance of injuries under various loading conditions but it has not been applied in the development of child models. More details about the test procedure and the application of test data in this research will be presented in chapters 4 and 5.

### **2.5.2 Numerical simulations with human models in children injury studies**

Numerical simulation models can be applied in practically all areas of research and development of vehicle crash safety technologies and occupant protection [48]. The advantage of numerical crash simulations over crash tests with crash dummies is that the

safety performance of design concepts and the effect of changes in the design can be studied efficiently, sometimes even without the use of a prototype. The models can be used as a tool of dynamic simulations and analyses to reconstruct real world accidents, to study biomechanical response of human body, and to evaluate vehicle performance during crashes. The numerical simulation models are classified as either lumped mass models, multi-body models, or finite element models. Since the lumped mass model is created by simplifying the whole vehicle to a few discrete parts, springs and/or dampers using the masses of the vehicle regions in one or two dimensions, it is typically used in vehicle development in the concept phase. The multi-body model and finite element model can be used towards both vehicle development and occupant protection studies.

Research and development in the field of child occupant crash protection relies heavily on the biofidelity of anthropomorphic test devices (ATDs) used in testing and the ability to relate measured parameters on the ATD to injury [23]. The Hybrid III dummy family including male, female and child dummies have been officially used as ATD's for vehicle crash tests. The Hybrid III 3-year-old child dummy is one of the child dummy series from the Hybrid III family. As previously mentioned, the Hybrid III 3-year-old child dummy has limited accuracy in predicting child injury from vehicle crashes due to a lack of biofidelity. However, there is no easy way to improve the biofidelity of the physical test dummy in a short period of time. A human-like model developed for simulating human responses in a vehicle crash event and predicting injury and fatality holds advantages over a test dummy. The detailed human anatomic geometries, material properties, and the results of the latest experimental tests and clinical findings can be more easily implemented in a human model. With a human model, parametric and multiple case studies can be performed.

One such human model is the THUMS (Total Human Model for Safety) which was developed by a Toyota research laboratory [49]. THUMS has very detailed human body parts, organs and soft tissues based on the anatomic and geometric data of a 50 percentile American male as Figure 2.21 illustrates. THUMS was introduced by Oshita et al. in 2002 [50]. It was developed to investigate the behaviour and injuries to various body regions of a mid-size adult American male (AM50) in vehicle crashes. This model was developed for the purpose of simulating the responses of the human body

under different impact loading conditions. THUMS was first validated for frontal and side impacts to the thorax, abdomen, and the hip area using available cadaver test data. In 2003 Iwamoto et al. [51] presented the new development of many internal organ models and a detailed brain model for THUMS which allows researchers and crash safety engineers to investigate human body responses and injuries with more detail for impact loads. This also applies to other models such as the small female model and the pedestrian model, which were developed based on THUMS. THUMS has been used and validated to predict lower extremity injuries. In addition, its kinematics has been compared with Hybrid III dummy sled tests by Ipek et al. in 2004 [52] with modifications at the lower extremity joints. Sawada and Hasegawa successfully applied the THUMS model in developing the new whiplash prevention seat in 2005 [14].

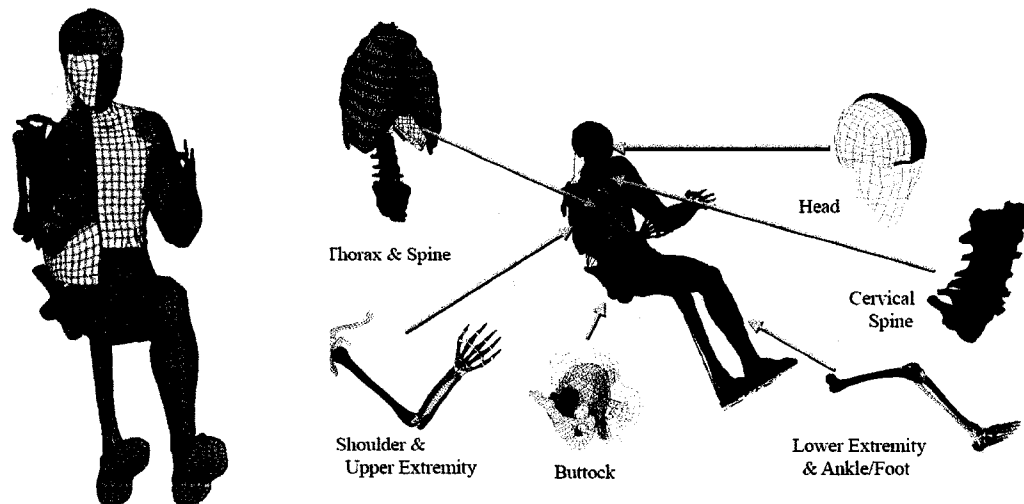


**Figure 2.21 Total Human Model for Safety (THUMS) developed by Toyota research laboratory [49].**

By comparison, there are not many validated FE child models. Information on child cadaver test data as well as child body injuries in car crashes is also very limited. A child dummy FE model based on the Hybrid III 3-year-old was developed to predict, through numerical simulations the performance of child restraint seats and the behaviour of the Hybrid III child dummy in a frontal vehicle crash. A comparison between the experimental crash test results using the Hybrid III 3-year-old child dummy in a forward facing child safety seat and the numerical simulation results using the FE child dummy

model with the same CRS configurations was performed by Turchi et al. in 2004 [42] based on the FMVSS 213 standard. The results have shown a good agreement in predicting the child dummy head and neck injuries. This model was further used to investigate the potential head and neck injuries of a 3-year-old child in rearward facing child safety seats. Recently, Wang et al. in 2006 [41] incorporated the FE Hybrid III 3-year-old child dummy model to numerically and experimentally investigate the child occupant injury potential and the performance of child restraint systems with different CRS configurations, in accordance with FMVSS 213 and CMVSS 208 safety standards. They concluded that the FE model is able to predict the injury potential of the test dummy with percentage errors within 5 to 10% and that the completely deformable CRS model is more realistic in comparison with the previously developed rigid model.

A human-like 3-year-old child FE model was presented by Mizuno et al. in [6]. This model was developed by scaling from the aforementioned THUMS male adult FE model AM50 using the model-based scaling method. Different body parts of the child model were scaled using specific scaling factors in accordance to a child's anatomy and the anthropometry, and material properties of 3-year-old children. The responses of the FE child model were compared with observations from a Hybrid III 3-year-old child dummy in a series of sled tests which followed the requirements of UNECE R44. The comparison shows that there is a significant deformation difference between the child model in FE simulation and the Hybrid III 3-year-old child dummy in the sled test. In the study of Mizuno et al. [7] in 2006, a new model of the pelvis region was developed and incorporated into the THUMS child model based upon a child's anatomical structure. The behaviour of this new model was observed to be more representative of that of a real child's pelvis under impact load conditions. As part of this research, comparisons between the THUMS numerical model and the Hybrid III 3-year-old dummy using a validated fully deformable CRS model under CMVSS 208 crash testing conditions were performed [53].

The biofidelity of the cervical spine in the child model is critical not only for the kinematic and biomechanical responses of the child neck but also for predicting child head injury potentials. Since the cervical spine in the child model was scaled from the THUMS model, it does not accurately reflect the anatomic geometry and the material

properties of a 3-year-old. In 2005 Ouyang et al. [8] performed a series of pediatric cadaver tests with subjects of 10 head/neck complexes of ages from 2 to 12 years. This invaluable pediatric data is only currently available for understanding child neck tolerance and injury potentials. Figure 2.22 shows the pediatric cadaver cervical spine extension at C2 and Figure 2.23 shows the pediatric cadaver cervical spine load deflection curves. The average deformation when a failure occurred in pediatric cadaver head/neck complex tensile tests was about 20 mm.

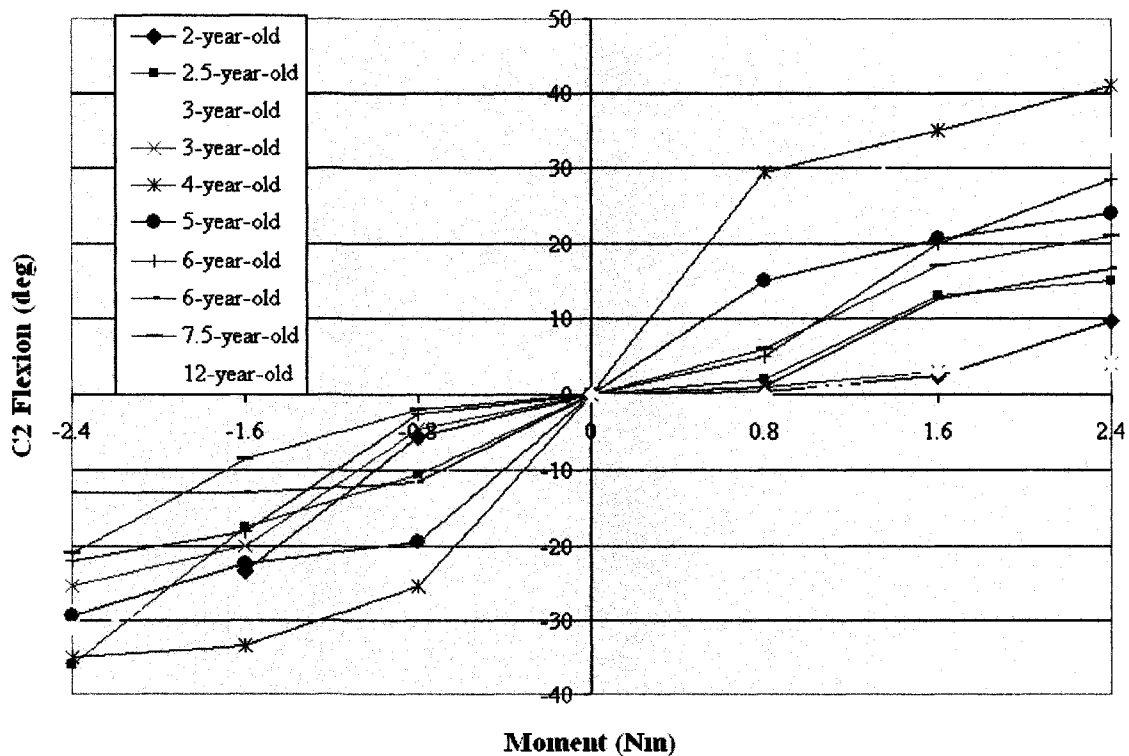


**Figure 2.22 Pediatric cadaver cervical extension at C2, unfiltered data [8].**

The original source and copyright owner: LIPPINCOTT WILLIAMS & WILKINS.

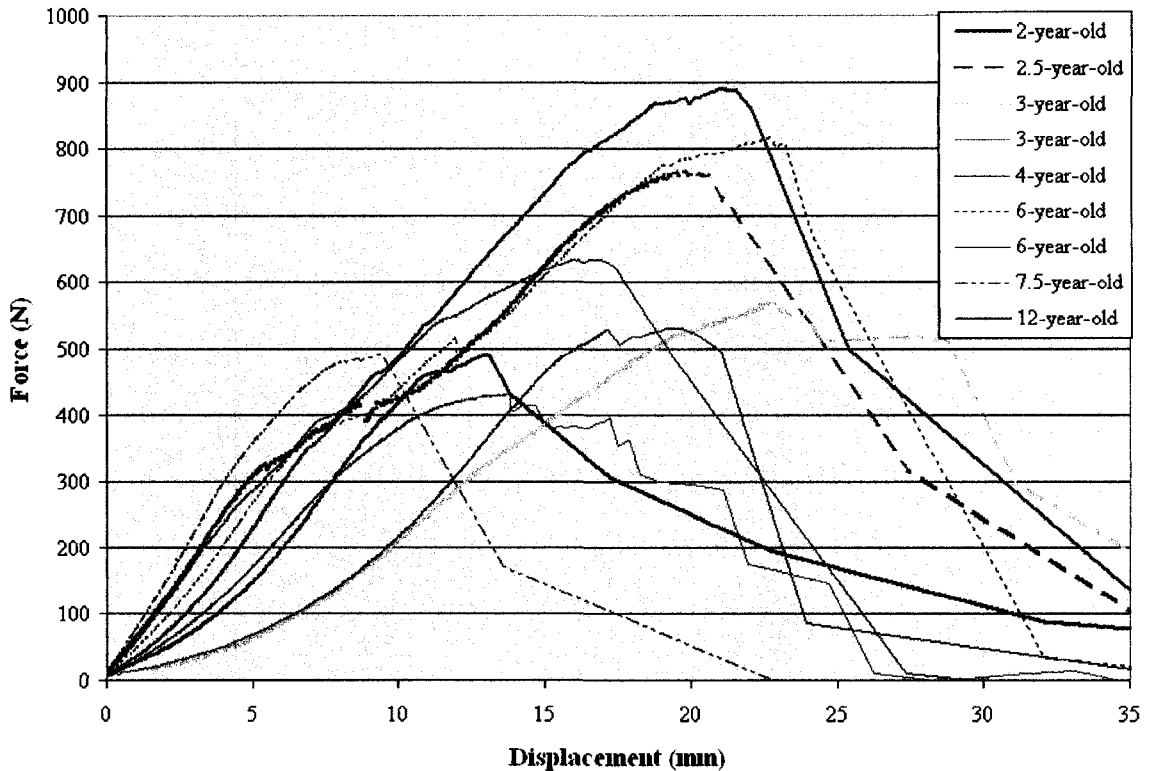


**Figure 2.23 Pediatric cadaver cervical load deflection curve, unfiltered data [8].**

The original source and copyright owner: LIPPINCOTT WILLIAMS & WILKINS.

There are some existing child cervical spine and head/neck FE models. One of them was created by Dupuis et al. in 2005 [10] using the anatomic geometric data from the neck of a three-year-old through CT scan and validated through a head/neck component sled tests based on the Q3 dummy. The sled test set up is illustrated in Figure 2.24. Figure 2.25 shows the physical model of the cervical spine and the finite element model of the head/neck complex based on the CT scan data of a 3-year-old child. This model was presented by Meyer et al. in 2006 with an updated version [54].

The FE model includes the head, seven cervical vertebrae C1-C7, the first thoracic vertebra T1, the intervertebral discs, and the principle ligaments. The material properties of this model were either adopted from the numbers available from literatures or scaled down from adults. The vertebrae were rigid, the ligaments were modeled using nonlinear material properties, and the intervertebral discs were scaled down from an adult model using elastic material properties.

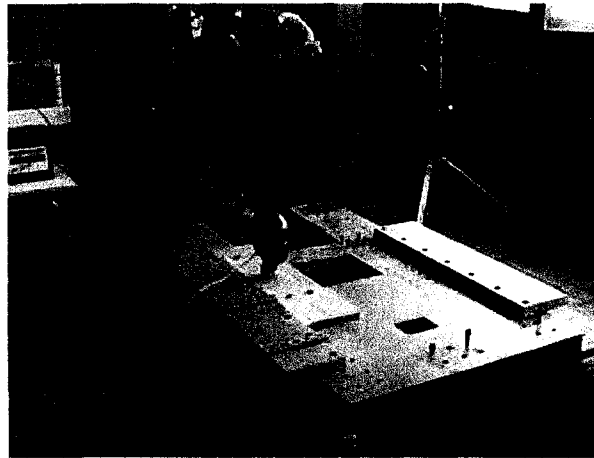


**Figure 2.24 Q3 dummy head/neck component sled test [10].**

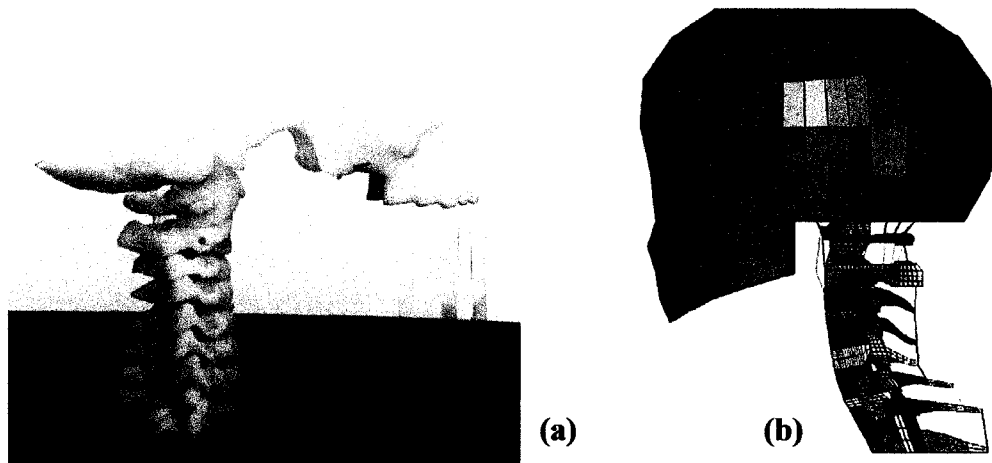


**Figure 2.25 (a) Physical model of the cervical spine based on CT scan of a three-year-old child including skull base (C0) and (b) Complete finite element model of the head and neck complex [10].**

Another study on the FE pediatric cervical spine which was presented by Kumaresan et al. in 2000 [11] [55] and in 2001 [30] involved building child cervical spine models (C4-C5-C6), as shown in Figure 2.27, using three different approaches to investigate the child neck biomechanical responses under various loading conditions:



- Approach 1: Geometrically scaled down from an adult human model (see Figure 2.26),
- Approach 2: Incorporated the local anatomic geometry and material properties of a three-year-old into the adult human model,
- Approach 3: Geometrically scaled down from an adult human model and incorporated the local anatomic geometry and material properties of a three-year-old.

Responses obtained using purely overall structural scaling, as defined in Approach 1, increased the flexibility slightly. By contrast, the inclusion of local component geometrical changes and material property changes to create the three individual pediatric cervical spine models, as defined in Approach 2, produced significantly higher changes in the flexibilities under all loading modes. When overall structural scaling effects were added to the three pediatric models, as defined in Approach 3, the increase was not considerably greater. The conclusion drawn from this research was that the flexibility of the cervical spine of a child was predominantly controlled by local anatomic geometry and material properties.

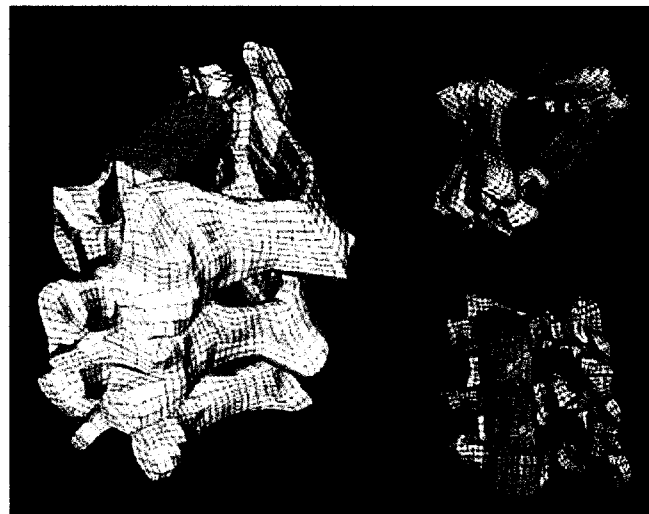


**Fig. 2.26 Different views of finite element mesh of ligamentous of adult C4–C5–C6 spine [30].**

It should be noted that the material properties of these models were not based on the data taken directly from pediatric test data. It is difficult to state that the biomechanical responses of these models actually reflect a real life child of the same age due to a lack of implementation of child biomechanical neck behaviour.

To improve a child model's kinematics and biofidelity to a 3-year-old, it is necessary to utilize first-hand pediatric data and clinical findings in developing child models. Therefore, the objective of the proposed research is to correlate biomechanical responses of the cervical spine of the child model with pediatric cadaver data from the subjects of head/neck complex specimens. The head kinematics and the neck injury potentials will be compared with a 3-year-old cadaver sled test in a frontal impact event and real cases of car crash accidents.

### 3. FOCUS OF RESEARCH

A human-like FE child model is a very useful tool in studying the biomechanical response and kinematics of a child in vehicle crashes and to predict the accompanying injuries. The child model developed at Nagoya University is one of the few child models. This model was scaled from an adult human model, THUMS, which was developed by a Toyota Research Laboratory. Though this child model was correlated with the Hybrid III 3-year-old child dummy and with data from some of the literature available during the time of its development, some of the body parts, such as the pelvis and the extremities, were modified based on child anatomy and biomechanics. Most of the body parts of this child model have not been validated directly with pediatric biomechanical data and clinic findings from crashes and/or sled tests.

The biofidelity of the neck of a child model is critical not only to the prediction of child neck injury but also to appropriately predict the kinematics and injuries of a child's head in a vehicle crash. The kinematics and the biomechanical response of a child's head and neck in vehicle frontal impact is mainly dependent on the tensile and extension/flexion bending stiffness of the neck. To the best of the author's knowledge, there exists only one study on pediatric cadaver component tests which was completed by Ouyang et al. in 2005 [8] with ten subjects of head/neck complexes from children aged 2 to 12 years old. This study provided pediatric data on the tensile and extension/flexion bending stiffness of the neck. Another pediatric cadaver test, which was carried out at University of Heidelberg under a sled test condition, provided information about the kinematics of children in frontal impact.

To utilize the invaluable pediatric data from the above mentioned two pediatric cadaver tests, this research focuses on:

1. A thorough comparison of the biomechanical response of the child head/neck FE model with pediatric cadaver head/neck complex tests;
2. Implementation of the biomechanical behaviour of representative samples from Ouyang et al. [8] through altered neck data from head/neck model into the child

model to improve its biofidelity and to more accurately predict child injury in a forward facing CRS during frontal impact crashes;

3. Comparison between predictions from the child model, utilizing the pediatric biomechanical neck behaviour, and results from child cadaver sled tests and cases of real world car crash accidents. This study will either prove or disprove the model's ability to better predict actual child responses in vehicle crash.

Due to the complexity of the child model, modifications to the model were conducted only on the ligaments, intervertebral discs, and facet joints of the cervical spine by adjusting the material properties in the range of elasticity. Alterations in the material behaviour of the cervical vertebrae were not considered in this research and should be included in future research. The musculature of a child's neck, which may be an important factor for the biomechanical response of a child in a vehicle crash, will also not be included in this research due to a lack of pediatric information.

## **4. CHILD HEAD/NECK COMPONENT MODEL DEVELOPMENT**

In this research a head/neck component model was first developed to simulate the pediatric cadaver head/neck complex tests by Ouyang et al. [8]. Further studies, incorporating the biomechanical response alterations of the child head/neck component model into the complete child model, will be considered in subsequent chapters.

### **4.1 Head/neck cadaver tests**

The pediatric cadaver tests used head/neck complexes from pediatric donors aged 2-12 years and were tested under the following loading conditions:

- Non-destructive flexion-extension bending;
- Non-destructive tensile step-and-hold test;
- Tensile distraction loading to failure.

The head/neck specimens consisted of the head, cervical spine (C1-C7) and thoracic spine (T1-T2) with the mandible and neck musculature removed for the purpose of improving the visualization of the cervical vertebrae. The T1 and T2 vertebrae were potted in polymethylmethacrylate prior to testing.

In the extension/flexion bending tests, the head/neck complexes were set in an inverted position and the skull was fixed level to the centre of mass (CG) of the head and a pure bending moment was applied to the T1-T2 vertebrae as shown in Figure 4.1(A)

In the tensile loading test, the thoracic vertebrae T1-T2 were fixed and the tensile load was applied at the centre of mass of the head in the vertical direction with freedom of anterior-posterior translation and rotation in the sagittal plane as shown in Figure 4.2 (A).

The numerical simulation models shown in Figure 4.1(B) and 4.2(B) will be presented in the following sections.

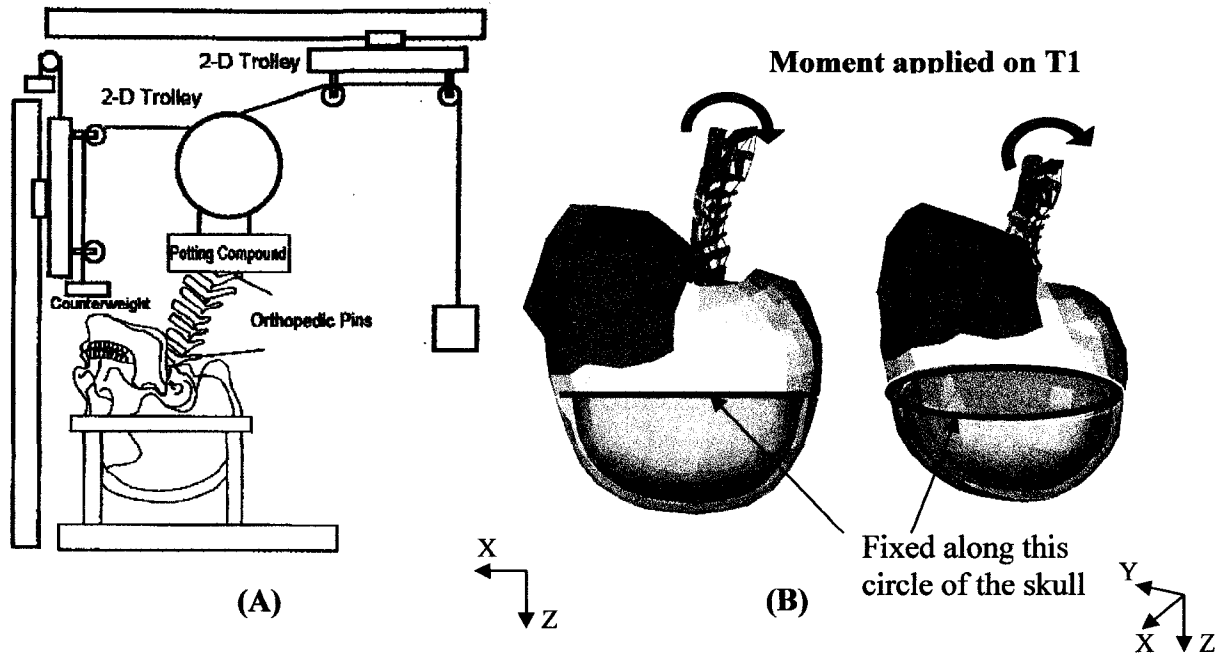


**Figure 4.1 Pediatric cadaver test and CAE simulation set-ups under bending load condition: (A) Cadaver bending test** (The original source and copyright owner: LIPPINCOTT WILLIAMS & WILKINS) **and (B) FE simulation set-up**

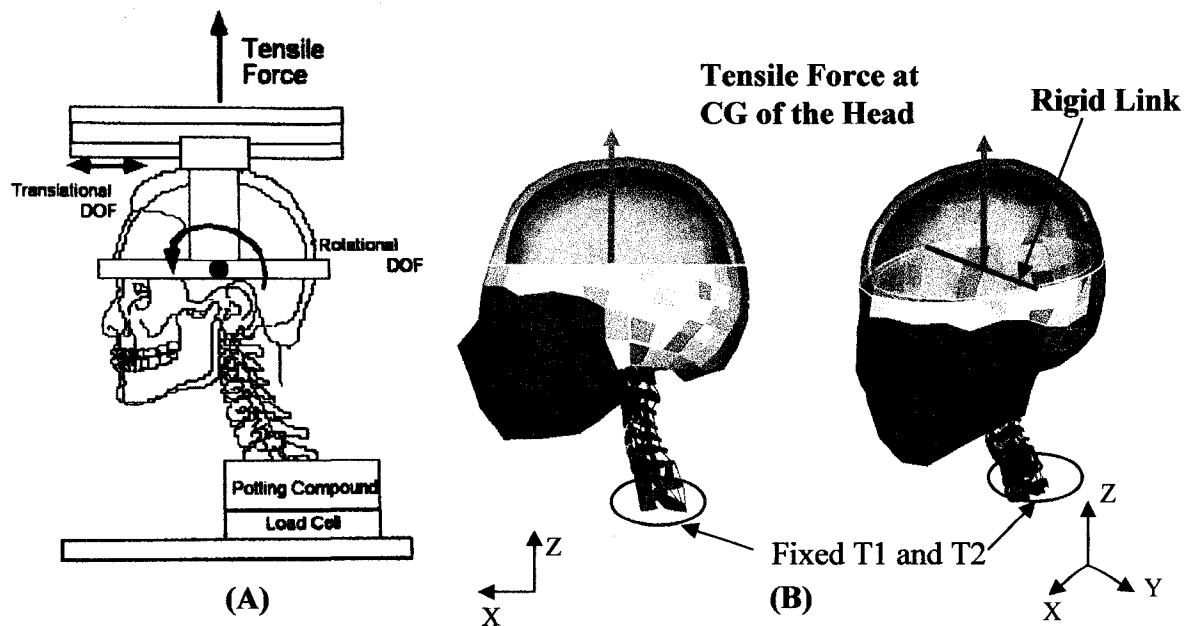


**Figure 4.2 Pediatric cadaver test and CAE simulation set-ups under tensile load condition: (A) Cadaver Tensile test** (The original source and copyright owner: LIPPINCOTT WILLIAMS & WILKINS) **and (B) FE simulation set-up.**

## 4.2 Head/neck component model development

### 4.2.1 From child model to head/neck component model

The base head/neck component model was developed by isolating the head, cervical spine and thoracic spine above T3 from the whole child model as shown in Figure 4.3. Figure 4.3 (B) illustrates the head/neck component model. This model contained all ligaments, intervertebral discs and facet joints above T1, and all other soft tissues including musculatures were removed in compliance with the pediatric cadaver head/neck complex test setup. The mandible, however, remained in the head/neck model (see Figure 4.3 (C)). In FE simulation this would not cause any visualization problems as would be experienced in the physical cadaver test. The contact interfaces and connections between the mandible and the cervical spine were carefully removed from the model, ensuring that the mandible's presence would not affect the simulation results. However, there was a contact interface between two adjacent vertebrae which was defined using a static coefficient of friction  $FS = 0.1$ , a dynamic coefficient of friction  $FD = 0.1$ , and a viscous damping coefficient  $VDC = 20$ .

This head/neck component model contained 6187 nodes, 9447 elements, and 152 parts.

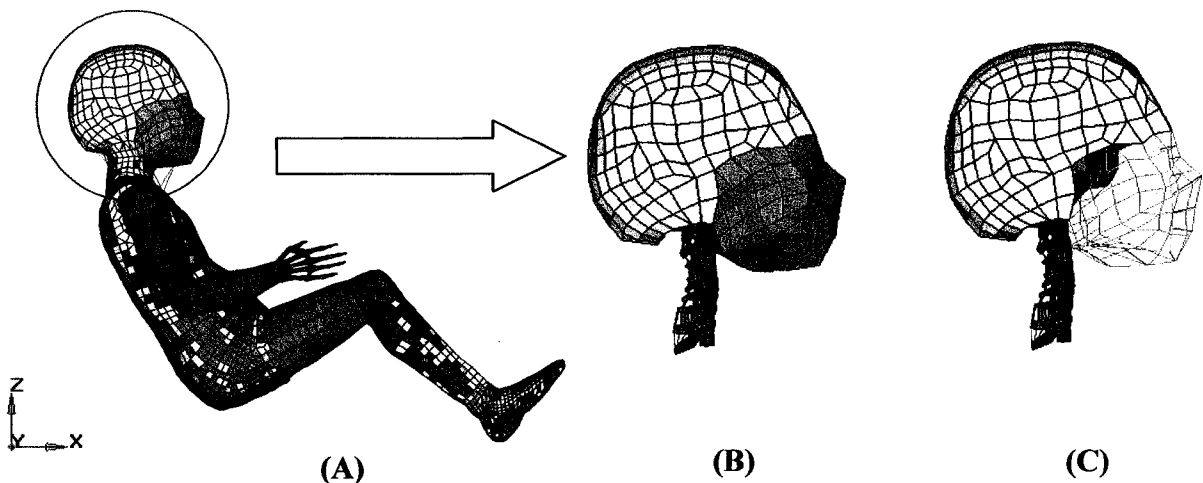
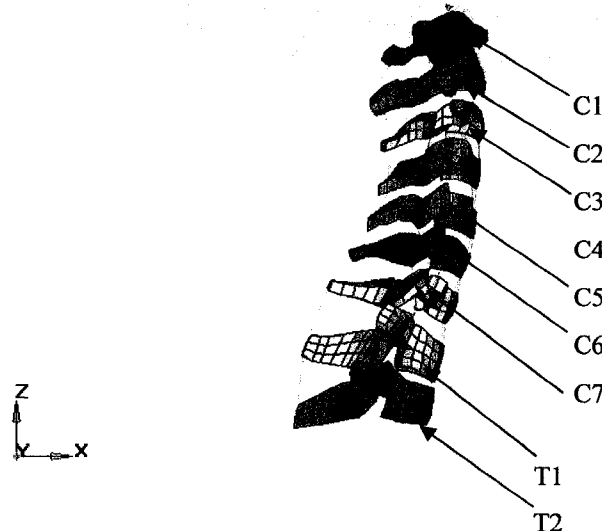


Figure 4.3 Head/neck component model developments: (A) child model, (B) and (C) isolated head/neck component model

Figure 4.4 illustrates the enlarged view of the cervical spine (C1 to C7) and a part of the thoracic spine (T1 to T2). All cervical vertebrae (C1-C7) and the two thoracic vertebrae T1 and T2 were modeled using solid elements and rigid material properties.



**Figure 4.4 Enlarged view of cervical spine (C1-C7) and partial thoracic spine (T1 to T2).**

Figure 4.5 shows groupings of soft tissues including ligaments, facet joints, and intervertebral discs. All of these soft tissues were modeled using elastic material properties in the child head/neck component model and in the child model. Ligaments of the cervical spine are divided into three groups, namely ligament 1, ligament 2 and ligament 3. Ligament 1, including interspinous ligaments (ISL), ligamentum flava (LF), anterior longitudinal ligaments (ALL), and posterior longitudinal ligaments (PLL), were modeled using membrane elements and fabric material with elastic modulus  $E = 150.8$  MPa. Both ALL and PLL are located around the intervertebral discs. Ligament 2 consisted of ligamentum flava between C7 and T1 and the posterior atlanto-occipital membrane, which used shell elements and elastic material ( $E = 15.08$  MPa); Ligament 3 contained only interspinous ligaments (ISL) between cervical vertebrae C2 and C3 and was modeled using membrane elements and fabric material ( $E = 75.4$  MPa). Solid



elements and elastic material ( $E = 0.84$  MPa) were used for modeling the facet joints between two adjacent vertebrae. Intervertebral discs consisted of nucleus pulposus and annulus fibrosus. Both nucleus pulposus and annulus fibrosus were modeled using solid elements and elastic material ( $E = 44.3$  MPa), and on the outer surface of these two portions of the disc there were seatbelt elements used as fiber that connect adjacent vertebrae.

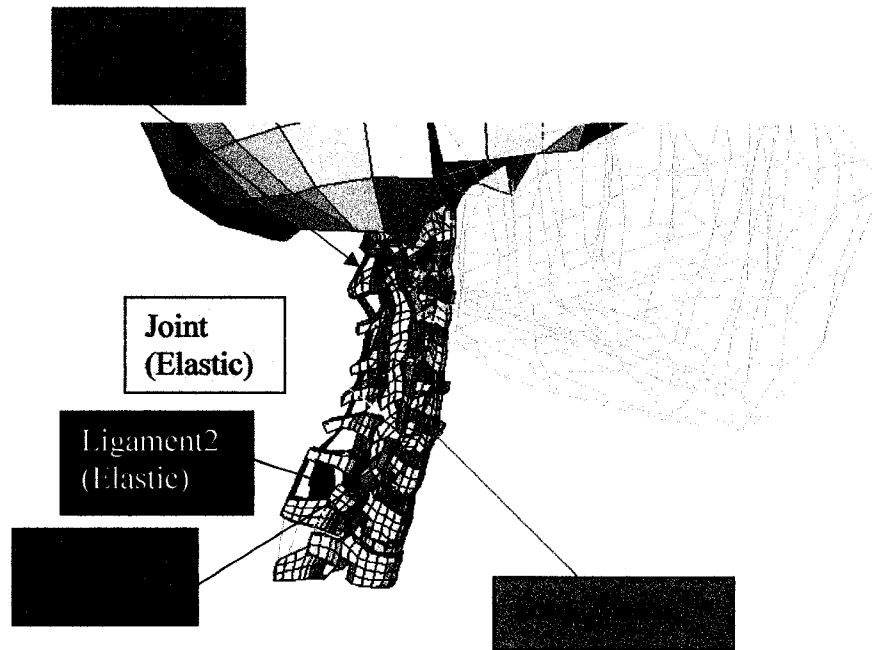


**Figure 4.5 Regions of soft tissue components in terms of different material properties.**

#### **4.2.2 Loading and Boundary Conditions**

According to the loading and boundary conditions of the pediatric cadaver head/neck complex tests there were, in total, three head/neck component models created for (i) tensile distraction, (ii) bending extension, and (iii) bending flexion. The loading procedures were in compliance with pediatric cadaver head/neck complex tests as detailed in the subsequent sections.

#### **4.2.2.1 Extension/flexion bending loading conditions**

The constraints of the two models for both bending extension and bending flexion were applied identically based on the description of boundary conditions in the cadaver head/neck complex tests in section 4.1. The nodes around the circumference of the skull at the level of the centre of mass of the head were fixed in all six directions, three translations and three rotations in/around the X, Y and Z axes. A pure moment was directly applied to T1 vertebra (rigid body) in the sagittal plane (X-Z plane) as shown in Figure 4.1 (B). The maximum absolute values of pure moments applied to the neck were -2.4 N·m for extension and 2.4 N·m for flexion within 100 ms. The magnitudes of the applied moment for both loading cases were the same as in the cadaver tests. The specimens were tested under a quasi-static loading condition. With the loading speed as indicated above, no significant dynamic effect was observed in the simulation predictions.

#### **4.2.2.2 Tensile loading condition**

The constraint for the head/neck component model under tensile distraction loading condition consists of totally fixed T1 and T2 vertebrae and free anterior-posterior translation and rotation in the sagittal plane of the head as shown in Figure 4.2(B). The quasi-static tensile loading was applied at a speed of 50 cm/s at the centre of mass of the head.

#### **4.2.3 Basic model simulation setup**

The three head/neck component models created so far were used as base models (referenced as Tensile\_Base, Extension\_Base and Flexion\_Base) as no material alterations were performed on any parts within the models. Table 4.1 shows a matrix of head/neck component models with associated simulations under different loading conditions. The head/neck component models with material alterations of the neck soft

tissues, including ligaments, facet joints, and intervertebral discs, shown in the table were discussed in chapter 5.

In the cadaver tests, the T1 and T2 vertebrae were positioned at an angle of 21 degrees to the horizontal to maintain the natural cervical lordosis. To match the pediatric cadaver test conditions the model was tilted forward by 10 degrees in the sagittal plane as shown in Figure 4.6. LS-DYNA version 970 revisions 5434a with double precision [57] was used for explicit analysis during the simulations. Bending extension/flexion loading cases ran for 100 ms while tensile loading cases ran for 40 ms.

To record normal sectional forces at the upper and lower cervical spine, three cross sections were defined separately at cervical spine C2-C3 for the upper neck and at C6-C7 for the lower spine (See Figure 4.7). For the upper neck one cross section contained all ligaments and joint parts while another contained only the disc. The cross section of the lower neck included all ligaments, facet joints, and intervertebral discs between C6 and C7. The disc fibre defined using seatbelt elements were eliminated from the definitions of both cross sections as it caused fluctuations in the simulation results.

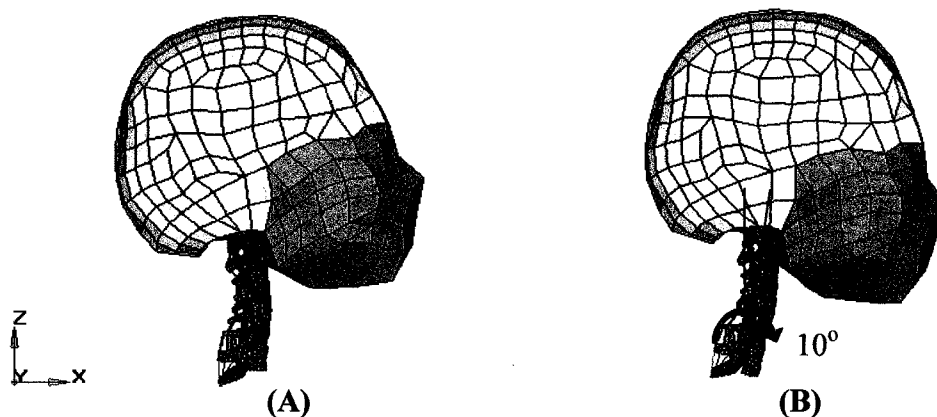


**Figure 4.6 Adjustment for the head/neck component model:  
(A) before tilted and (B) after tilted.**

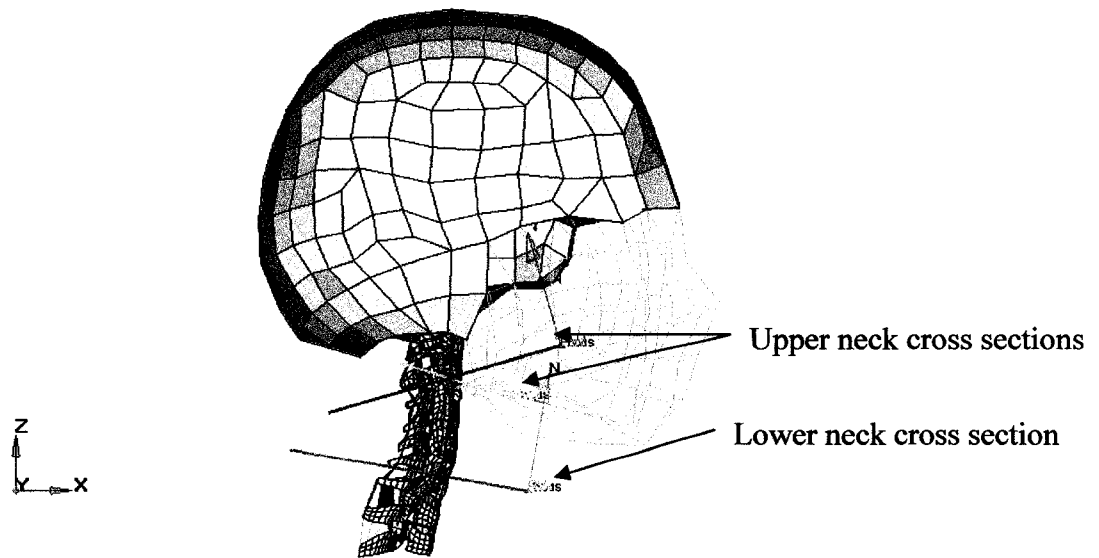


**Figure 4.7 Upper and lower neck cross section definitions.**

**Table 4.1 Matrix of head/neck component models under different loading conditions.**

Model	Tensile Loading	Bending Extension	Bending Flexion	Altered Neck
Tensile_Base	<b>X</b>			
Extension_Base		<b>X</b>		
Flexion_Base			<b>X</b>	
Tensile_A	<b>X</b>			<b>X</b>
Extension_A		<b>X</b>		<b>X</b>
Flexion_A			<b>X</b>	<b>X</b>

#### **4.3 Data extraction of the head/neck simulation model**

In the pediatric cadaver head/neck complex tensile test, a multi-axial load cell in a polling compound under thoracic vertebrae T1 and T2 was used for the measurement of the neck tensile force while a displacement transducer on the skull was used to record the

head displacement. The force/displacement curves from the tests of the subjects of different ages were compared as shown in Figure 2.24. To compare the simulation results with the pediatric cadaver head/neck complex tests, the curve of displacement versus time was first created using the time history data from a pre-defined node at the centre of mass of the head. Then, the normal section force was extracted from the recorded time history data. The neck force versus displacement curve was obtained by cross plotting the two time history responses from the numerical simulations.

In the pediatric cadaver head/neck complex bending test a protractor measured the absolute T2 rotation at each loading step. The neck rotation/moment response predicted from simulation was developed by cross plotting the angular rotation time history of the T2 vertebra, being a rigid body, with the applied bending moment.

## **5. COMPARISON OF HEAD/NECK MODEL WITH PEDIATRIC DATA**

In Ouyang's research, ten pediatric cadaver head/neck complex tests were conducted. Test data from subjects aged 2 to 7.5 years (9 for bending and 8 for tensile) was used for the comparison. The pediatric cervical spine within this age range exhibited similar biomechanical conditions, but the anatomic differences between the pediatric and adult cervical spine are prominent until approximately 8 years of age. From ages 8 to 12 there is a transitional period and after age 12, the cervical spine is almost fully developed and is comparable to that of an adult [32].

It was noticed that one of the test subjects (aged 5 years) was invalid for tensile test comparison as damage to the specimen resulted. In order to perform a comparison with the pediatric cadaver test data, two groups of simulation models were developed. Within the first group, three base head/neck component models, Tensile\_Base, Extension\_Base and Flexion\_Base, were developed and used to simulate tensile distraction, bending extension, and bending flexion, respectively. These models were developed for comparison with the pediatric cadaver head/neck complex tests as an initial evaluation of the CAE models. The second group consisted of three head/neck component models with altered neck materials (referred to as Tensile\_A, Extension\_A and Flexion\_A as indicated in Table 4.1) which were created using the base models to compare the pediatric cadaver head/neck complex tests by adjusting the material properties of the cervical spine in terms of the energy and stiffness distribution of the parts in the neck region. Details about the material adjustments of the cervical spine are described in section 5.2.

### **5.1 Comparison of the base model and the cadaver head/neck complex test**

#### **5.1.1 Tensile loading condition**

Under tensile loading conditions, without any alterations in the material properties of the parts of the head/neck component model, the maximum sectional force sustained by the cervical spine was 4656 N when the skull displacement reached approximately

20 mm. The stiffness was 232.8 N/mm while the average tensile stiffness from pediatric test data was 35.2 N/mm. Figure 5.1 illustrates the load/skull displacement for the pediatric tests and base simulation models. Using linear regression, the stiffness of the head/neck component model was observed to be approximately 6.6 times greater than the pediatric cadaver finding. This outcome was expected as the FE model of the whole neck was scaled down geometrically from an adult human model (THUMS) and the cervical vertebrae were modeled using rigid material properties while the ossification process during the development of the pediatric cervical spine was not taken into account. Although the material properties of the ligament, facet joints, and intervertebral discs were modified based on the data of available literature and the flexion of the neck in the child model was compared with the corridor of the Hybrid III 3-year-old dummy, the current child model exhibits a stiff tensile neck response relative to pediatric biomechanical behaviour.

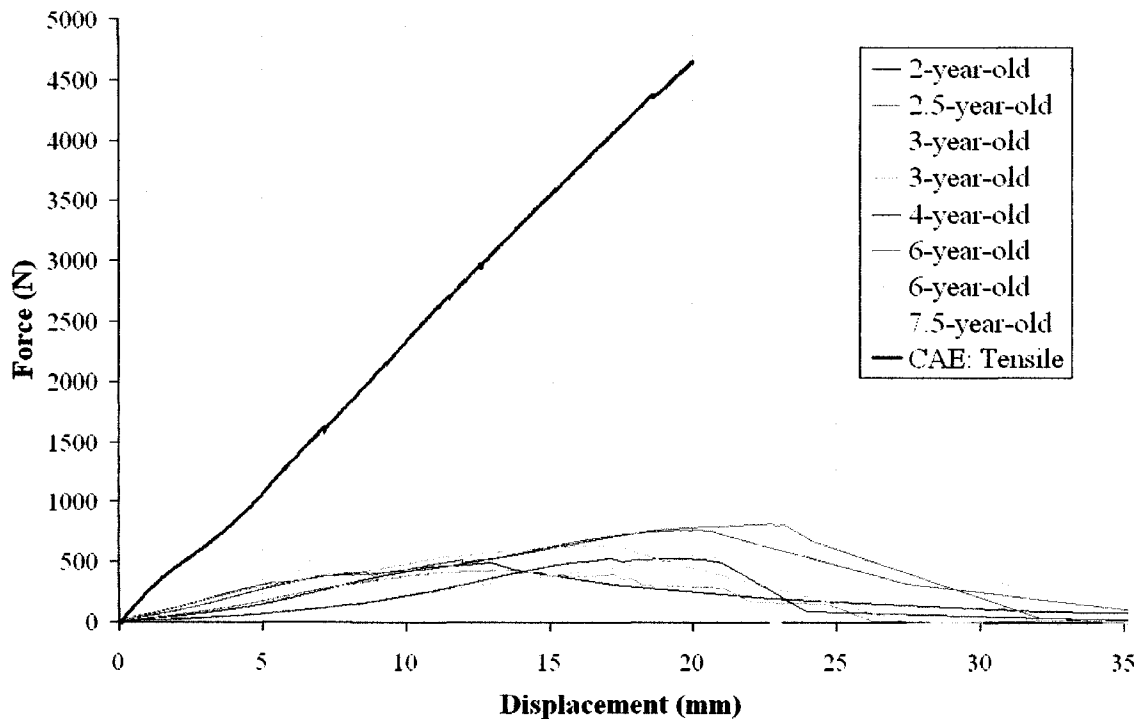


**Figure 5.1 Load/deflection response of the head/neck base model simulation and pediatric cadaver head/neck complex tests of 8 specimens aged 2 to 7.5 years.**

### 5.1.2 Extension/flexion bending condition

Figure 5.2 illustrates the rotation versus bending load curve of the cervical spine. Angular displacement which was measured at T2 was consistent with the experimental testing procedure. The extension and flexion loading behaviour was basically linear while the pediatric cadaver head/neck complex test data generally varied in a nonlinear fashion. From these findings it is observed that the cervical spine in the base head/neck component model was stiff relative to pediatric biomechanical behaviour. The mean bending stiffness of the pediatric neck was 0.041 N·m/degree while the maximum bending stiffness of the neck in the base head/neck component model was 0.189 N·m/degree.

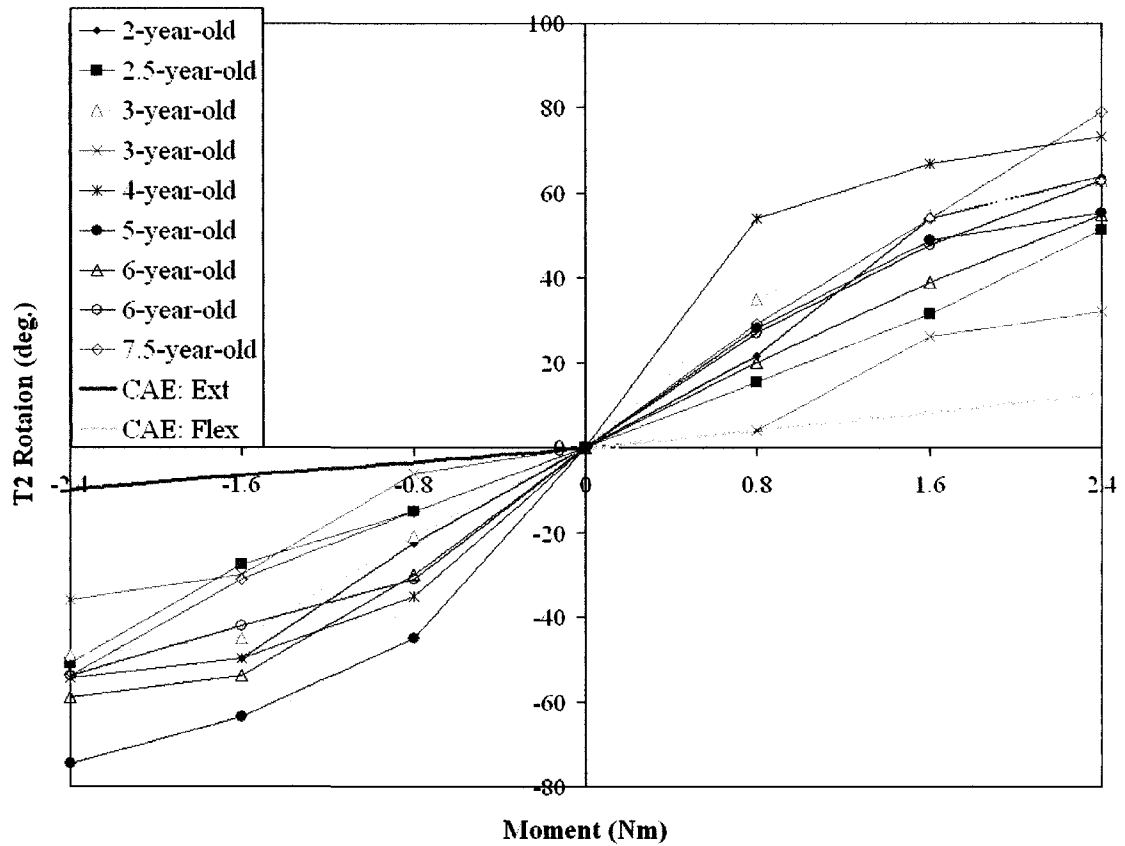


**Figure 5.2 Neck's moment-rotation range (T2) comparison of head/neck base model simulation and pediatric cadaver head/neck complex tests of 9 specimens aged 2 to 7.5 years.**



## **5.2 Parametric Study**

Many factors influence the neck tensile and rotational stiffnesses. The following two sections present studies in terms of the energy absorption and stiffness distribution of the materials within the child FE head/neck component model.

### **5.2.1 Energy absorption in the cervical spine**

Since child cervical spine injuries usually occur in the vicinity of the atlas to C3 and in the vicinity of C5 to C7, the energy absorption by the ligaments, joints and discs in these areas were assessed. Appendix C illustrates the time history of the strain energy for the parts identified in the regions of interest. The most effective parts in terms of energy absorption (greater than 0.5 J) were identified within the C2-C3 area to be the annulus fibrosus (AF), interspinous ligaments (ISL), anterior longitudinal ligaments (ALL) and posterior longitudinal ligaments (PLL). Additionally, within the C6-C7 area the annulus fibrosus, ligamentum flavum (LF), anterior longitudinal ligament and posterior longitudinal ligament dominated the strain energy. Figure 5.3 illustrates a subset of data within Appendix C illustrating the strain energy as a function of time in the tensile simulation.

Strain energy for parts in the bending simulation illustrated no significant contribution. It was believed this may be a result of contact occurring between the cervical vertebrae. Material behaviour alteration was based upon parts which illustrated significant energy contributions.

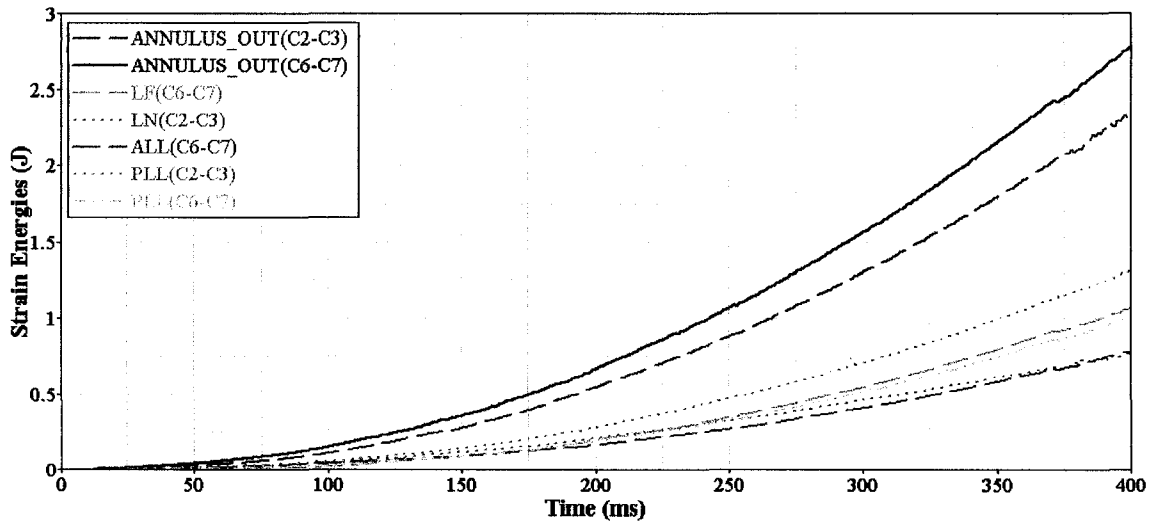


**Figure 5.3 Energy-time curves of the most effective ligaments for energy absorption in the vicinities of C2-C3 and C6-C7 of the cervical spine under tensile loading condition.**

### 5.2.2 Altering the material properties

Kumaresan et al. [11] showed that the biomechanical response is mostly influenced by changes in the local geometry and the material properties of the pediatric cervical spine and that it is very important to consider the developmental anatomical features in pediatric structures to better predict their biomechanical behaviour. To improve the neck biofidelity in the current child model, this study focused only on material property alterations.

Based on the energy and stiffness distributions, the elastic modulus of the ligaments, facet joints, and intervertebral discs of the cervical spine were altered through comparisons of numerical simulation predictions with the pediatric cadaver head/neck complex test data in a trial and error process. A uniform reduction scale factor of 1/10 as a final choice applied to scale down all ligaments or other soft tissues of the cervical spine except the facet joints which utilized a scale factor of 1/4 throughout the parametric study as its stiffness contribution was relatively low compared to that of other parts of the region. During the material behaviour alteration analysis, it was observed that the interspinous ligament (ISL) had a significant influence on the moment/angular

displacement response during flexion. Additionally it was found that the annulus fibrosus (AF) of the intervertebral discs, anterior longitudinal ligament (ALL) and posterior longitudinal ligament (PLL) strongly influenced rotational deformation under extension. In order to balance the extension/flexion stiffness of the cervical spine, the reduction in the elastic modulus factor (1/8) of interspinous ligaments (ISL) was more than that of the annulus fibrosus (AF), anterior longitudinal ligaments (ALL) and posterior longitudinal ligaments (PLL) with the exception of the facet joints. Figure 5.4 shows regions of soft tissue components with different material definitions (fabric for membrane element or elastic for shell or solid element). Both of them used elastic material properties.

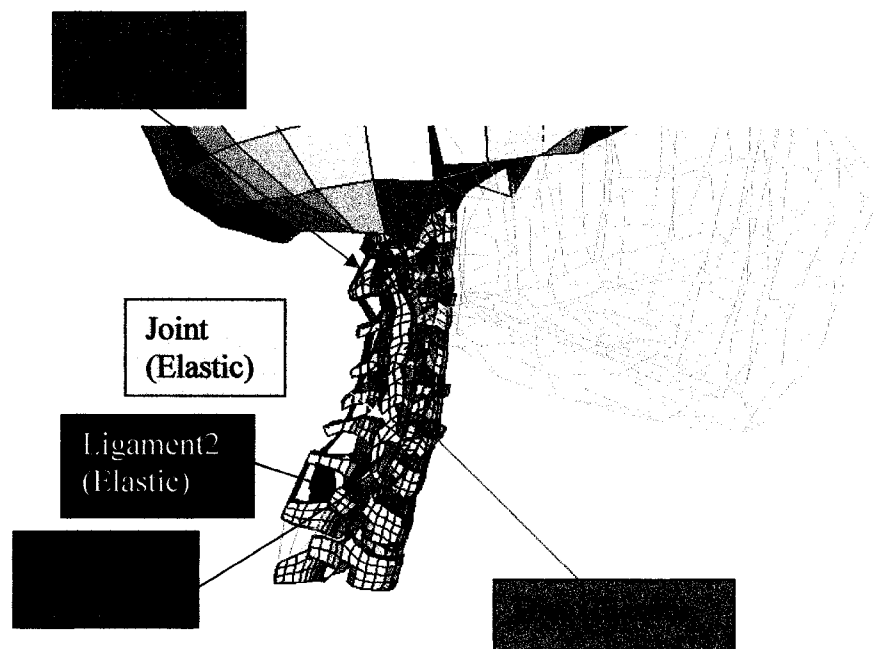


**Figure 5.4 Groups of soft tissue components in terms of different material properties (elastic modulus).**

Figures 5.5 and 5.6 illustrate some of the intermediate simulation results with comparisons of neck force-distraction and moment-flexion/extension time histories with the child cadaver head/neck complex tests in the trial and error process of this research. It was found that there was clear trend that the maximum neck force decreased with deductions of elastic moduli of the neck soft tissues. Table 5.1 shows the original elastic

moduli ( $E$ ) and final reduction factors selected after several times of trial and error. The final defined elastic moduli for the material properties were applied in all three head/neck component models. Comparisons of the simulation results with the pediatric cadaver head/neck complex tests will be presented in section 5.3.

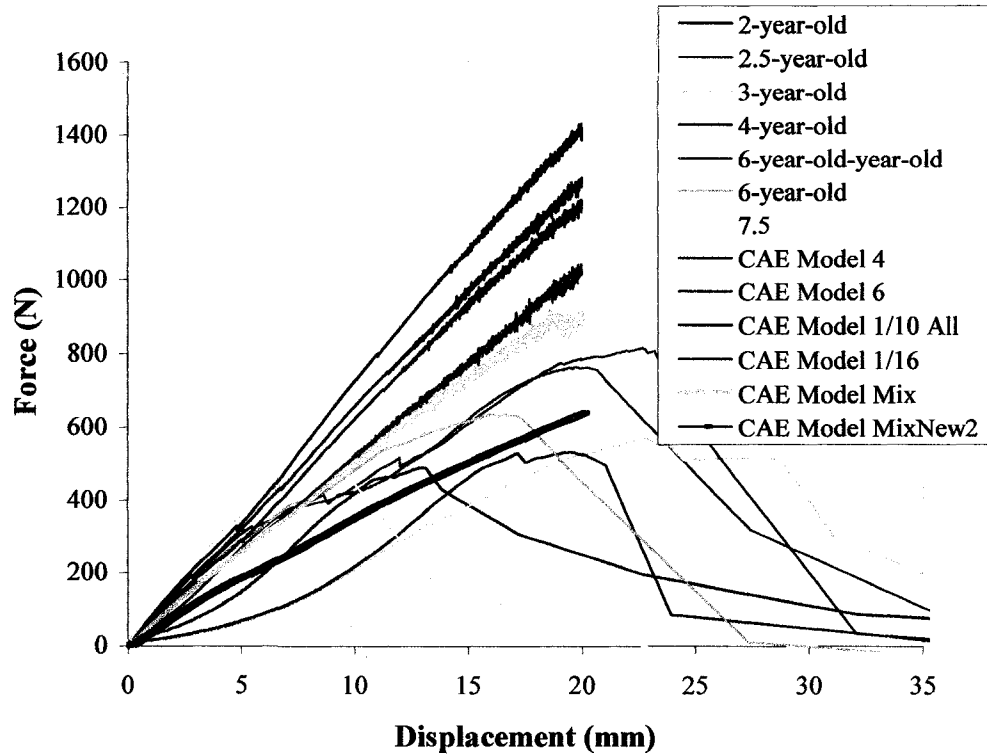


**Figure 5.5 Force-deflection curve comparison of some head/neck altered model simulations and pediatric cadaver tests of specimens aged 2 to 7.5 years.**

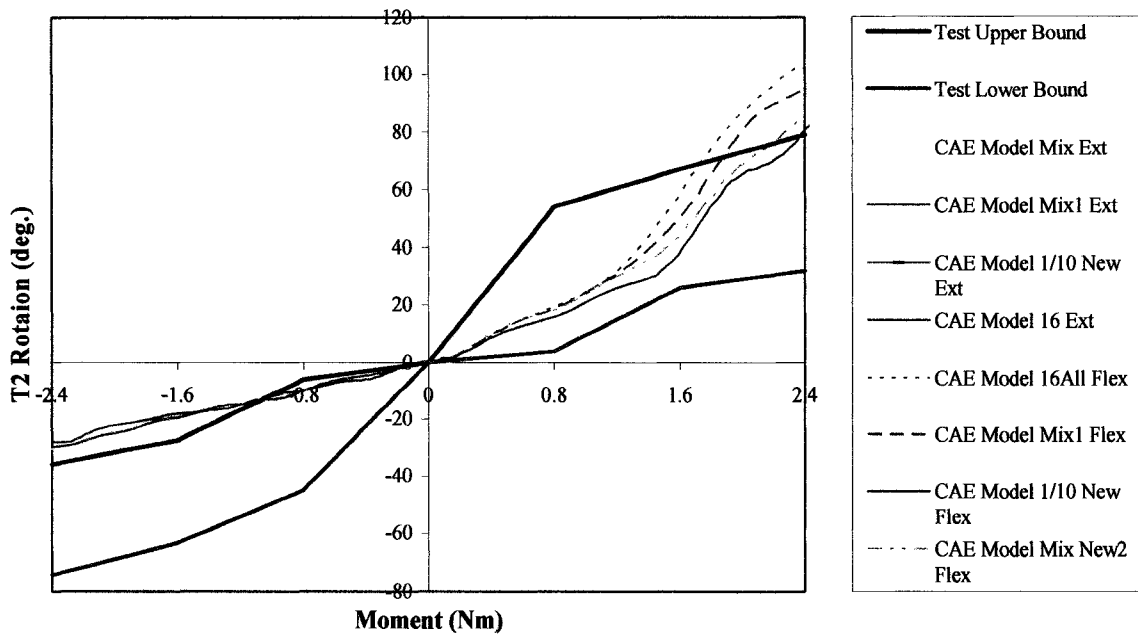


**Figure 5.6 Moment-flexion/extension curve comparison of some head/neck altered model simulations and upper and lower bounds of pediatric cadaver head/neck complex tests.**

**Table 5.1 Cervical spine material property alternations.**

Model	Material Property ( <i>elastic modulus</i> ) Scale Factor						Comments
	Ligament1 (Fabric)	Joint (Elastic)	Disc (Elastic)	Ligament2 (Elastic)	Ligament3 (Fabric)	Disc Fiber	
<b>Model 1 (Base1)</b>	1.0 <i>E=150.8MPa</i>	1.0 <i>E=0.84 MPa</i>	1.0 <i>E=44.3 MPa</i>	1.0 <i>E=15.08 MPa</i>	1.0 <i>E=75.4 MPa</i>	1.0	Tensile
<b>Model 2</b>	1/8-1/10	1/4	1/10	1/10	1/8	1/10	Tensile w/o disc fiber
<b>Model 3</b>	1/8-1/10	1/4	1/10	1/10	1/8	1/10	Tensile w/ disc fiber
<b>Model 4 (Base2)</b>	1.0	1.0	1.0	1.0	1.0	1.0	Bending Extension
<b>Model 5 (Base2)</b>	1.0	1.0	1.0	1.0	1.0	1.0	Bending Flexion
<b>Model 6</b>	1/8-1/10	1/4	1/10	1/8-1/10	1/8	1/10	Bending Extension
<b>Model 7</b>	1/8-1/10	1/4	1/10	1/8-1/10	1/8	1/10	Bending Flexion

Note: *E* - elastic modulus; Ligament1 - LF, ISL, ALL and PLL; Joint - facet joint (cartilage); Disc-AF; Ligament2 - posterior atlanto-occipital membrane; LF(C7-T1); Ligament3 - ISL(C2-C3)

### 5.3 Comparison of altered head/neck model with cadaver head/neck complex tests

#### 5.3.1 Tensile loading condition

Under tensile loading, the stiffness of the cervical spine in the model after neck alterations was observed to be in the range of the pediatric cadaver head/neck complex tests of eight 2 to 7.5 year old samples, with an average stiffness of 35.26 N/mm. As Figure 5.7 illustrates, the numerical predictions of the force-displacement curve corresponded to the estimated average corridor of the pediatric cadaver head/neck complex tests before the neck deformation reached 10 mm and remained close to the upper bound afterwards. The disc fibre that was modeled using one dimensional seatbelt elements in the cross section definition caused significant fluctuations in the simulation force-displacement observations. From this study it has been found that the ligament and intervertebral discs predominantly control the tensile stiffness of the cervical spine while the tensile deformation of the neck is less affected by the cervical vertebrae.

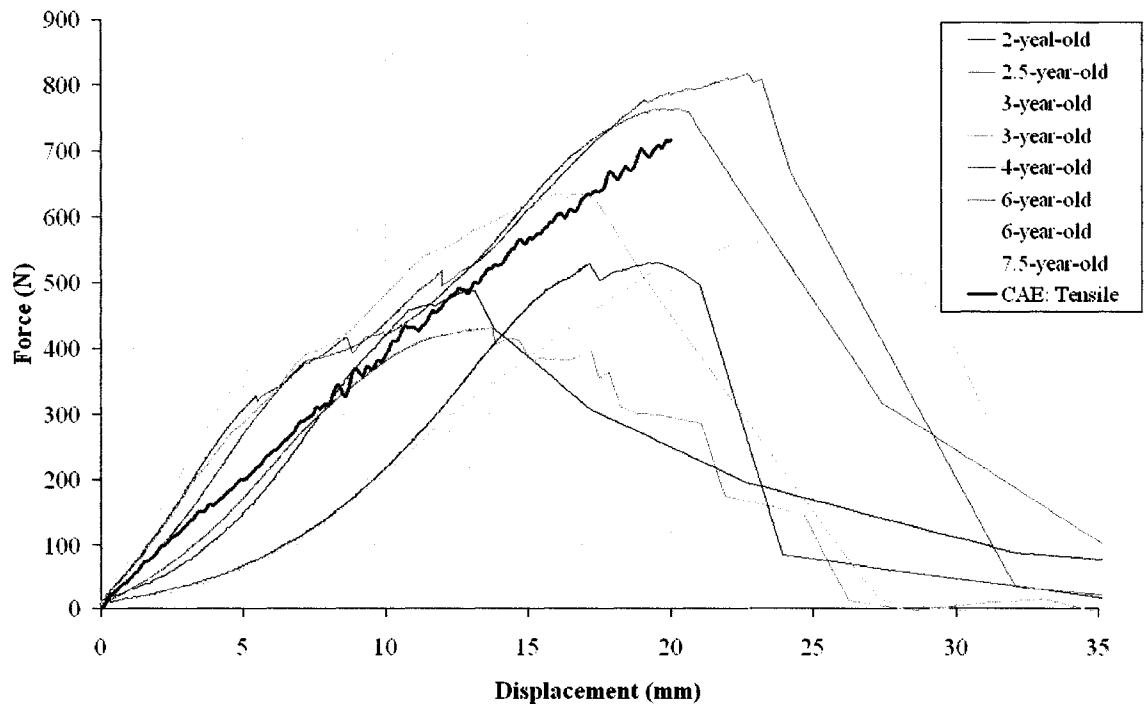


**Figure 5.7 Load-deflection curve comparison of head/neck altered model simulation and pediatric cadaver tests of 8 specimens aged 2 to 7.5 years.**

### 5.3.2 Extension/flexion bending condition

The rotational stiffness of the cervical spine under extension/flexion bending conditions was sensitive to the changes to the material properties of the ligaments while the sensitivity to changes of intervertebral discs was only within a certain range which the scale factor changed to be approximately between 1/16 and 1/8. Figure 5.8 shows the comparison between the rotation time histories from the pediatric cadaver head/neck complex tests and from the head/neck component model simulations that have implemented the altered material characteristics. In this figure, the vertical axis represents the rotation deformation of the neck at T2 relative to the head at the level of the centre of mass where the constraint was applied, and the horizontal axis represents the extension (to the left hand side of the vertical axis) and flexion (to the right hand side of the vertical axis) moment applied to T2 of the head/neck component model.

When the head/neck component model was subjected to extension, the rotation-moment curve fell in the corridor of the pediatric cadaver head/neck complex tests with the moment less than 0.8 N·m. An increase in the applied moment (greater than 0.8 N·m) caused the extension stiffness of the cervical spine to be higher than the pediatric cadaver head/neck complex tests suggested. In the moment range of 0.8 N·m to 2.4 N·m the rotation-moment curve, however, was considered to have a good agreement with the corridor of the pediatric cadaver head/neck complex tests.

Under the applied flexion moment load, the head/neck component model showed a better agreement with the pediatric cadaver had/neck complex tests in rotation deformation. The rotation-moment curve fell inside the corridor of the pediatric cadaver head/neck complex tests. In Figure 5.8, the FE prediction of the flexion/rotation response was somewhat stiffer in the applied moment ranging from 0 N·m and 1.6 N·m, and tended to be softer after the moment reached approximately 1.6 N·m. The simulation illustrates a shear deformation between cervical vertebra C1 and C2 when the flexion moment approached 1.6 N·m, causing the flexion rotation stiffness reduction. This might be a result of the rigid material properties currently used for the cervical vertebrae since the immaturity of the pediatric spine and its ossification process are among the major influencing factors of the biomechanical response of the pediatric cervical spine.

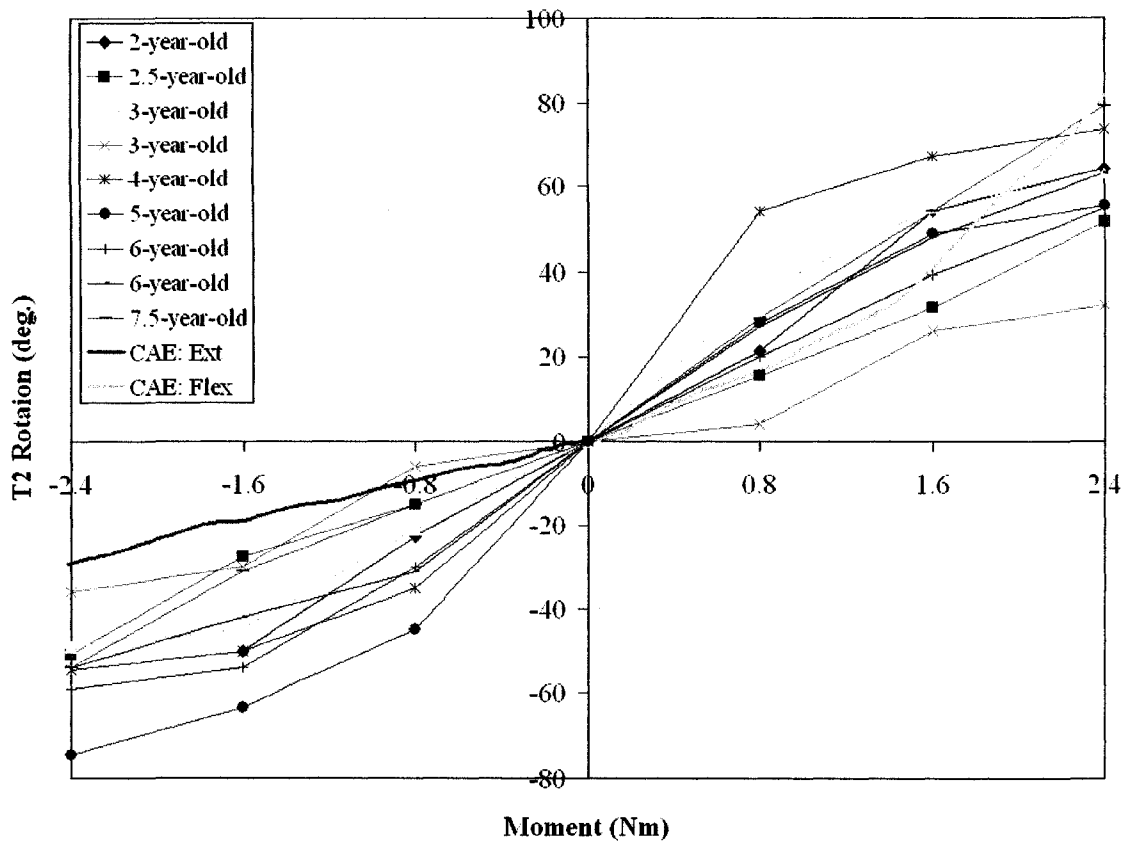


**Figure 5.8 Neck's moment-rotation range (T2) comparison of altered head/neck component model simulation and pediatric cadaver tests 9 specimens aged 2 to 7.5 years.**

In comparing the head/neck model simulations before and after alteration of the material properties of the cervical spine, significant improvement of the neck biomechanical response was observed. The tensile stiffness and the extension/flexion rotation stiffness illustrated a good agreement with results of pediatric cadaver head/neck complex tests after the alteration of the soft tissue material properties.



## **6. IMPLEMENTATION OF CHILD BIOMECHANICAL NECK BEHAVIOUR INTO THE CHILD MODEL**

The objective of this research is to improve the biofidelity of the child model and to increase the accuracy of predictions of child injury in frontal vehicle crash. The biofidelity of the neck in a child FE model is very important as it affects the kinematics of the whole child model in the simulations and the accuracy of the child injury predictions. The altered material properties of the cervical spine in the head/neck component model were obtained based on comparisons with the pediatric cadaver tests by Ouyang et al. [8] as presented previously in chapters 4 and 5. Implementation of the altered neck data into the child model will be presented in this chapter. A comparison of the simulation results before and after the implementation of the altered neck data will be discussed in chapter 7. Simulations using the child model were conducted under two different crash test conditions, namely, a FMVSS 213 frontal impact sled test condition and a cadaver frontal impact sled test condition.

### **6.1 FMVSS 213 sled simulation with the child model**

The simulation model consists of the child model, a five-point forward facing child restraint system, and a FMVSS 213 bench seat. The setup was in accordance with FMVSS 213 requirements.

The acceleration pulse utilized in the FMVSS 213 sled test simulation was obtained from testing completed by Turchi et al. [42]. During this test, the sled was accelerated towards a fixed seismic mass using pneumatic pressure with an impact velocity of 41.7 km/h (25.9 mph). The acceleration pulse experienced by the sled during the impact was controlled by a hydraulic damper at the front of the sled. The acceleration pulse which the sled experienced in a direction opposite to the impact velocity and the lower and upper limits of sled acceleration outlined in FMVSS 213 are illustrated in Figure 6.1. This acceleration pulse was applied in the numerical simulations in this research.

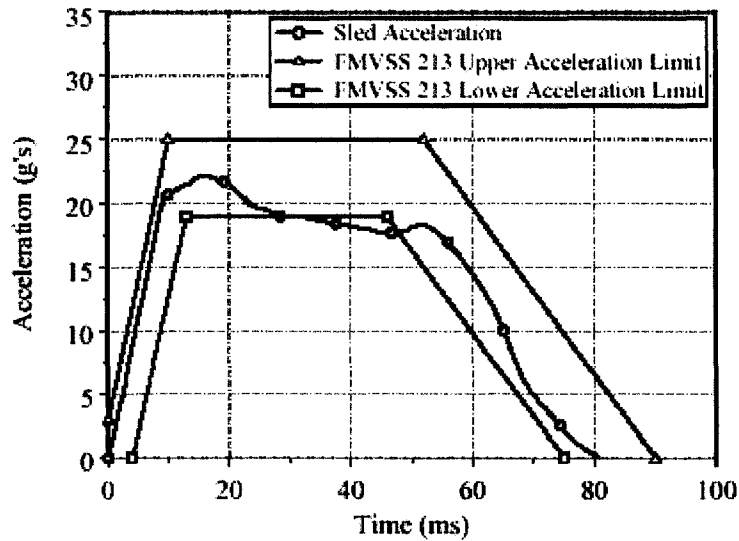


**Figure 6.1. Upper and lower FMVSS 213 acceleration/time responses and the actual test acceleration /time response [41].**

Reprinted with permission from SAE Paper # 2006-01-1141 © 2006 SAE International.

### 6.1.1 Child model

The 3-year-old child model presented by Mizuno et al. in 2005 [6] and 2006 [7] was developed to investigate injuries to various body regions of a child and to provide information that can be difficult to obtain from crash test dummies. Responses of this child FE model were compared to the response-based scaling corridor of a 3-year-old. The mass of the 3-year-old child model is 16.6 kg and the stature height is approximately 99.5 cm.

The dimensions of each body region of the child model were based upon the anthropometry data of children from the United States and the material properties of child bone were defined based on available data. The response-based corridors and impact tests on the Hybrid III 3-year-old child dummy were used to validate the impact responses of the neck, thorax, torso, and abdomen of the 3-year-old child FE model. The child model

is presented in Figure 6.2. This model is comprised of 66,778 nodes and 97,803 elements. Compared to the previous version of the child model developed before 2006 (version 1), the child model used in this research (version 2) is a more detailed model including implementation of deformability in the skull and brain as well as modeling of a child anatomical pelvis. More details about the development of the child model can be found in references [6] and [7]. As part of this research, a comparison between simulations with the 3-year-old child FE model (version 1) and the Hybrid III 3-year-old child dummy model (completed in accordance to CMVSS 208 frontal impact test configurations) was conducted and the comparison results can be found in reference [53]. Findings from the comparison between the Hybrid III 3-year-old child dummy model and the child model indicated the neck of the Hybrid III 3-year-old child dummy model was significantly stiffer than the child model and did not predict the appropriate degree of flexion associated with the neck. Figure 6.3 illustrate a sectional comparison of the Hybrid III 3-year-old dummy model and the child model and comparison of the head rotation about the Y-axis. Appendix A presents the modeling differences and comparisons of the simulation results between the two versions of the child models through simulations of frontal impact following FMVSS 213 sled test requirements.

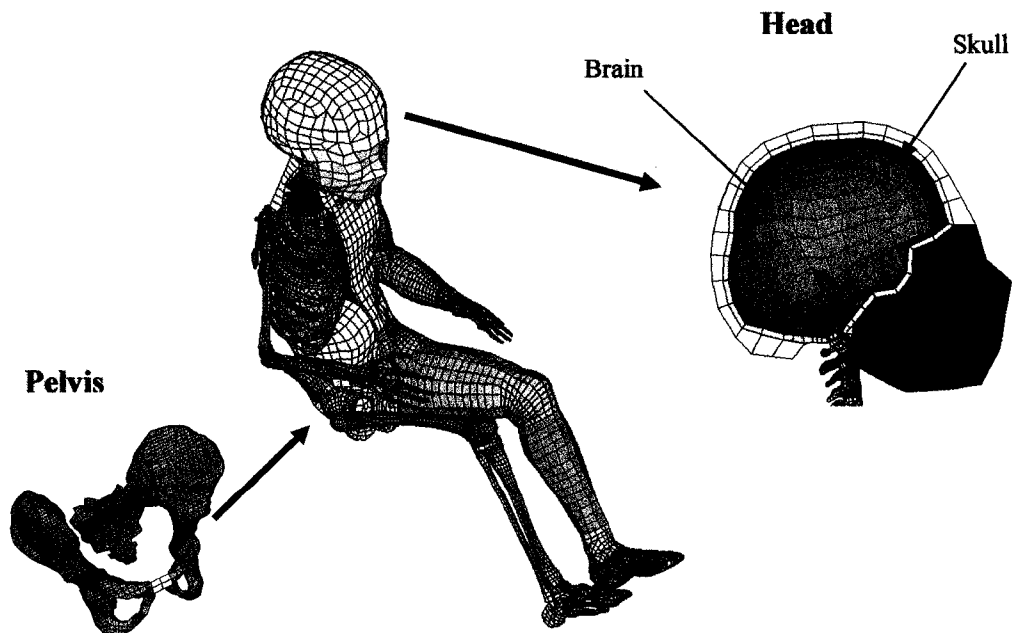


**Figure 6.2 Three-year-old child model.**

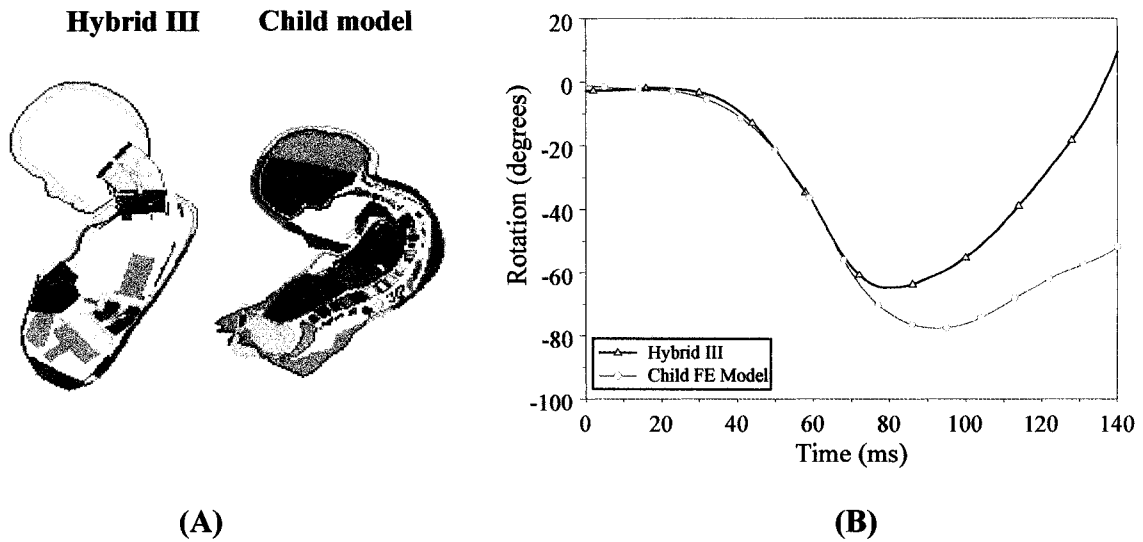


**Figure 6.3 (A) Sectional comparison of the behaviour of the Hybrid III 3-year-old dummy model and the child model and (B) Comparison of the head rotation about the Y-axis.**

### 6.1.2 Child restraint system (CRS) and FMVSS 213 bench seat

Numerical models of the CRS and FMVSS 213 bench seat used in this research were based upon the work of Wang et al. [41] and Turchi et al. [42]. Details about these models can be found in references [41] and [42]. However, a brief summary of the important aspects of these models is presented. The child safety seat, as well as all other components of the numerical model including the bench seat, the CRS webbing, and the CRS foam pad, was meshed using the Finite Element Model Builder (FEMB). The child seat was modeled using computer aided design (CAD) surfaces provided by Century/Graco Corp. The CRS was modeled using the elastic/plastic material properties based upon tensile test data. The Belytschko-Tsay shell elements (shell element formulation number 2 in LS-DYNA [56]) were assigned with thicknesses of 3.5 mm and 4.5 mm for specific regions of the CRS. Values for the density, Young's modulus, and Poisson's ratio were  $800 \text{ kg/m}^3$ , 0.842 GPa, and 0.3 respectively. Additionally, a stress versus effective plastic strain curve obtained from the tensile testing results was assigned

to the CRS material model. The material model implemented for the CRS utilized the von Mises yield criteria.

The mesh of the child seat was comprised of 12,728 nodes and 13,379 shell elements, of which 11935 elements were quadrilateral elements and 1444 elements were triangular elements. The final mesh of the deformable child safety seat is illustrated in Figure 6.4. Figure 6.5 illustrates the seatbelt, LATCH, top tether, and the five-point restraint system. The foam pad was modeled using a selectively reduced solid element formulation and the mesh of the foam pad is shown in Figure 6.6. The complete FE model including CRS, seat belt webbing, the waist and chest buckles, LATCH and the top tether, and the FMVSS 213 bench seat is illustrated in Figure 6.7.

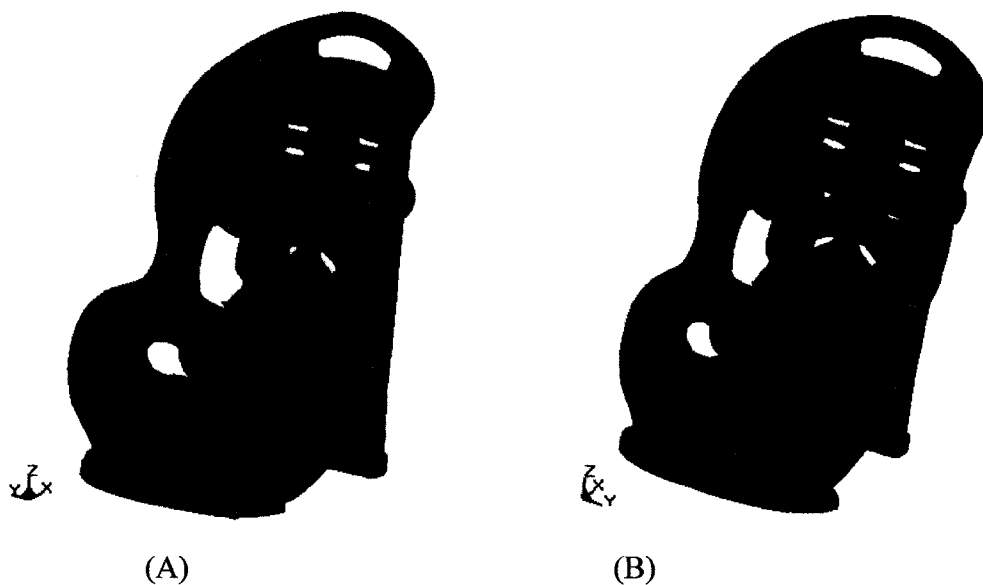


**Figure 6.4. (A) Front isometric view of the deformable CRS, (B) Rear isometric view of the deformable CRS [41].**

Reprinted with permission from SAE Paper # 2006-01-1141 © 2006 SAE International.

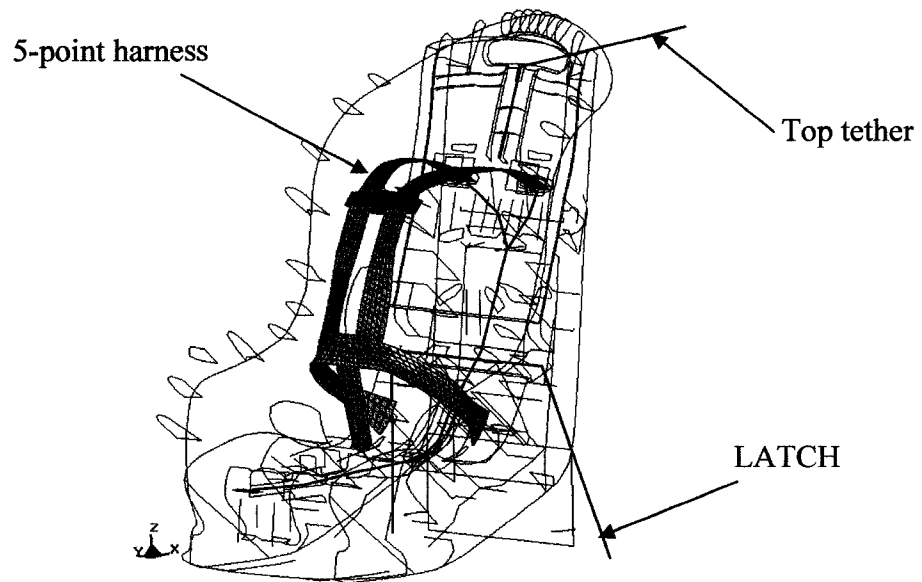


**Figure 6.5 The seatbelt, LATCH, top tether, and the five point restraint system [41].**

Reprinted with permission from SAE Paper # 2006-01-1141 © 2006 SAE International.

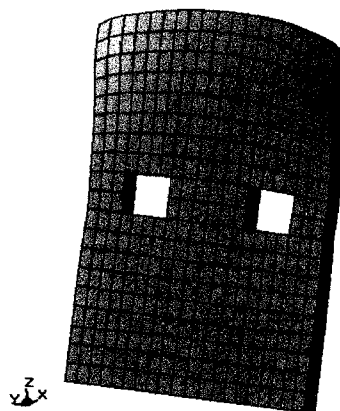


**Figure 6.6 The model of the foam pad [41].**

Reprinted with permission from SAE Paper # 2006-01-1141 © 2006 SAE International.

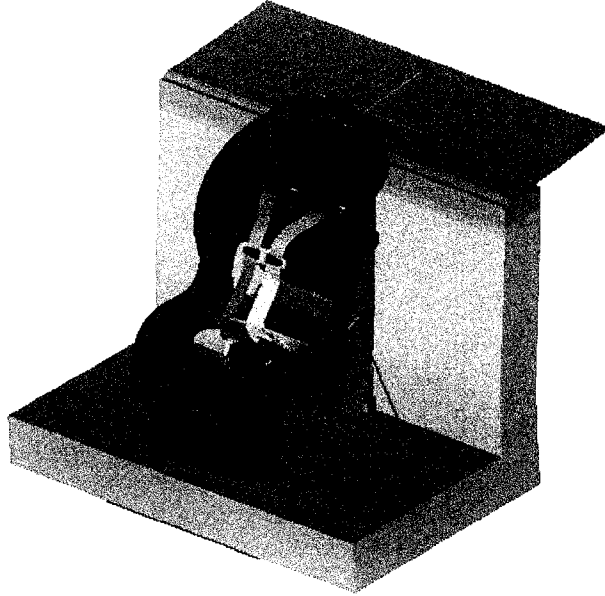


**Figure 6.7 Complete FE model of the deformable CRS and FMVSS 213 bench seat.**

### **6.1.3 Numerical simulation setup under FMVSS 213 sled test condition**

To simulate the FMVSS 213 sled test, the child model was combined with the CRS and FMVSS 213 bench seat. The units and the orientation of all components in the CRS and bench seat were unified with the child model as illustrated in Figure 6.8. The child model, without alterations to the material properties of the neck, was positioned into the CRS with adjustment of the harness to match the profile of the child model. The simulations were carried out using LS-DYNA version 971, release 7600-1077. The total simulation duration was 150 ms for the explicit dynamic analysis. Preloading was completed in a dynamic relaxation simulation. Before the dynamic simulation commenced, a 200 N preload was applied to the LATCH system and the top tether was loaded to 90 N. These preloads are consistent with FMVSS 213 requirements. Tightening of the front-adjusting harness strap which was simulated to properly position the child model into the CRS was also performed in the dynamic relaxation phase. The length of time for this preloading phase depends on the analysis convergence. The dynamic relaxation convergence tolerance was set to 0.0001 for all crash simulations.

Since this model is large in size (about 152,000 elements) and complicated for a variety of human-like components and material properties, the following countermeasures were implemented to improve the stability of the numerical simulation:

- The ligaments of the cervical spine, which were modeled using a membrane element formulation and shell elements, were coarsened to reduce the numerical instabilities observed in trial simulations;
- Material properties of the upper abdomen were adjusted such that at large strains (approximately 80%) the material begins to significantly harden. This technique permits a somewhat stiffer response than may be expected at large values of strain but will allow for a more realistic distribution of loading to neighbouring finite elements.

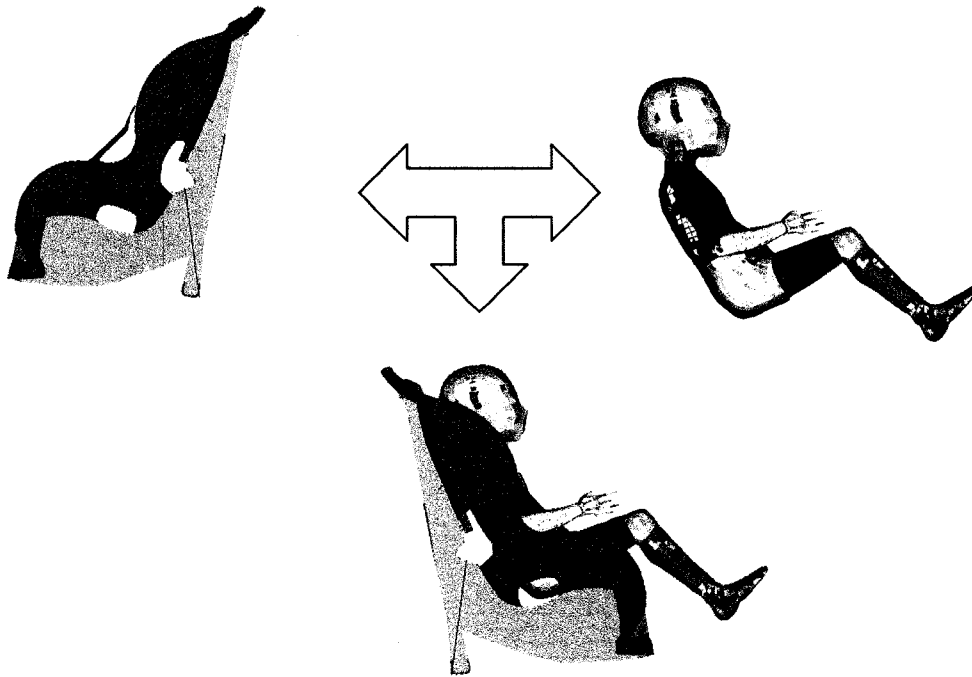


**Figure 6.8 Combination of child model with CRS and FMVSS213 bench seat.**



An acceleration pulse with the magnitude/time history as recorded from the experimental tests (as shown in Figure 6.1) was prescribed to the rigid bench seat in the positive global X-direction after preloading was completed. No other motion of the rigid bench seat in the global Y or Z axes directions was permitted. The ends of the top tether and LATCH were constrained to the rigid bench seat. Gravity was applied to the entire system.

There were no changes to the contact interfaces within the original child model and the CRS and bench seat. However different contact algorithms were added for modeling the contact between the child model and the CRS. The penalty method, which consists of placing normal interface springs between all penetrating nodes and contact surfaces, was used for all contact algorithms. The contact algorithm \*CONTACT\_AUTOMATIC\_SURFACE\_TO\_SURFACE with a static coefficient of friction FS = 0.5 and dynamic coefficient of friction FD = 0.45 was used to simulate contact between the child model, CRS and the foam padding. Additional contacts were added to simulate interactions between the hands, arms, head, and legs of the child model. Soft constraint formulation was applied to the contact interfaces between all body parts except bones. Interfaces between bones used a viscous damping coefficient.

All simulations were conducted using LS-DYNA on a personal computer with dual 2.6 GHz AMD Athlon processors with 2 gigabytes of random access memory (RAM). A double precision version of the FE solver was used. Numerical instabilities such as inverted solid elements (negative volumes) were observed to occur in the model as a result of inappropriate contact. The time step scale factor was reduced to 0.25 to counteract the effects of instability. The computational time for each simulation was approximately 80 hours.

A DVD containing the LS-DYNA input file for this simulation (and others) accompanies this thesis.

#### **6.1.4 Implementation of neck data from the altered head/neck component model**

The child model in combination with the CRS and FMVSS 213 bench seat was developed as a base model. The adjusted material properties for all parts altered in the

head/neck component model were incorporated into this base model and referred to as the “child model with neck alterations.” The simulation setup of the child model with neck alterations was identical to that of the base model.

Simulation results, in terms of head accelerations, neck deformation, motion, and cross-sectional forces, from both child models before and after neck alterations were investigated. The bio-fidelity and biomechanical responses of the two child models were compared and will be discussed in chapter 7.

To further evaluate the child model (both the base model and the altered model), an additional FE simulation incorporating an acceleration pulse from Kallieris et al. [45] was completed. This simulation was conducted as the test in reference [45] incorporated a child cadaver and represents an excellent validation metric for the child models. Section 6.2 will provide brief details on the test completed in reference [45].

## **6.2 Child model simulating a cadaver frontal impact sled test**

### **6.2.1 Cadaver frontal impact sled test**

Cassan et al. [46] summarized all pediatric cadaver tests performed prior to 1993. There were 11 pediatric cadaver tests completed by three different research groups. Eight cadaver sled tests were carried out and complete details from the testing were presented by Kallieris et al. in 1976 [45]. A comparison study of the kinematics observed in restrained child dummies and child cadavers in frontal crashes was also conducted in this study. One of the experimental child cadaver tests referenced in this research involved a 2½ year old male with a mass of 16 kg and a length of 97 cm who is similar to the child model.

The acceleration pulse which this child cadaver was subjected to is illustrated in Figure 6.9. The pulse was of trapezoidal shape and had an average deceleration of 18g’s with a pulse duration of approximately 75 ms. The initial impact velocity of the sled was 8.6 m/s. A shield type restraint system with trade name Vario (Britax) was utilized in the child cadaver test, which is different from the CRS in the numerical simulations. However, the model shared similar physical characteristics with the child cadaver in terms of mass and height. Furthermore, to the best of the authors’ knowledge,

observations from this test are the only data available which incorporate a child cadaver of similar stature and physical characteristics to the child FE model. Therefore a comparison of the kinematics experienced by the child cadaver and the child model was completed utilizing the acceleration pulse presented in Figure 6.9.

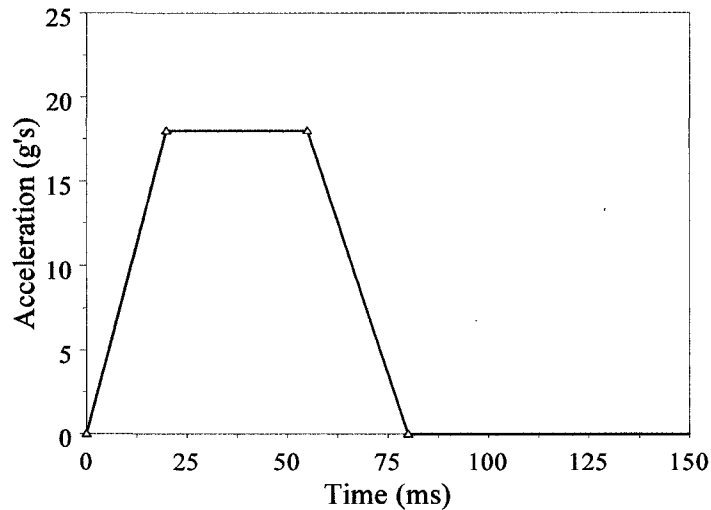


**Figure 6.9 Child cadaver testing acceleration pulse [45].**

### **6.2.2 Simulation setup under cadaver sled test condition**

The simulation setup under the cadaver sled test condition was identical to that of the FMVSS 213 numerical simulation with the exception of the acceleration pulse applied to the sled bench seat.

### **6.3 Data extraction from the child model**

Occupant injury data were extracted from time history information from nodes on the head and chest of the child model. Cross sections of the upper and lower neck were defined in the child model and used for assessing neck forces. Neck rotation was assessed using rigid body time histories of the neck vertebrae.

Head kinematics was assessed from the time history information of the kinematics associated with three nodes contained in the head. One nodal location was at the centre of

mass of the head and the remaining two nodes were located on each side of the skull in line with the centre of mass when viewed perpendicular to the sagittal plan. Time history information of a node located at vertebra T3 of the thoracic spine was used to record the translational and rotational response of the chest.

Head trajectory was determined based upon the motion of the head's centre of mass relative to the rigid portion of the bench seat. The neck tensile deformation was determined by calculating the distance between C1 and T1 and rotational motion was based upon the difference in rotation angles associated with C1 and T1.

The standard SAE J211 [57] was used to filter the time history data from all aspects of the child model. SAE J211 was developed for filtering all the experimental and numerical data of the vehicle body and of the anthropomorphic test device (ATD). A second order butterworth filter was developed as specified in SAE J211 for filtering all data. The filters for dummy data channels prescribed by SAE J211 are listed in Table 6.1. The child model is different from the ATD as most of the parts of the child model are human like and deformable. The data extracted from the simulation contained significant oscillations such that the levels of the filters used in this research were adjusted to the different result data.

**Table 6.1 SAE J211 filters for child occupant injury data.**

Injury data	Data channel
Head Acceleration	Class 1000
Neck Force	Class 1000
Neck Moment	Class 600
Chest Acceleration	Class 180

#### **6.4 Injury parameters**

Pediatric ATD's and their associated injury criteria were used as one of the primary tools for predicting child injuries and child occupant protection in motor vehicles [5]. The following sections provide details of these injury criteria.

### 6.4.1 Head injury criteria

The head injury criteria (HIC) are required by the standard FMVSS 213 to calculate the risk of head injury for child occupants during vehicle crashes. Equation (1), which is used to determine the head injury criteria for the Hybrid III 3-year-old child dummy, was applied for various simulations considered in this research.

$$HIC = \left[ \frac{1}{t_2 - t_1} \int_{t_1}^{t_2} a_{\text{resultant}} \cdot dt \right]^{2.5} \cdot (t_2 - t_1) \quad (1)$$

Where

$$a_{\text{resultant}} = \sqrt{a_x^2 + a_y^2 + a_z^2} \quad (2)$$

The resultant head accelerations in units of g's are calculated using Equation (2) where  $x$ ,  $y$  and  $z$ -axes formed the local coordinate system located in the head following the SAE J211 conversion. The time interval to calculate the head injury criteria is 36 ms which followed the FMVSS 213 final rule. The acceptable value of HIC should be less than 1000 and the acceleration level of the child's head should not exceed 60 g's for any period greater than 36 ms. There is also a proposed value of 570 for the HIC evaluation over a 15 ms window for the Hybrid III 3-year-old child dummy.

### 6.4.2 Neck injury criteria

Neck injury criteria are required by the standard CMVSS 208 to calculate the neck injury risks of child occupants during vehicle crashes. Equation 3 was used to determine the neck injury criteria for the Hybrid III 3-year-old child dummy.

$$N_{ij} = \left( \frac{F_z}{F_{zc}} \right) + \left( \frac{M_y}{M_{yc}} \right) \quad (3)$$

Though FMVSS 208 contains child neck injury criteria, the current FMVSS 213 does not regulate neck tolerance measurements due to the increasing concern about the biofidelity or artifacts of the Hybrid III child dummy [38]. For this reason, the neck injury criteria were not applied to the neck injury prediction in this research.

## **7. COMPARISON OF CHILD MODEL BEFORE/AFTER NECK ALTERATION**

Simulations of frontal crash following the FMVSS 213 protocols were conducted using the child model before and after neck alterations. In the following sections, comparisons of the kinematics and biomechanical responses of the two child models will be presented qualitatively and quantitatively. The head excursion and the neck injury potential of the child models will also be compared with the cadaver sled test and a traffic accident case.

### **7.1 Qualitative Comparison**

The kinematic response of the child models before and after neck alterations at different time intervals throughout the simulations are shown in Figure 7.1 for the side view and in Figure 7.2 for the cross sectional view. The difference in the kinematic response of the two models in the simulations is not obvious until contact between the chin and chest occurs at approximately 60 ms. Excursions of the head of both child models commence at 27.5 ms and the arms and legs stretch out completely at approximately 57.5 ms.

At 62.5 ms the rotation and excursion of the child head increase more significantly in the child model with neck alterations. A greater degree of neck flexion is observed at the same time for the altered model. The arms come to contact with the head at 85 ms for both child models. Arm/head contact, however, occurs for a longer duration for the child model without neck alterations. It was observed that chin/chest contact occurred over a longer duration for the child model with neck alterations while the separation between the head and chest occurred before 120 ms of simulation time for the child model without neck alterations. Both child models rebound and contact the backing of the child seat at a time of approximately 105 ms.

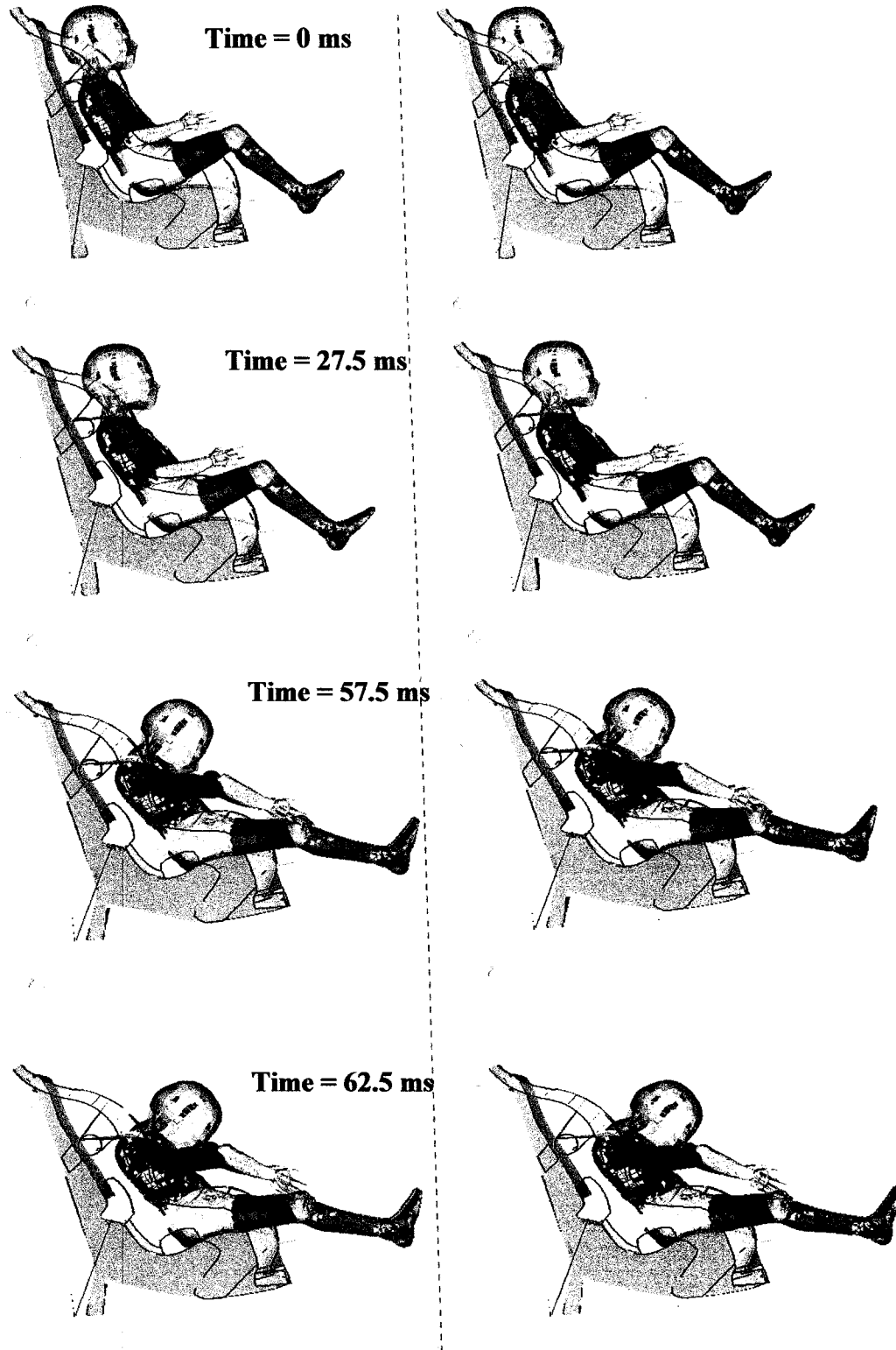


**Figure 7.1 Child model simulating FMVSS 213 frontal crash side view: before neck alterations on the left and after neck alterations on the right (continued on the next page)**

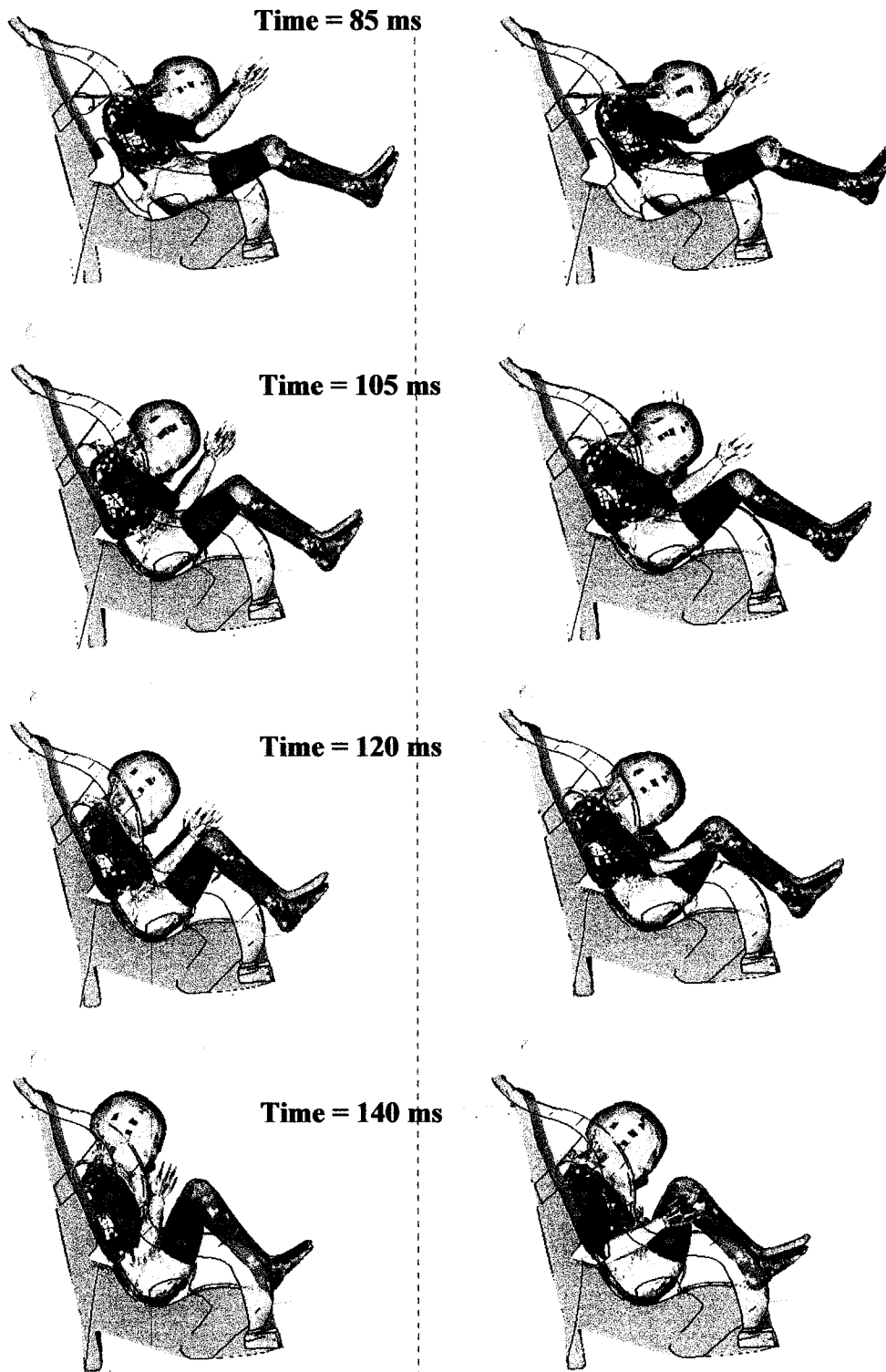


**Figure 7.1 (continued) Child model simulating FMVSS 213 frontal crash side view: before neck alterations on left and after neck alterations on the right**



**Before neck alteration**

**After neck alteration**

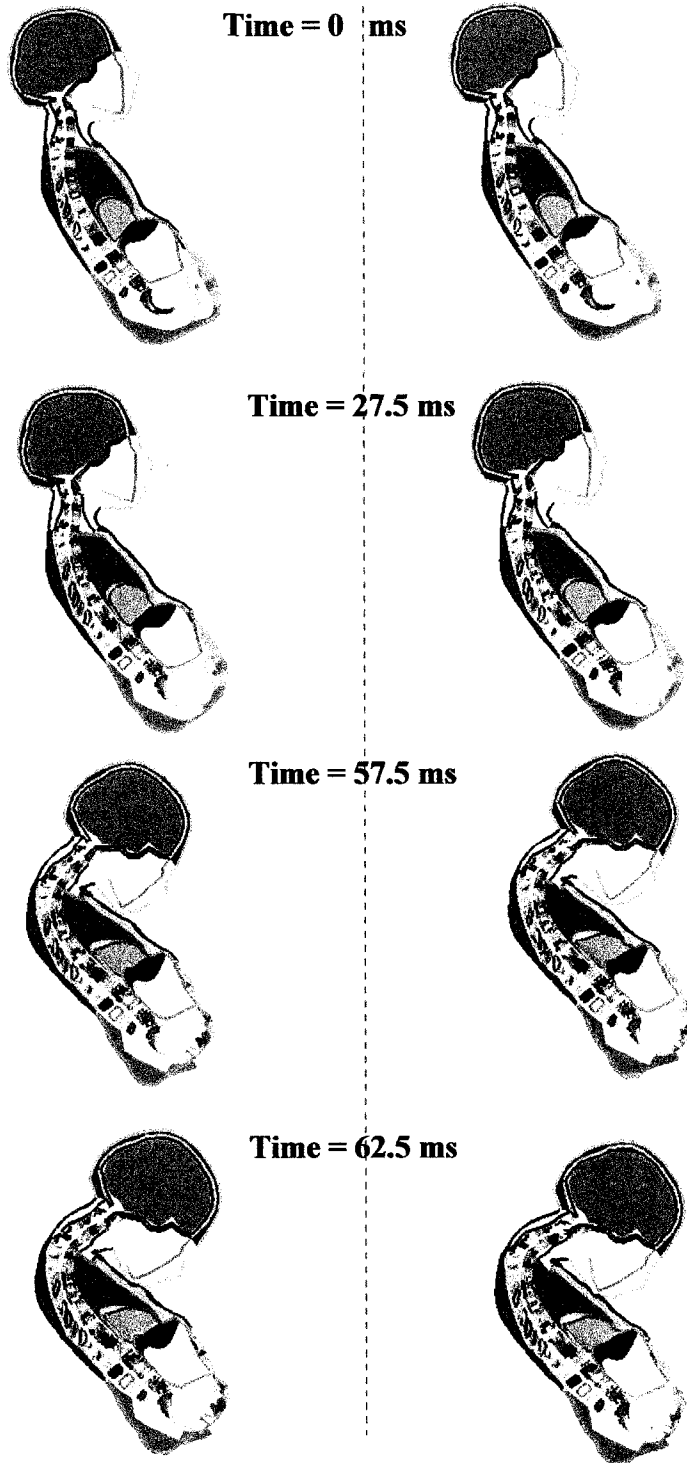


**Figure 7.2 Child model simulating FMVSS 213 frontal crash cross sectional view:  
before neck alterations on left and after neck alterations on the right  
(continued on the next page).**

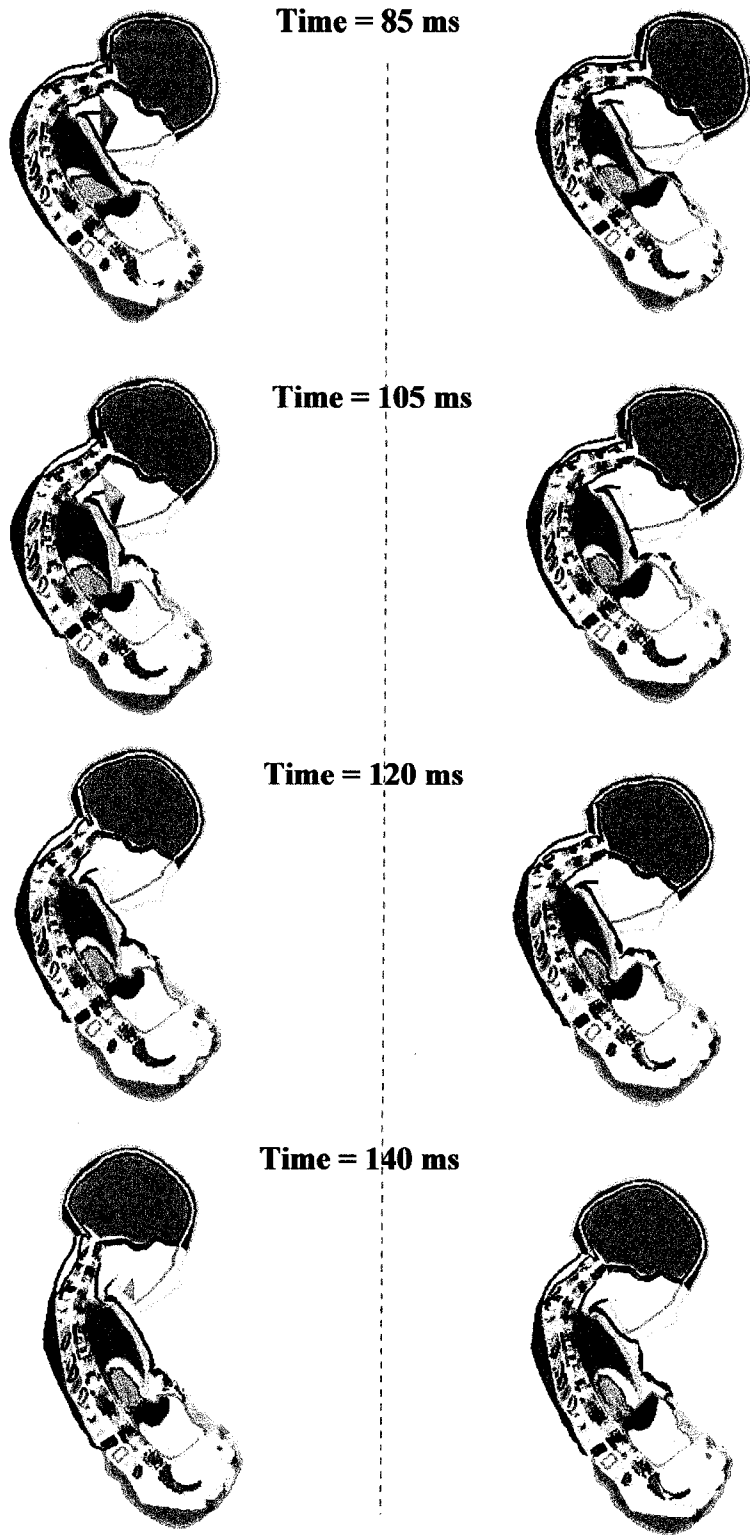


**Figure 7.2 (continued) Child model simulating FMVSS 213 frontal crash cross sectional view: before neck alterations on left and after neck alterations on the right**

At approximately 92.5 ms, significant shear deformation along with the flexion of the neck at cervical vertebrae C1-C2 was observed in the simulation of the child model with neck alterations. These details are illustrated in Figure 7.3. As the arrow in the enlarged local view of this figure indicates, the cervical vertebra C2 has exhibited significant position change relative to the C1 and the basion of the skull. This phenomenon predicts a clinical finding, called an atlanto-occipital dislocation (A. O. D), which is often a fatal neck injury for young children. This is not easily identifiable prior to the reduction of the elastic characteristics of the soft tissues associated with the cervical spine.

In general, the child model with neck alterations has notably more head rotation, larger neck distraction, and longer contact duration between the head and chest.

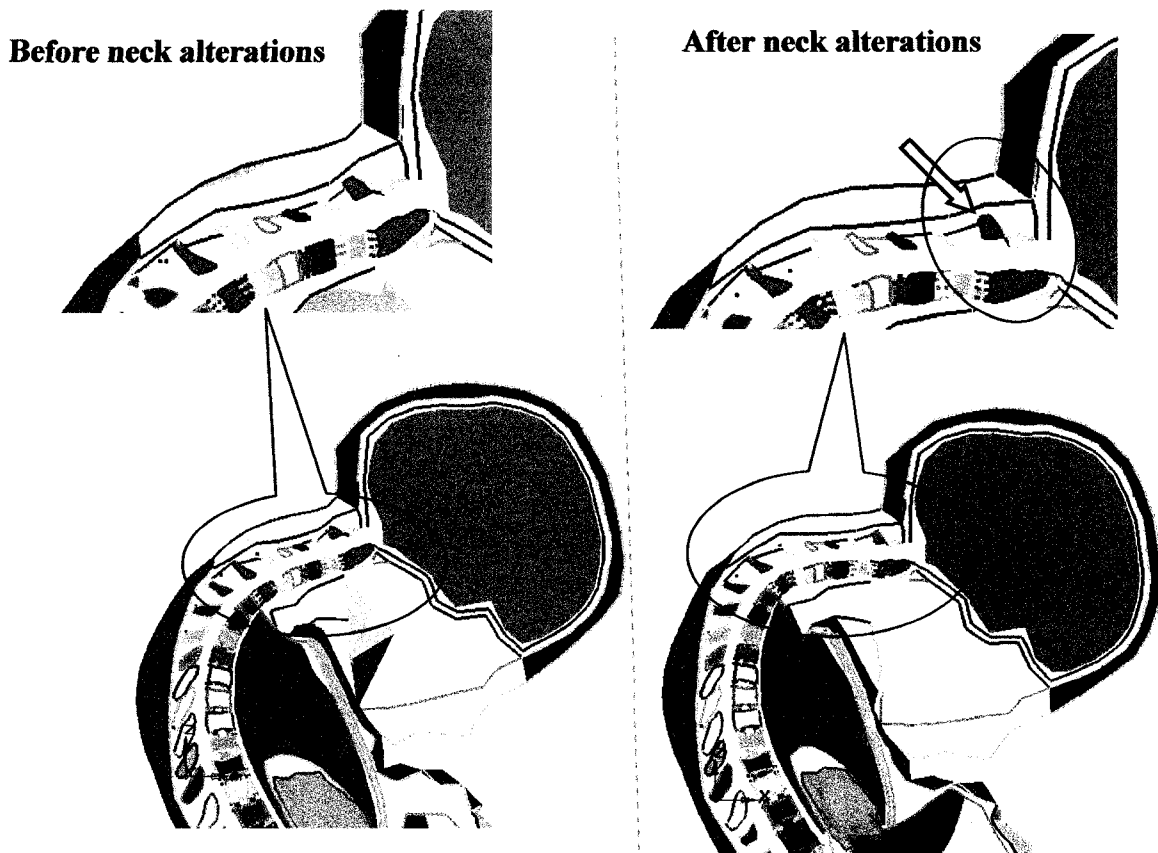


**Figure 7.3 Detail of neck deformation of the child model at 92.5 ms in cross sectional view: the shear deformation of C1-C2 of the child model after neck alterations as indicated in the area with an arrow.**

## **7.2 Quantitative Comparison of Kinematic and Biomechanical Responses**

In the following sections, a quantitative comparison of the kinematic and biomechanical responses of the two child models before and after neck alterations will be presented. Specifically, time histories of the following variables will be presented:

- acceleration, excursion and rotation of the head,
- tensile forces, deflection and rotational deformation of the neck, and
- accelerations and deflection of the chest.

In addition to these variables, the head displacement of the child models will be compared with the head trajectory of a similar child from a pediatric cadaver test. The prediction of neck injury will be discussed and compared with the case of a crash in a documented traffic accident in section 7.3.

### **7.2.1 Head Response**

#### **7.2.1.1 Head accelerations and head injury criteria (HIC)**

Figures 7.4 and 7.5 illustrate comparisons of the head accelerations in the global X and Z directions of the child models before and after neck alterations. Figure 7.6 illustrates the resultant acceleration. The accelerations from the two models are almost identical to each other in profile, magnitude, and peak duration. The acceleration pulses from both models, however, contained significant noise even after a much lower class filter (180) was utilized instead of the filter class 1000 recommended in SAE J211 for the ATD used in FMVSS 213 crash tests.

There are two notable peaks observed in the global X and Z head accelerations of the child model without neck alterations prior to 65 ms. The first peak occurred at approximately 57.5 ms and was caused by the brief contact between the chin and the front clip of the child seatbelt before the chin reached the chest. The second peak was observed to occur at 62.5 ms and a detailed discussion of the reason for this observation

will be provided in section 7.3. Additionally, rationales as to why this was observed in the child model will also be addressed in section 7.3.

Figure 7.7 illustrates a time history of the chin to chest contact force. The peak of the contact force occurs at approximately 72 ms. The time history curves are relatively smooth before the contact forces reach their peaks. The chin and chest in the child model without neck alterations separated from each other at approximately 130 ms.

Differences in the head accelerations of the two child models during rebound, which was estimated to occur at 105 ms, resulted from contact between the arms and head which generally occurred from 85 to 97.5 ms.

Since the head acceleration time history responses do not differ significantly, the values of the head injury criteria (HIC) (as shown in Table 7.1) calculated from the simulation results for both child models are also similar.

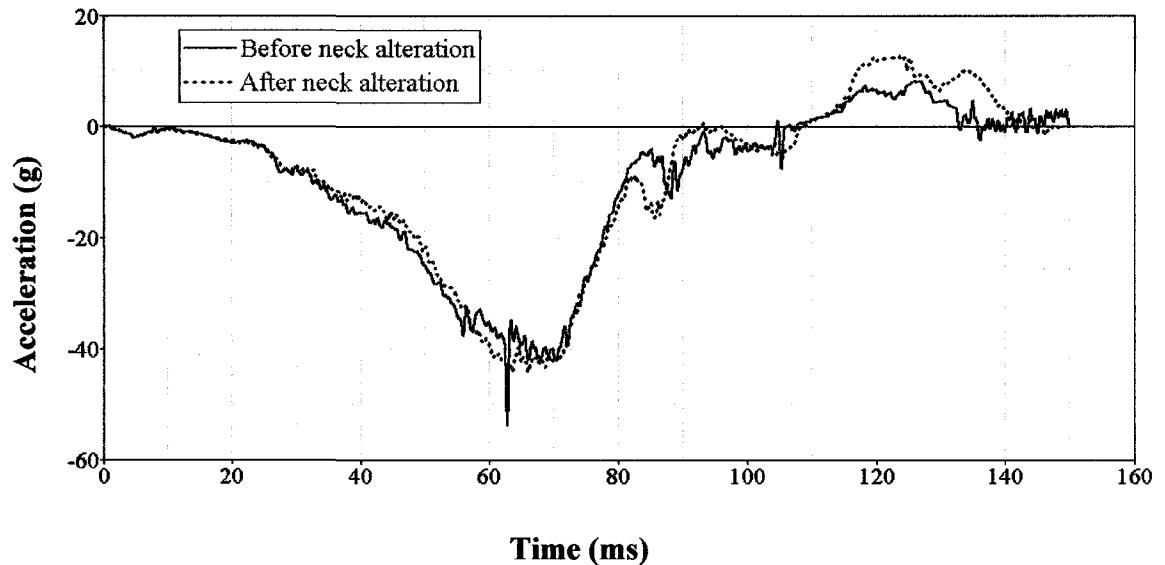


**Figure 7.4 Head acceleration in X direction.**

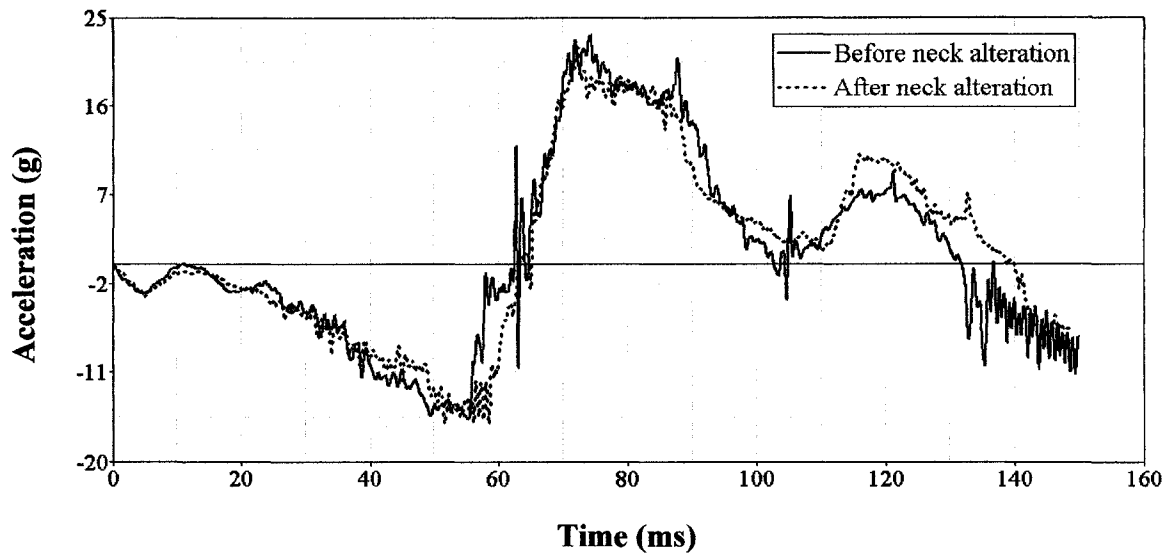


**Figure 7.5 Head acceleration in Z direction.**

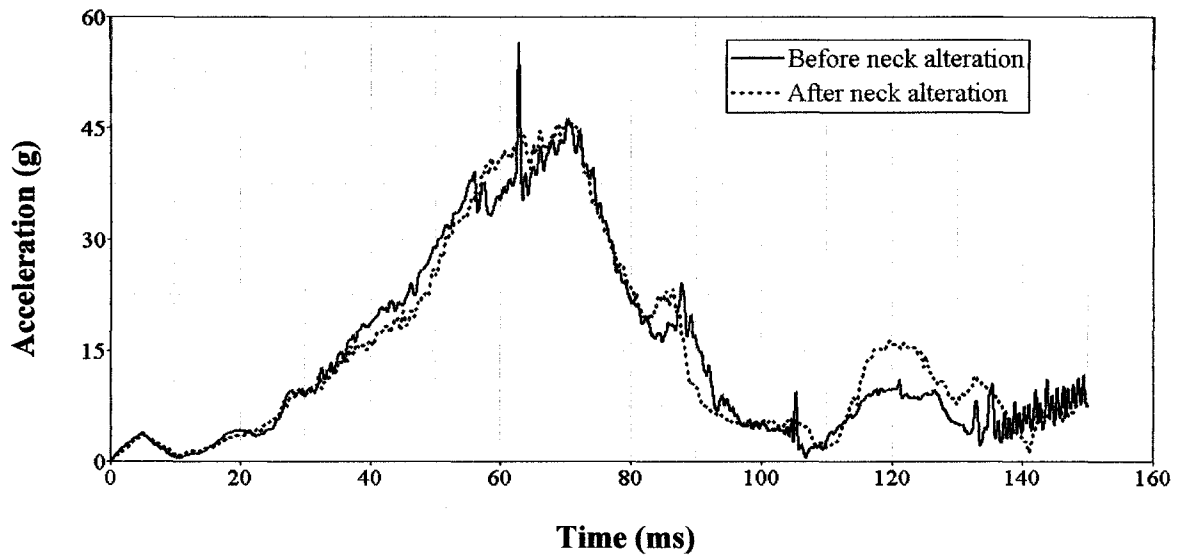


**Figure 7.6 Head resultant acceleration.**

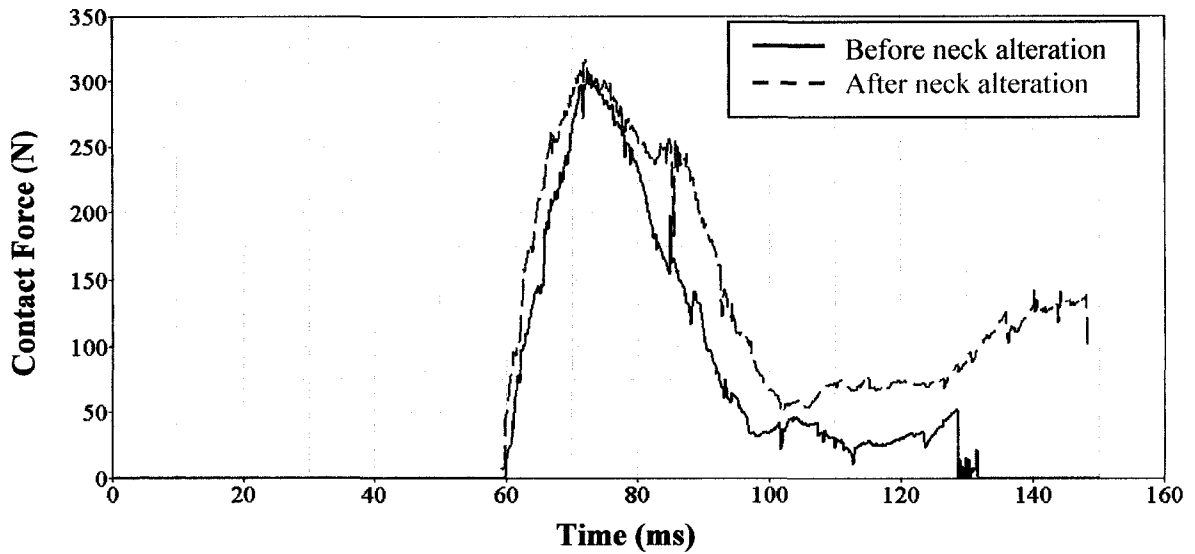


**Figure 7.7 Chin to chest contact force time.**

**Table 7.1: Values of the Head Injury Criteria (HIC)**

<b>Model</b>	<b>HIC 15</b>	<b>HIC 36</b>
<b>Child Model Before Neck Alteration</b>	<b>201</b>	<b>292</b>
<b>Child Model After Neck Alteration</b>	<b>202</b>	<b>305</b>

### 7.2.1.2 Head rotation

Figure 7.8 illustrates a comparison of the head rotation in the sagittal plane of the child models before and after neck alterations. It was observed that a difference in head rotation commenced at approximately 70 ms. The head of the child model, incorporating the child biomechanical response, exhibited more rotation (maximum 125 degrees at 95 ms) than the unaltered child model (maximum 119 degrees at 85 ms).

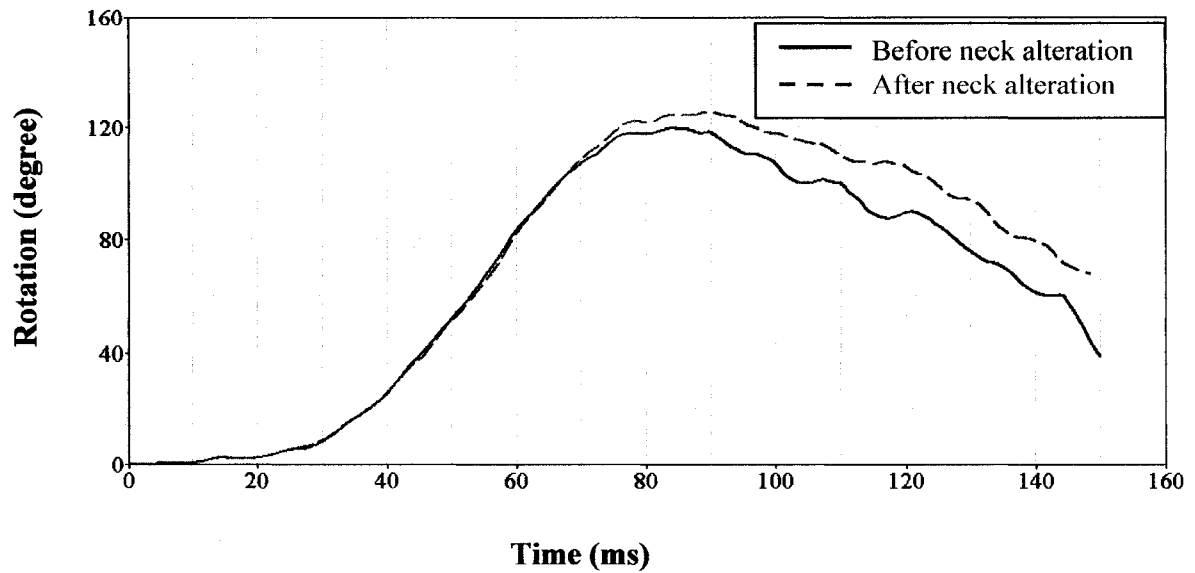


**Figure 7.8 Head rotations in the sagittal plane.**

### 7.2.1.3 Head displacement and trajectory

The displacement of the head at the center of gravity has been measured relative to the rigid seat bench. Figure 7.9 illustrates the X and Z displacements (relative to the rigid seat bench) on the abscissa and ordinate respectively. These profiles represent the trajectories of the head mass centre. Greater excursions in both the X and Z directions in the child model after neck alterations were observed. This is consistent with results (as shown in figure 7.10) from the simulations of the two child models that were subjected to the acceleration pulse of the experimental child cadaver test. The head displacement of the child model was increased in the X and Z directions by 3% and 5%, respectively, by altering the neck material properties.

Figure 7.10 indicates that the head of the child cadaver appeared to have no rebound. This was a result of the failure of the child restraint system and the overturn of the child cadaver in the later stage of the test as noted in the high speed video footage of the cadaver test. As a result, the comparison between the child model and cadaver was limited to simulation timing from the commencement of head rebound. It is obvious that the head excursion of the child model after neck alterations is more consistent with the findings from the child cadaver tests. The maximum displacements of the head have a



percentage error of approximately 16% and 13.5% for the child model before and after neck alterations when compared with the child cadaver test.

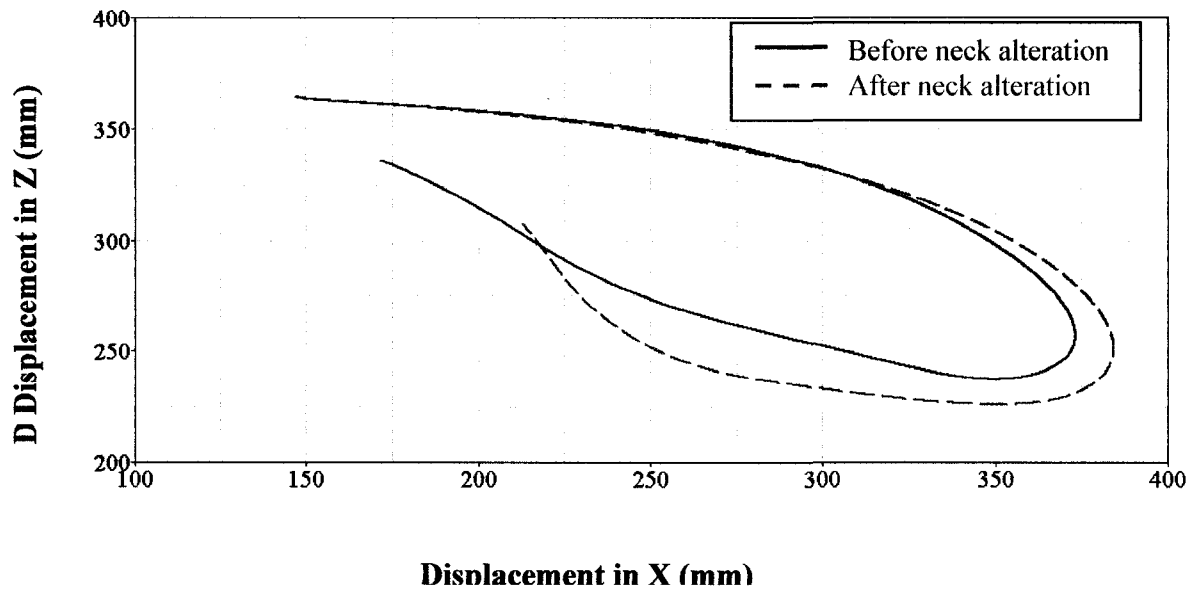


**Figure 7.9 Head trajectories under FMVSS 213 frontal impact sled test conditions.**

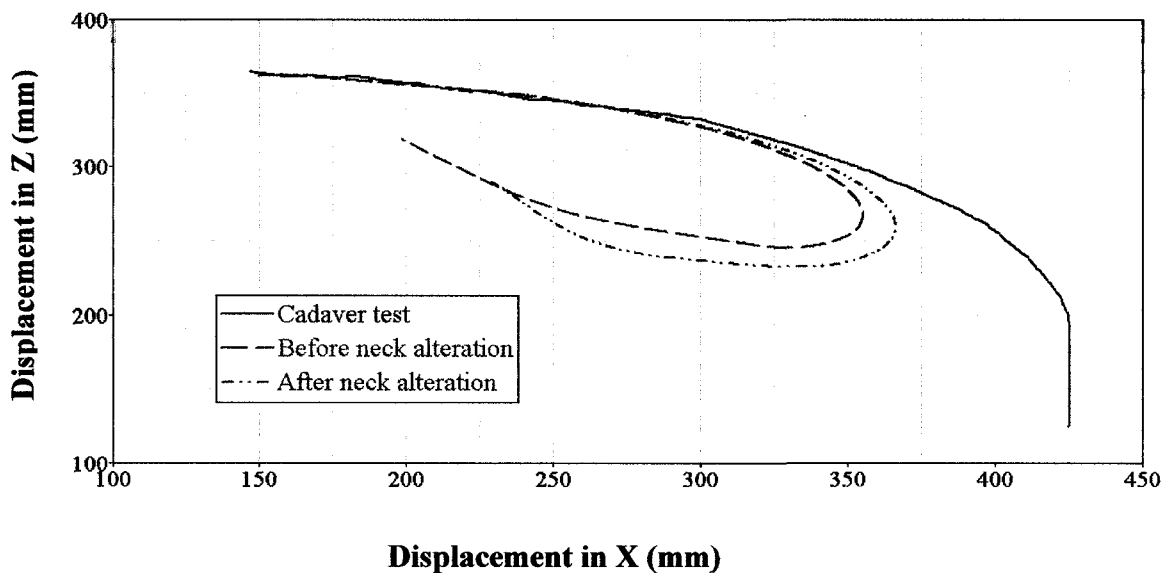


**Figure 7.10 Head trajectory under cadaver frontal impact sled test conditions.**

## 7.2.2 Neck response

### 7.2.2.1 Upper neck forces

Figure 7.11 illustrates the difference in the upper neck (C2-C3) tensile forces between the child models. The maximum upper neck tensile force was 1228 N at 70 ms and 793 N at 75 ms in the child models before and after neck alterations, respectively. The alterations of the neck in the child model reduce the upper neck tensile force by approximately 35% and delay the time when the neck force reaches the peak value by approximately 5 ms.

A shift in the upper neck force from distraction to compression emerges at approximately 110 ms for the unaltered neck child model when the torso of the child contacts the child seat back. The compression force reaches its peak value of 205 N at approximately 125 ms. No significant neck compression force is observed in the child model after neck alterations.

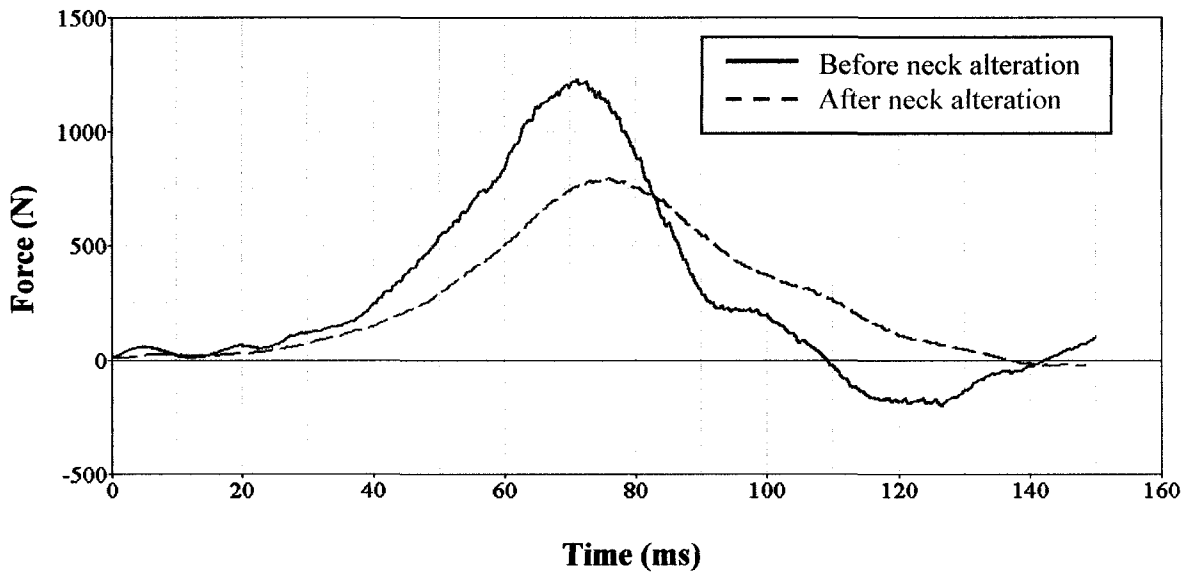


Figure 7.11 Upper neck tensile forces.

### 7.2.2.2 Lower neck forces

As illustrated in Figure 7.12, the time history of the lower neck (C6-C7) force varies noticeably in both child models before and after neck alterations. The child model after neck alterations exhibited much lower peak values. The duration of the lower neck force was increased in both compression and tension throughout the simulations. It was observed that for the model without neck alterations that the lower neck force first appeared to be in compression until 49 ms. Then, the lower neck was subjected to a tensile force between 49ms and 108 ms. The neck force returned to compression between 108 ms and 134 ms. By contrast, before 132 ms, the neck force from the child model incorporating the neck alterations had only one shift from compression to tension at 57 ms and remained in the tension region until 132 ms. Maximum values of the lower neck force were observed to be 624 N in tension and 272 N in compression for the child model without neck alterations. Incorporating the biomechanical behaviour of the cervical spine into the child model resulted in a peak tensile force of 366 N and 147 N in compression. The lower neck force has been reduced by 41% for tensile force and 46% for compressive force, respectively, as a result of the neck alteration under the simulated FMVSS 213 test.

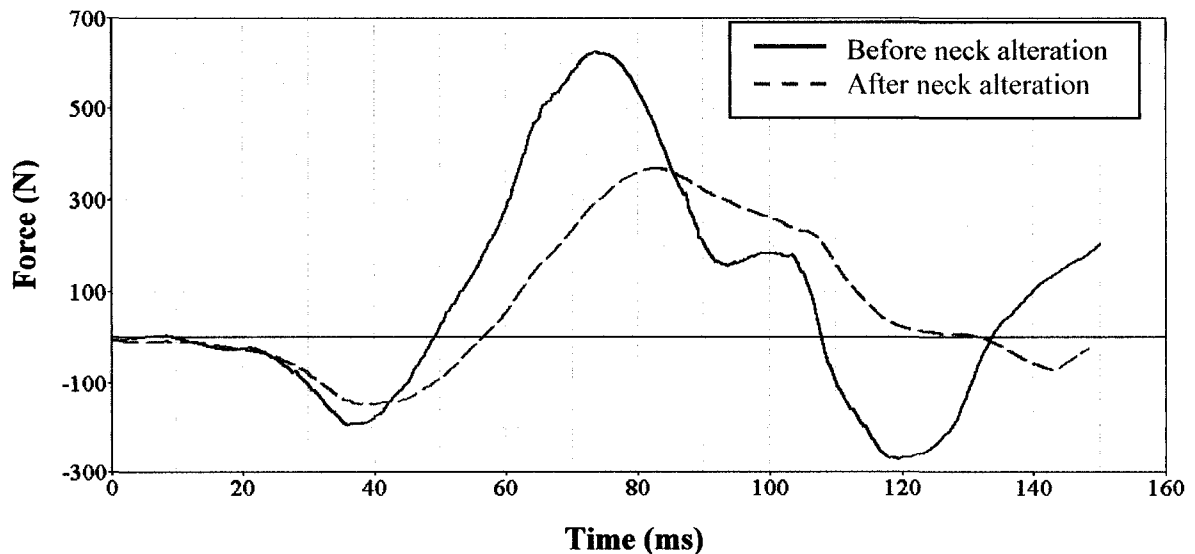
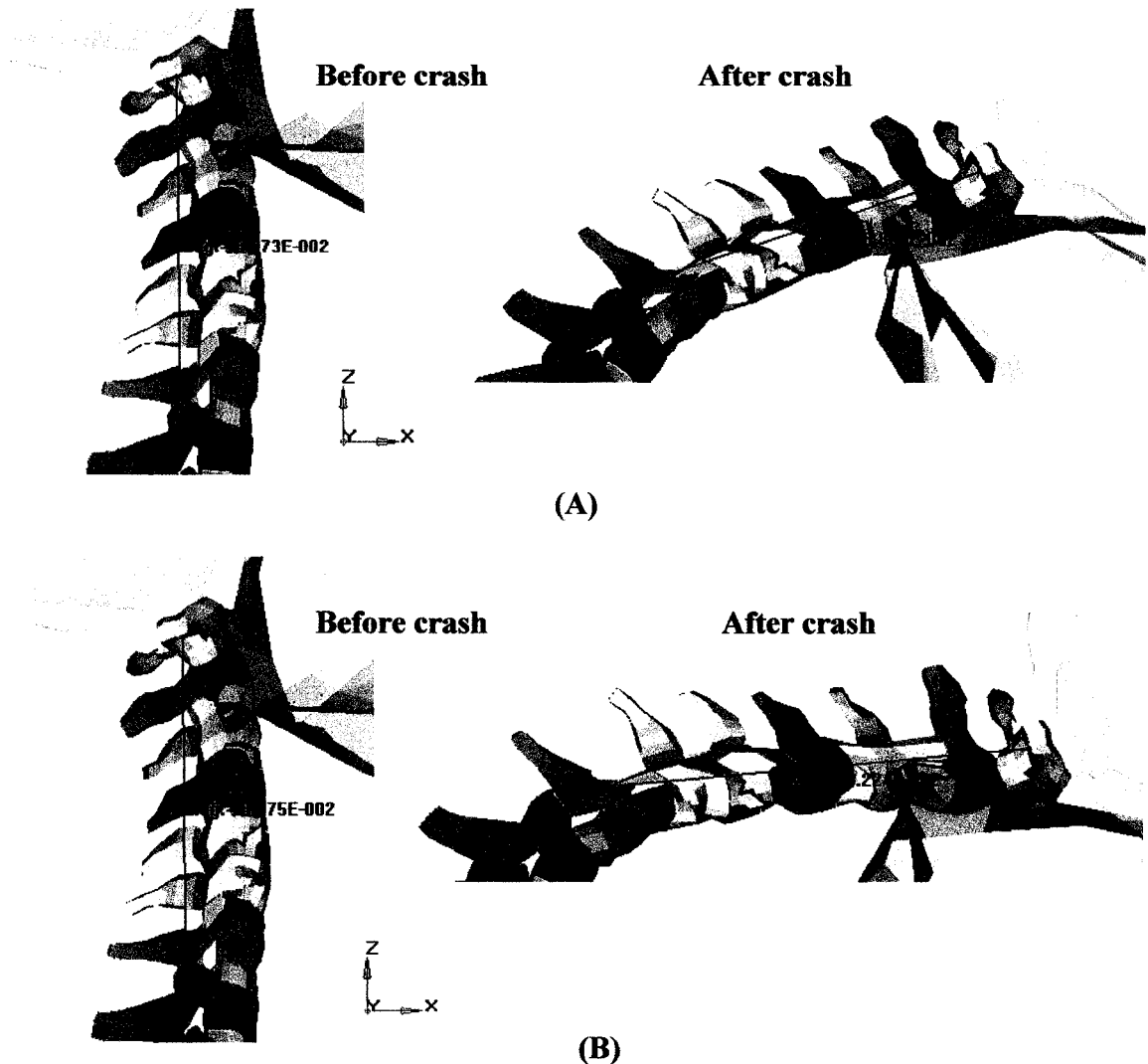


Figure 7.12 Lower neck tensile forces.

### 7.2.2.3 Neck deflection

Throughout the simulations of frontal crash under FMVSS 213 test conditions, the necks of both child models experience tensile deformation as shown in Figure 7.13. It is observed that the maximum deflection of the child neck is 8 mm at approximately 73 ms and 22.5 mm at approximately 78 ms for the child models before and after neck alterations, respectively. An increase of 14.5 mm in neck tensile deformation results from neck alterations. Note that the locations of the measurements are at the pedicles of the cervical vertebra C1 and the thoracic vertebra T1.



**Figure 7.13 Measurement of Neck Deflection (C1-T1): (A) without neck alterations and (B) with neck alterations.**

#### 7.2.2.4 Neck Rotation

The neck rotation in the sagittal plane is determined by calculating the difference in rotation angles between the cervical vertebra C1 and thoracic vertebra T1. Figure 7.14 presents a comparison of neck rotations from the child models before and after neck alterations. An increased rotation angle of 19 degrees after neck alterations was observed. It can also be observed that the rotation time history has second peaks when contact between the torso of the child and the child seatback occurred. Overall, the maximum rotation is 51 degrees at 77 ms and 70 degrees at 82.5 ms for the child models before and after neck alterations, respectively.

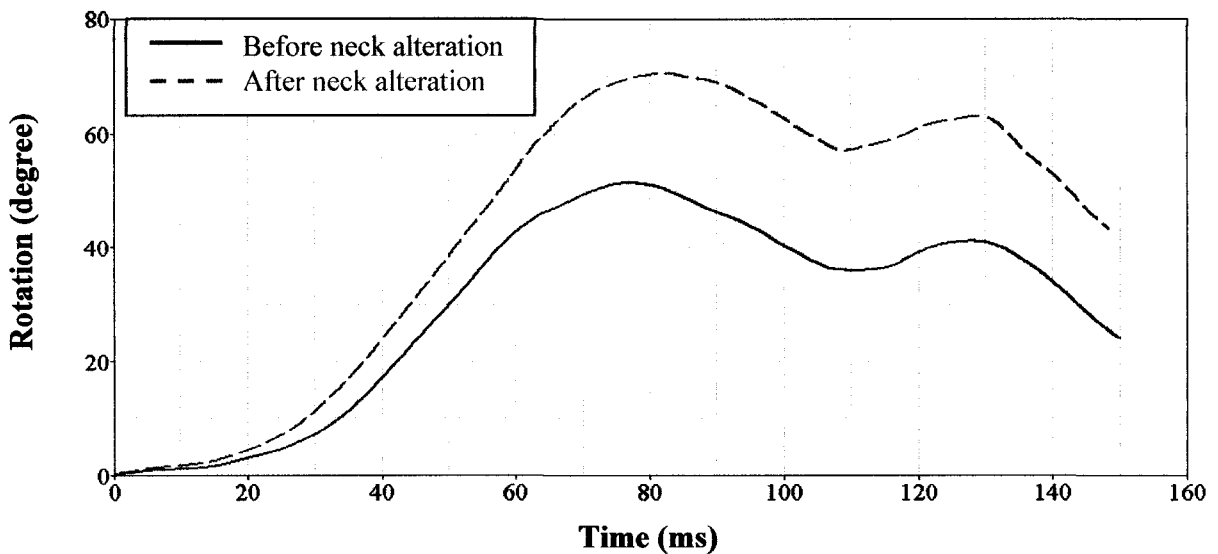


Figure 7.14 Neck rotation in sagittal plane.

#### 7.2.3 Chest response

##### 7.2.3.1 Chest accelerations

Since no significant modifications in the chest area were employed, it is expected that the chest acceleration pulses should not change considerably. Figures 7.15, 7.16 and 7.17 illustrate the chest resultant acceleration and the chest accelerations in the X and Z directions. It is important to note that initial accelerations in their unfiltered forms are approximately zero at the start of the simulation. Filtered values are not zero due to the

filtering of the data. Predictions from the two models were found to be very similar in profile and magnitude until the simulation time of approximately 100 ms. After this time, contact between the torso and the child seatback pad and the seatback occurred. During torso/seatback contact, the chest acceleration pulses display some variation in peak values and timing. These changes are due to the differences in head/neck rotations and chin/chest contact durations resulting from the biomechanical modifications of the neck.

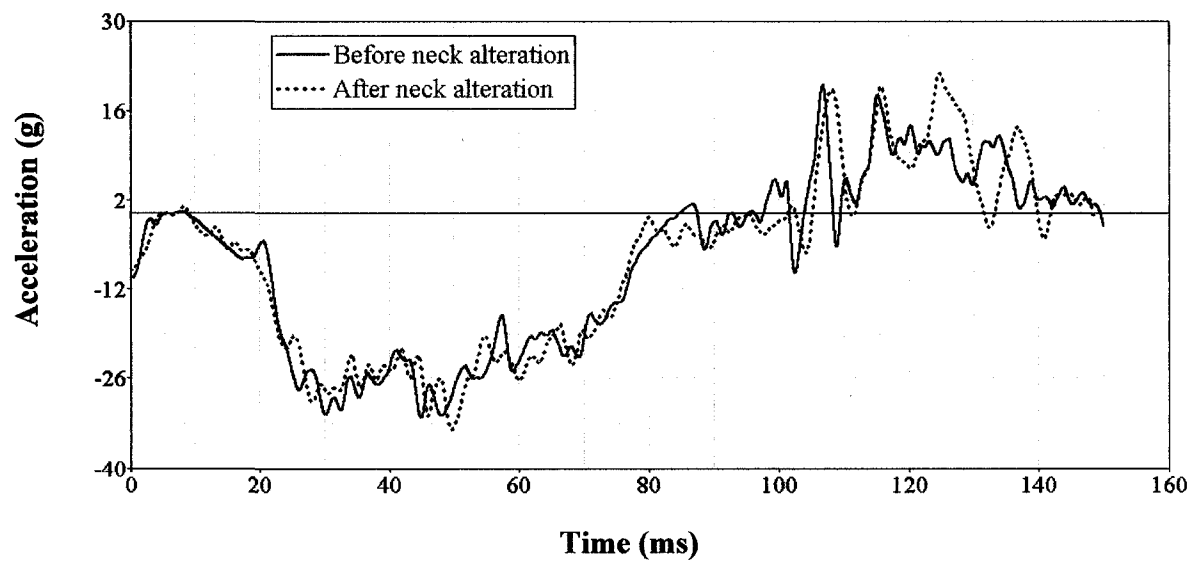


**Figure 7.15 Chest Acceleration in the X direction.**

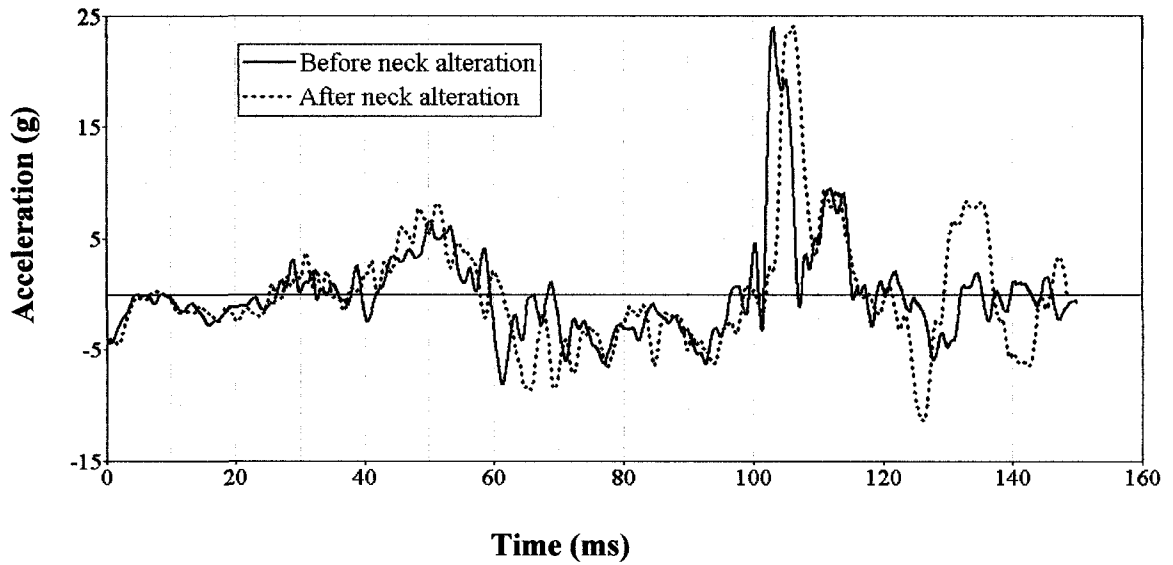


**Figure 7.16 Chest acceleration in the Z direction.**

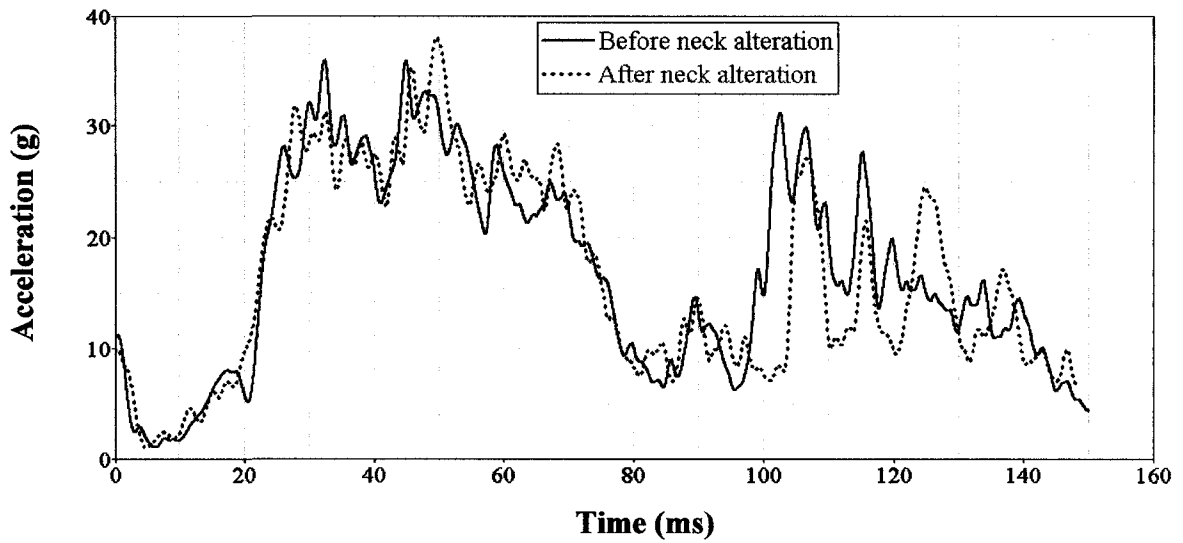


**Figure 7.17 Chest resultant accelerations.**

### 7.2.3.2 Chest deflection

Chest deflection is one parameter used for predicting child injury risks. Figure 7.18 illustrates chest deflection versus time response for both models. The maximum chest deflection is 21.9 mm at approximately 88 ms and 19.5 mm at 91 ms. The reduced

peak value and its delayed timing is a result of the observed downward motion of the head and neck after the neck alterations and will be discussed in detail in section 7.3

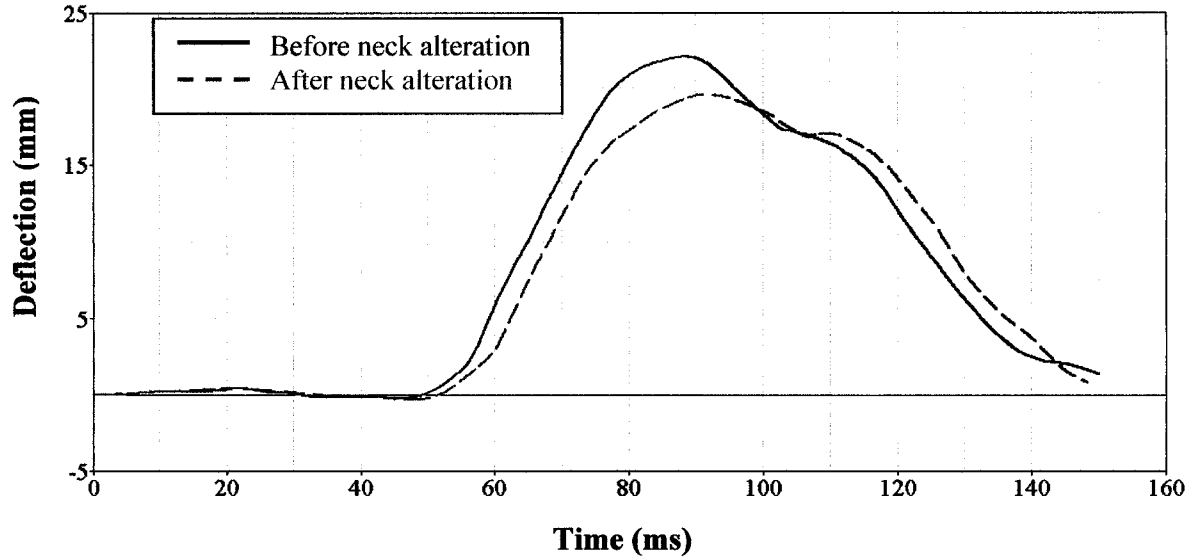


**Figure 7.18 Chest deflections.**

### **7.3 Discussions**

#### **Head response**

As Figures 7.4 to 7.6 illustrate, the head acceleration time history in the X and Z directions and the resultant head acceleration of the child model with neck alterations were of similar profile and magnitude as the child model without neck alterations. This is essentially because there are no changes in the head mass and the material properties used for modeling the head. Secondly, there is evidence that the neck shear force considerably increased (as shown in Figure 7.3) while the tensile force decreased. The similar resultant acceleration values of the original and modified models illustrate that the head injury criteria  $HIC_{15}$  and  $HIC_{36}$  of both child models are consistent as expected. The HIC values listed in Table 7.1 are considerably below the critical values of 1000 for  $HIC_{36}$  and 570 for  $HIC_{15}$  as recommended by the NHTSA for a 3-year-old child in frontal crash. This implies that predicting head injury using this child model will lower the risk of head injuries for children. This finding is consistent with the 2006 NHTSA report [3]. It is also



compliant with the argument that the inertial force from vehicle crash may not reach the level necessary to cause child head injuries without direct impact [34].

The change in the stiffness of the neck illustrated some local effects on the head acceleration pulses. For example, at 57.5ms and 62.5 ms, the local fluctuation of the acceleration pulses from the child model before neck alterations still appear even after the application of a low level filter, SAE 180, which is of a much lower filter class than is required in SAE J211 [57] (SAE 1000 is recommended). With the reduction in the neck stiffness of the child model, it was observed that accelerations associated with the head did not illustrate significant fluctuations in the time intervals mentioned above.

Vibrations throughout the simulation are caused by the deformable material used for the brain and skull. Originally, there were two versions of the child model as presented in chapter 2. In version 1 the brain and skull were not deformable, similar to those of the Hybrid III 3-year-old child dummy model. The second version of the child model, which is used in this research, employs a deformable material with a low elastic modulus for the brain and a high elastic modulus for the skull. The material properties used for the brain and skull influence the head acceleration in the frontal crash simulations. A comparison of the child models (version 1 and version 2) was conducted during this research. Graphs of the results can be found in Appendix A. The figures show that the head acceleration time histories exhibit much less fluctuation in version 1 than in version 2.

The majority of head injuries are contact based and may result from contact with a seatback or other vehicle interior components. As indicated in Figures 7.8 to 7.10, after the neck was altered, the head of the child model exhibits more excursion and rotation, and its displacement trajectory is more consistent with a pediatric cadaver. The reduction in neck tensile and rotational stiffness increases the risk of child head contact injuries. This is in agreement with the findings of Arbogast et al [5] indicating that increased compliance in the spine may create an entirely different head trajectory and result in severe head contact with interior vehicle structures.

## Neck response

Neck injury in children is rare but usually fatal when it occurs. Some of the injuries are difficult to diagnose [4] [36] [37]. The biomechanical response of the neck in the child model not only influences the head kinematics but is also critical to the accuracy of neck injury predictions in the simulations.

Due to issues the surrounding biofidelity of the Hybrid III dummy in the neck and torso [4] [5] [23], it cannot properly predict child neck injury. Because of this, the neck injury criteria have been excluded from FMVSS 213. The child model, prior to neck alterations, also exhibited unrealistically high neck tensile and rotational stiffnesses in comparison with the pediatric cadaver head/neck complex tests under quasi-static tensile and extension/flexion bending load conditions [8].

There are many factors that influence the tensile and bending stiffnesses of the child neck. The musculature, material properties, and local anatomic geometry are the most dominate parameters. Active muscles have a more significant effect on the biomechanical response than inactive muscles. Clinical findings [58] show that extension loading of the neck often leads to injuries in the upper cervical spine. The neck muscles act to stabilize and protect the cervical spine as well as to support and move the head. The local anatomic geometry and material properties of the child cervical vertebrae are other important factors [11] [55]. But as the comparison of the head/neck component model showed, the material properties of soft tissues associated with the cervical spine, the ligaments, the intervertebral discs, and facet joints, predominately influence the stiffness of the child cervical spine. This is consistent with the findings in other studies on the biomechanical response of an adult cervical spine [30].

Implementation of the adjusted material properties of the cervical spine in the child model has resulted in reductions in the upper and lower neck forces in the simulation of frontal crashes under FMVSS 213. The maximum upper and lower neck tensile forces are decreased by approximately 35% and 41%, respectively. The maximum lower neck compression force is also reduced by 46%.

When comparing the magnitudes of the neck forces as shown in Figure 7.11 and 7.12, the peak value of the lower neck force is only about half of that of the upper neck force in the simulations. Calculations of the neck forces include the ligaments, the

cervical intervertebral discs, and the facet joints but exclude the musculatures and other soft tissues in the neck area. These calculations are similar to the calculations from the head/neck component model. The effects of the musculatures of the child neck, however, should not be ignored in the prediction of child neck injuries. The active neck can take a considerable amount of load and reduce the force subjected to the cervical spine. This is true for an adult occupant [58]. However, due to its underdeveloped muscles and premature cervical spine, a 3-year-old child experiences the neck injury more often in the upper neck region than in the lower neck region. The force distribution along the neck of the child model is consistent with clinical findings [28] [36] [3] [38].

Ivancic et al. in 2007 [32] found that the joint of the head/C1 was generally more flexible than that of the other spinal levels for both adults and children. A typical child neck injury is traumatic atlanto-occipital dislocation [37]. Cervical spine injuries in the upper level neck are seen two and a half times more often in children than in adults. It has been suggested that atlanto-occipital dislocation should be considered in all children involved in motor vehicle accidents [37]. Diagnosis of atlanto-occipital dislocation has been based on the distance between the tip of the dens to the basion of the skull (DB distance). Encouragingly, this child model with the altered neck has demonstrated similar injury characteristics in frontal crash simulation as those from clinical findings, as Figure 7.3 illustrates. It clearly shows a shear deformation between the skull basion and cervical vertebra C2 and relative position changes between the C1 and C2 due to the cervical vertebra rotation and bending flexion deformation of the neck. Howard et al. [28] presented a similar child injury and riding condition in a real world crash as shown in Figure 2.17 (A). This phenomenon cannot be observed in the child model before the neck alteration and in the commonly used Hybrid III 3-year-old child dummy model for frontal crash simulations.

### **Chest response**

It has been demonstrated by Oi et al. in 2004 [58] that chest resultant acceleration increased with increasing delta-V and as the crash severity increased, the peak chest deflections also increased. To predict child chest injuries, there are critical values for chest acceleration and chest deflection which are currently being proposed by

FMVSS 213 for a 3-year-old child; 56 g's for a resultant chest acceleration and 34 mm for chest deflection. Peak values of chest acceleration and deflection are in the ranges of 36 g's to 38 g's and 19 mm to 13 mm, respectively, for both child models before and after neck alterations. All values are well below the proposed critical values.

The chest response of the child model illustrates some changes after the adjustment of the neck material properties. Some variations appear later (after 100 ms) in the simulations in terms of delayed peak timing and magnitude changes. This is a result of the greater levels of neck distraction and rotation in the altered child model. Increased head excursion and neck flexion deformation also delayed the influence of head/chest contact on chest acceleration and deflection.

## 8. CONCLUSIONS, LIMITATIONS AND FUTURE WORK

### 8.1 Conclusions

A head/neck component model was developed based on the child model developed by Nagoya University and compared with pediatric cadaver head/neck complex tests under distraction and extension/flexion bending loading conditions. After the material properties of the cervical spine in the head/neck component model were altered, the tensile and bending stiffnesses of the cervical spine were significantly reduced and the force/displacement and rotation/moment responses were in good agreement with the corridors of the pediatric cadaver head/neck complex tests. The kinematics and the biomechanical response of the child model were notably improved once the altered neck data from the head/neck component model were implemented.

For the research associated with the component testing the following conclusions can be made:

1. Soft tissues, such as ligaments, intervertebral discs, and facet joints, are most responsible for the tensile and rotational stiffness of the cervical spine for the child model.
2. The material properties of the soft tissues of the cervical spine in the child model, such as the ligaments, intervertebral discs, and facet joints, were altered by reducing the elastic modulus by 10 to 12.5 percent. After the material alteration, the neck tensile force was within the range of the cadaver head/neck complex tests and the rotation-moment curves were in good agreement to the corridor of the pediatric cadaver head/neck complex tests.

For the research associated with the implementation of the neck alterations in the child model considering FMVSS 213 and a cadaver sled test the following conclusions can be made:

3. Reduction in the neck tensile and rotational stiffness in the child model after the neck alterations reduced the upper neck tensile force by approximately 35% while the lower neck tensile force was reduced by 41% and 46% under a compression state.

4. The head and chest acceleration profiles from the simulations with and without the neck alterations remained similar. Values of  $HIC_{15}$  and  $HIC_{36}$  for both models are almost identical.
5. This child model was able to predict detailed mechanisms for neck injury, such as atlanto-occipital dislocation, under the same severity as a real world vehicle crash.
6. The kinematics of the head of the child model has been improved based on comparisons between the head trajectory and the pediatric cadaver sled test. The head displacement was increased by 3% and 5% in the X and in Z directions, respectively. The head rotation was also increased by 5%. Utilizing the altered neck biomechanical behaviour, the head trajectory was more consistent with child cadaver tests.
7. The time of contact between the head and chest increased after incorporating biomechanical behaviour into the neck of the child model. There was no complete separation from the beginning of the head/chest contact to the end of the simulation.
8. Alteration of the neck material properties in the child model illustrated an insignificant influence on chest acceleration but some notable differences to chest deflection. The chest deflection is approximately 3 mm lower in the child model with neck alterations.

In general, after the material properties of the child neck were altered, the child FE model provided more accurate biomechanical responses and kinematics in simulations of vehicle frontal impact. Its bio-fidelity has been improved compared to the child model without the alterations and the current Hybrid III 3-year-old child dummy FE model.

## **8.2 Limitations**

Since the moment/rotation curve of the cervical spine under the extension bending load condition deviated slightly from the corridor of the pediatric cadaver head/neck complex tests, there is a limitation in this research associated with the rotational stiffness of the cervical spine. This could also be due to a lack of modification to the local anatomic geometry and material properties of the child cervical vertebrae. Adjustments to

the material properties of the neck of the child model were based on strain energy and considered only elastic material characteristics (elastic modulus) due to the complexity of the model and the limited available clinical and experimental pediatric data.

### **8.3 Future Work**

Considerations for the musculature, local anatomic geometry, and biomechanics of the cervical vertebrae of children should be a part of future study on the child model. Future research should also consider the effect of child brain modeling and its contribution to head injury prediction so as to further improve the biofidelity of the child model.

## REFERENCES

1. Report of World Health Organization (WHO), Youth and Road Safety, 2007. [http://www.who.int/violence\\_injury\\_prevention](http://www.who.int/violence_injury_prevention), accessed December, 2007.
2. A. Williamson, P. Irvine and S. Sadural, "Analysis of motor vehicle-related fatalities involving children under the age of six years (1995-2000)", NSW Injury Risk Management Research Centre, Report for the Motor Accidents Authority, pp. 1-47, July 2002.
3. NHTSA report: 2004 Motor Vehicle Occupant Protection Facts: Children, Youth, Young Adult. 2006, <http://dms.dot.gov>, accessed January, 2008.
4. J. Kang, G. Nusholtz and V. Agaram, "Hybrid III Dummy Neck Issues", SAE Technical Paper Series No. 2005-01-1704, 2005.
5. K. B. Arbogast and F. K. Winston, "Advanced Safety Technology for Children and Young Adults: Trends and Future Challenges", SAE International Convergence 2006, Detroit, Michigan, October 16-18, SAE Technical Paper Series No. 2006-21-0007.
6. K. Mizuno, K. Iwata, T. Deguchi and T. Ikami, "Development of a Three-Year-Old Child FE Model", Traffic Injury Prevention, Vol. 6, pp. 361-371, 2005.
7. K. Mizuno, K. Iwata, T. Namikiri and N. Tanaka, "Comparison of human FE model and crash dummy response in various child restraint systems", 2006 International Crashworthiness Conference, Athens Greece, 2006.
8. J. Ouyang, Q. Zhu, W. Zhao, Y. Xu, W. Chen and S. Zhong, "Biomechanical Assessment of the Pediatric Cervical Spine Under Bending and Tensile Loading", SPINE Volume 30 Number 24, pp. E716-E723, 2005.
9. M. Tot, "A Comparison of the Kinematic Response and Biofidelity of the Neck of Pediatric Cadaver Data and the Hybrid III Three-Year-Old Child Finite Element Model", Thesis of Master Degree of Human Kinetics at the University of Windsor, 2007, Windsor Ontario Canada.
10. R. Dupuis, F. Meyer, R. Willinger, "THREE YEARS OLD CHILD NECK FINITE ELEMENT MODELISATION", Université Louis Pasteur, France, Paper Number 05-0081 <http://www-nrd.nhtsa.dot.gov/pdf/nrd-01/esv/esv19/05-0081-W.pdf>, accessed January, 2008.
11. S. Kumaesan, N. Yoganandan, F. A. Pintar, D. J. Maiman and S. Kuppa, "Biomechanical Study of Pediatric Human Cervical Spine: A Finite Element Approach", Journal of Biomechanical Engineering, Vol. 122, pp. 60-71, February 2000.



12. Transport Canada report: Canadian Motor Vehicle Traffic Collision Statistics: 2005, <http://www.tc.gc.ca/roadsafety/tp/tp3322/2005/menu.htm>, accessed January, 2008.
13. NHTSA DOT HS 810 837: Motor Vehicle Traffic Crash Fatality Counts and Estimates of People Injured for 2006, September 2007. <http://dms.dot.gov>. accessed January, 2008.
14. M. Sawada and J. Hasegawa “Development of New Whiplash Prevention Seat”, Toyota Motor Corporation, Japan, Paper Number 05-0288, 19<sup>th</sup> International Technical Conference on the Enhanced Safety of Vehicles, Washington DC, United States, 2005.
15. NHTSA DOT HS 809 784, Technical Report: Child Passenger Fatalities and Injuries, Based on Restraint Use, Vehicle Type, Seat Position, and Number of Vehicles in the Crash, April 2005.
16. D. R. Durbin, I. Chen, R. Smith, M. R. Elliott and F. K. Winston, “Effects of Seating Position and Appropriate Restraint Use on the Risk of Injury to Children in Motor Vehicle Crashes”, *Pediatrics* 2005, 115, pp. 305-309.
17. NHTSA Traffic Safety Facts 2005 Data Children: DOT HS 810 618, <http://www-nrd.nhtsa.dot.gov/Pubs/810618.PDF>, accessed January, 2008.
18. C. Parenteau and D. C. Viano, “Field Data Analysis of Rear Occupant Injuries Part II: Children, Toddlers and Infants”, SAE Technical Paper Series No. 2003-01-0154, 2003.
19. D. J. Nuckley, R. P. Ching, “Developmental biomechanics of the cervical spine: Tension and compression”, *Journal of Biomechanics* 39 (2006) pp. 3045–3054.
20. J. A. Goldwitz, W. W. Van Arsdell, “FMVSS Child Occupant Protection Regulations”, SAE Technical Paper Series No. 2006-01-1138, 2006.
21. Federal Motor Vehicle Safety Standards No. 208; Occupant crash protection, Docket No. 571.208, *Federal Register*, Vol. 63, 28935, May 27, pp. 497-580, 1998.
22. W. W. Van Arsdell, “The Evolution of FMVSS 213: Child Restraint System”, SAE Technical Paper Series No. 2005-01-1840.
23. J. Yannaccone, F. Whitman, L. Sicher and L. D’Aulerio, “Analysis of Nij in simulated real-world crashes with a 3-year-old Hybrid-III”, *IJCrash* 2006 Vol. 11 No. 5 pp. 443-457.
24. R. Menon, Y. Ghata, S. Ridella, D. Roberts, F. Winston, “Evaluation of Restraint Type and Performance Tested with 3- and 6-Year-Old Hybrid III Dummies at a Range of Speeds”, SAE Technical Paper Series No. 2004-01-0319, 2004.

25. NHTSA: TRAVELING SAFELY WITH CHILDREN: THE BASICS, <http://www.nhtsa.dot.gov/people/injury/childps/newtips/pages/Tip1.htm>, accessed January, 2008.
26. Volvo Car Corporation, "A SAFETY MANUAL: CHILDREN IN CARS", Second edition 2004.
27. NHTSA DOT HS 809 489: LATCH Makes Child Safety Seat Installation As Easy As 1,2,3. August 2002.
28. A. Howard, A. M. McKeag, A. German, I Hale, W. Altenhof and R. Turchi, "Cervical Spine Injuries in Children Restrained in Forward Facing Child Restraints", Proceedings of the Canadian Multidisciplinary Road Safety Conference XIII, June 8-11, 2003, Banff, Alberta.
29. "Techniques for developing child dummy protection reference values, Event report", Child injury protection team, October 1996, pp. 1-87, <http://www-nrd.nhtsa.dot.gov/pdf/nrd-51/kid.pdf>. accessed January, 2008.
30. N. Yoganandan, S. Kumaresan, F. A. Pintar, "Biomechanics of the cervical spine Part2. Cervical spine soft tissue responses and biomechanical modeling", Clinical Biomechanics 16 (2001) pp. 1-27. Reprinted with permission from Elsevier, Copyright (2001).
31. <http://commons.wikimedia.org/wiki/Image> , accessed June, 2008.
32. P. Viccellio, H. Simon, B. D. Pressman, M. N. Shah, W. R. Mower, J. R. Hoffman, "A prospective Multicenter Study of Cervical Spine Injury in Children", Pediatrics 2001; 108;e20.
33. K. Arbogast, R. Cornejo, M. Kallan, F. Winston, and D. Durbin, "Injuries to children in forward facing child restraints", The Department of Pediatrics, [http://www.unece.org/trans/doc/2002/wp29grsp/Injuries\\_in\\_FFCRS\\_final.pdf](http://www.unece.org/trans/doc/2002/wp29grsp/Injuries_in_FFCRS_final.pdf), The Children's Hospital of Philadelphia, pp. 1-17. accessed January, 2008.
34. A. J. McLean and Robert W. G. Anderson, "BIOMECHANICS OF CLOSED HEAD INJURY, Head Injury", Published in 1997 by Chapman & Hall, London, ISBN 0 412 58540 5
35. M. Prange, W. Newberry, T. Moore, D. Peterson, B. Smyth and C. Corrigan, "Inertial Neck Injuries in Children Involved in Frontal Collisions", SAE International 2007 World Congress Detroit, Michigan, April 16-19, 2007, SAE Technical Paper Series No. 2007-01-1170.

36. E. S. Lustrin, S. P. Karakas, A. Orlando Ortiz, J. Cinnamon, M. Castillo, K. Vaheesan, J. H. Brown, A. S. Diamond, K. Black, S. Singh, "Pediatric Cervical Spine: Normal Anatomy, Variants, and Trauma", *RadioGraphics* 2003; 23: pp. 539–560.
37. D. I. Bulas, C. R. Fitz, D. L. Johnson, "Atlanto-Occipital Dislocation in Children", *Radiology* 1993; 188:155-158.
38. M. R. Sochor, D. P. Faust, K. F. Anderson, S. Barnes, S. A. Ridella, S. C. Wang, "Assessment of 3 and 6-Year-Old Neck Injury Criteria Based on Field Investigation, Modeling, and Sled Testing", SAE Technical Paper Series No. 2006-01-0253, 2006.
39. P. C. Ivancic, S. Ito, M. M. Panjabi, "Dynamic sagittal flexibility coefficients of the human cervical spine", *Accident Analysis and Prevention* 39 (2007) 688–695.
40. T. Kapoor, W. Altenhof, Q. Wang, A. Howard, "Injury potential of a three-year-old Hybrid III dummy in forward and rearward facing positions under CMVSS 208 testing conditions", *Accident Analysis and Prevention* 38, pp. 786-800,2006
41. Q. Wang, T. Kapoor, W. Altenhof, L. Chen and A. Howard, "Use of Rigid and Deformable Child Restraint Seats in Finite Element Simulations of Frontal Crashes", SAE Technical Paper Series, SAE paper no. 2006-01-1141, 2006.
42. R. Turchi, W. Altenhof, T. Kapoor, and A. Howard, "An investigation into the head and neck injury potential of three-year-old children in forward and rearward facing child safety seats", *International Journal of Crashworthiness*, Vol. 10, pp. 1–14, 2004.
43. L. L Greaves, Q. Zhu, P. A. Cripton, M.Cluff, C. Y. Greaves, A. Melnyk, A. Perdios, S. Tredwell and K. Mulpur, "The Effect of Age and Gender on the Three-Dimensional Kinematics of the Pediatric Cervical Spine", SAE Technical Paper Series No. 2007-01-2495, 2007.
44. F. Meyer, R. Willinger, F. Legall, "The Importance of modal validation for biomechanical models, demonstrated by application to the cervical spine", *Finite Elements in Analysis and Design* 40 (2004) pp. 1835-1855.
45. D. Kallieris, J Barz, G. Schmidt, G. Heess, and R. Mattern, "Comparison between child cadavers and child dummy by using child restraint systems in simulated collisions", 20th STAPP Car Crash Conference, SAE Technical Paper Series No 760815, 1976.
46. F. Brun Cassan, M. Page, Y. Pincemallie, D. Kallieris and C. Tarriere, "Comparative study of restrained child dummies and cadavers in experimental crashes", SAE Technical Paper Series, SAE paper no. 933105, 1993.
47. J. Wismans, J. Maltha, J.w. Melwin, R. L. Stalnaker, "Child Restraint Evaluation by Experimental Simulation", Twenty-Third STAPP Car Crash Conference, 1979.

48. J. Wismans, Design Tools: Human Body Modeling, pp. 227-268, 2007.  
<http://www.autosteel.org/AM/Template.cfm?Section=PDFs&CONTENTID=4277&TEMPLATE=/CM/ContentDisplay.cfm> accessed June, 2008.
49. Computational Human Model THUMS (Total HUMAN Model for Safety) Briefing Sheet Occupant Model: Version 1.52  $\beta$ -040526 TOYOTA CENTRAL R&D LABS., INC.
50. F. Oshita, K. Omori, Y. Nakahira and K. Miki, "Development of a Finite Element Model of The Human Body", 7th International LS-Dyna User Conference, pp (3-37)-(3-48), 2002.
51. M. Iwamoto, K. Omori, H. Kimpara, Y. Nakahira, A. Tamura, I. Watanabe, K. Miki, J. Hasegawa and F. Oshita, "Recent advances in THUMS: development of individual internal organs, brain, small female, and pedestrian model", 4th European LS-DYNA Users Conference, 2003.
52. H. Ipek, H. Steffan, M. Hofinger, A. Keding and Z. Karacay, "Enhanced Simulation Models for Lower Extremity Injuries", 3rd LS-DYNA Anwenderforum, Bamberg 2004.
53. W. Zhang, T. Kapoor, W. Altenhof, A. Howard and K. Mizuno, "A Comparison of Kinematics of a Child Finite Element Model and the HYBRID III 3-Year-Old Dummies in Frontal Crashes", SAE Technical Paper Series No. 2007-01-0977, 2007.
54. F. Meyer, F. Roth, R. Willinger, D. Baumgartner, "Child Neck Injury Mechanisms Based on FE Modeling", Child Injury Led Design, 2006
55. S. Kumaesan, N. Yoganandan, F. A. Pintar and W. M. Mueller, "Biomechanics of Pediatric Cervical Spine: Compression, Flexion and Extension Responses", J. Crash Prevention and Injury Control, Vol. 2 (2), pp. 87-101, 2000.
56. Livermore Software Technology Corporation, LS-Dyna Keyword User's Manual, Version 970, April 2003.
57. SAE J211/1, Instrumentation for Impact Test – Part 1 – Electronic Instrumentation, Society of Automotive Engineers, 2003.
58. N. Oi, M. G. Pandy, B. S. Myers, R. W. Nightingale, V. C. Chancey, "Variation of Neck Muscle Strength along the Human Cervical Spine", Stapp Car Crash Journal, Vol. 48 (November 2004), pp. 397-417.
59. <http://www.hughston.com/hha/a.cspine.htm> , accessed June, 2008.

## APPENDIX A

### Comparisons between FE Child Model Version 1 and Version 2

Child model version 1 was developed in 2005 [6] and version 2 was incorporated improvements to version 1 in 2006 [7]. Figure A.1 (A) illustrates the child model with some soft tissues removed to expose the skeletal structure. The known differences between the two versions are as follows:

**The head:** The material of brain and skull changed from rigid in version 1 to Isotropic\_Elastic\_Plastic in version 2. Figure A.1 (B) illustrates the sectional view of the head.

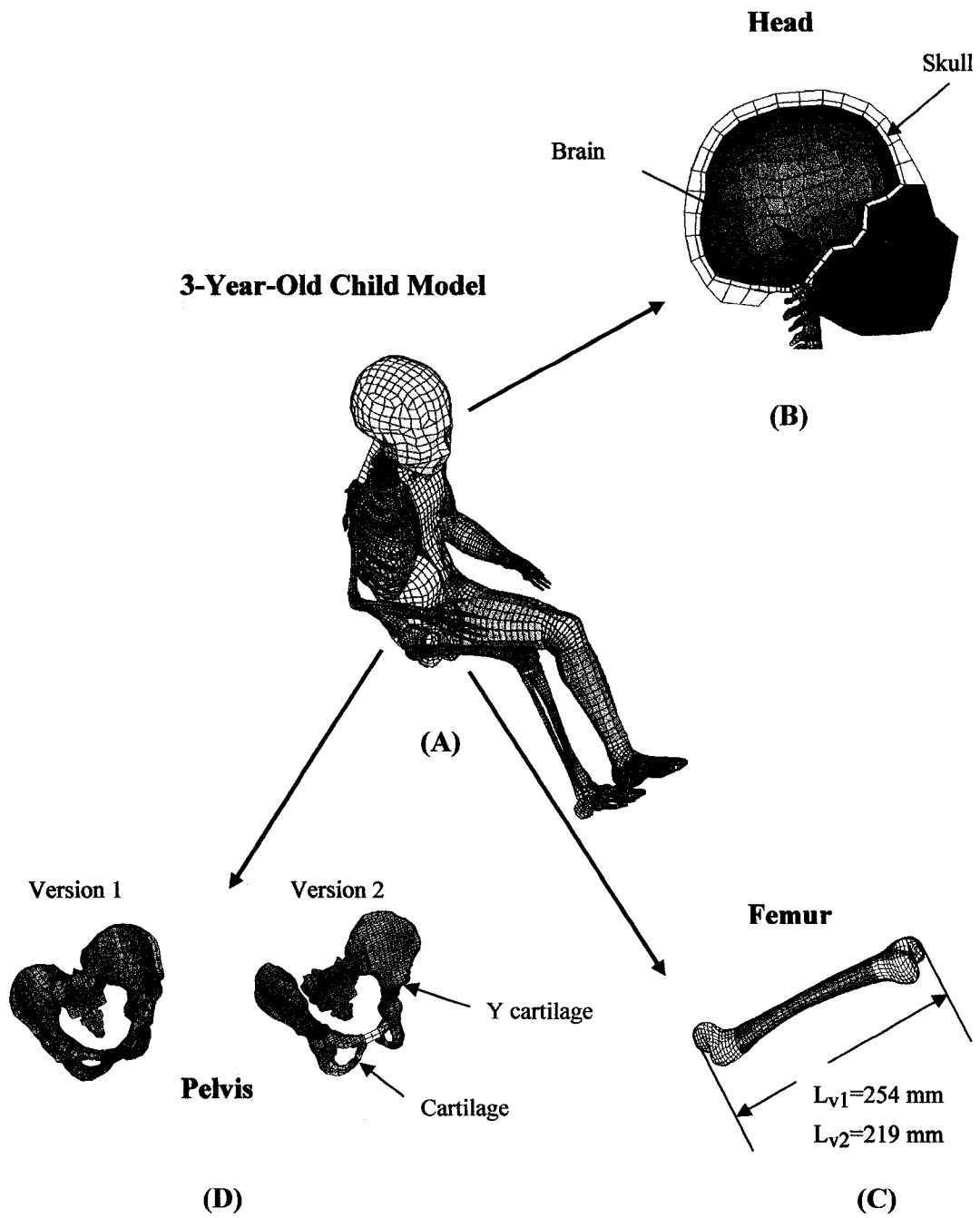
**The total weight of the child model:** 15.72 kg in version 1 and 14.91 kg in version 2.

**The femur length:**  $L_{v1} = 254$  mm for version 1 and  $L_{v2} = 219$  mm for version 2 as shown in Figure A1 (C).

**Pelvis:** The pelvis in version 1 is scaled down from the adult model (THUMS) and the pelvis in version 2 is based on the anatomical structures and material properties of a child. Cartilage and Y cartilage were added to the pelvis in the child model version 2. Figure A.1 (D) illustrates the differences between the two models.

#### Other changes in child model version 2 are:

- Change material of forearm bones and hand bones from deformable to rigid;
- Improvement of joint modeling in wrist region;
- Add more contact interfaces:
  1. Head - Arm Contact (soft constraint formulation)
  2. Humerus - Forearm bones Contact (FS = 0.3, FD = 0.3)
  3. Knee - Knee Surface Contact (soft constraint formulation)
  4. Head - Harness Contact (FS = 0.5, FD = 0.45)
  5. Buttock interior - Buttock Surface Contact (soft constraint formulation)
  6. Head - Thigh, Knee Contact (soft constraint formulation)
- Add seatbelt elements (M.serratus\_anterior) between scapula and rib



Note:  $L_{v1}$  - femur length for child model version 1;  $L_{v2}$  - femur length for child model version 2.

**Figure A.1 Child model and its modifications from version 1 to version 2.**

## Frontal Impact Simulations:

### Using FMVSS 213 Sled Test Pulse:

FMVSS 213 frontal dynamic sled test was completed at Graco Corporation's sled testing facilities using Hybrid III 3-year-old child dummy. The testing apparatus consisted of a sled with an approximate mass of 635 kg. During a typical impact test, the sled was accelerated towards a fixed seismic mass using pneumatic pressure with an impact velocity of 41.7 km/h (25.9 mph). The acceleration pulse experienced by the sled during the impact was controlled by a hydraulic damper at the front of the sled. Figure A.2 illustrates the crash testing facilities. The acceleration pulse which the sled experienced in a direction opposite to the impact velocity and the lower and upper limits of sled acceleration outlined in FMVSS 213 are illustrated in Figure A.3.

In the test, the child dummy was positioned and restrained in a forward facing five-point restraint system which was secured to the LATCH system. The setup and the procedure of the test can be found in the reference of Turchi et al. in 2004 [42] and Wang et al. in 2006 [41].



**Figure A.2 FMVSS 213 sled test at Graco Corporation's sled testing facilities (41).**

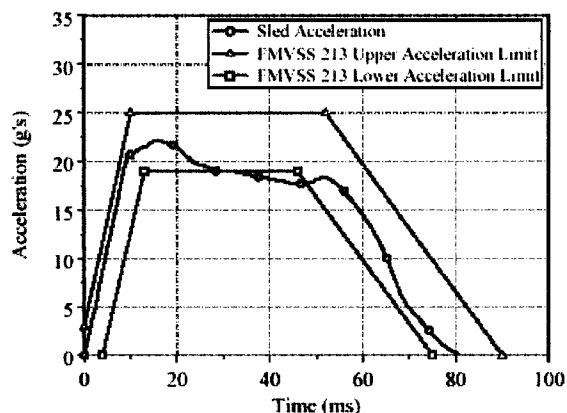


**Figure A.3 FMVSS 213 sled test acceleration (with the upper/lower limits) versus time curve [41].**

**Using Cadaver Test Pulse:**

Experimental child cadaver testing was conducted for frontal crashes at the University of Heidelberg. The experimental child cadaver is a 2½ year old male with a mass of 16 kg and length of 97 cm in a shield form CRS.

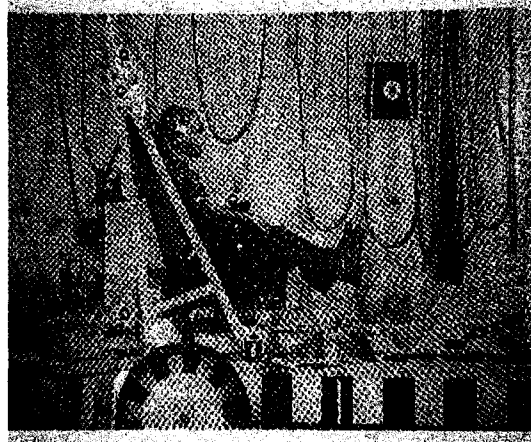


**Figure A.4 Sled test with test subject and CRS [45].**

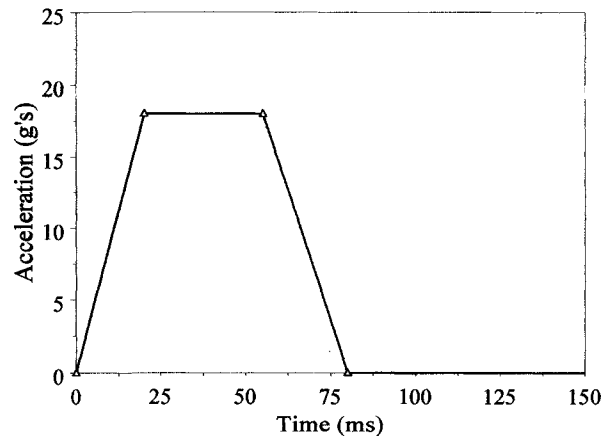


**Figure A .5 Child cadaver testing acceleration pulse [45].**



## Kinematics Comparison (FMVSS 213 Simulations)

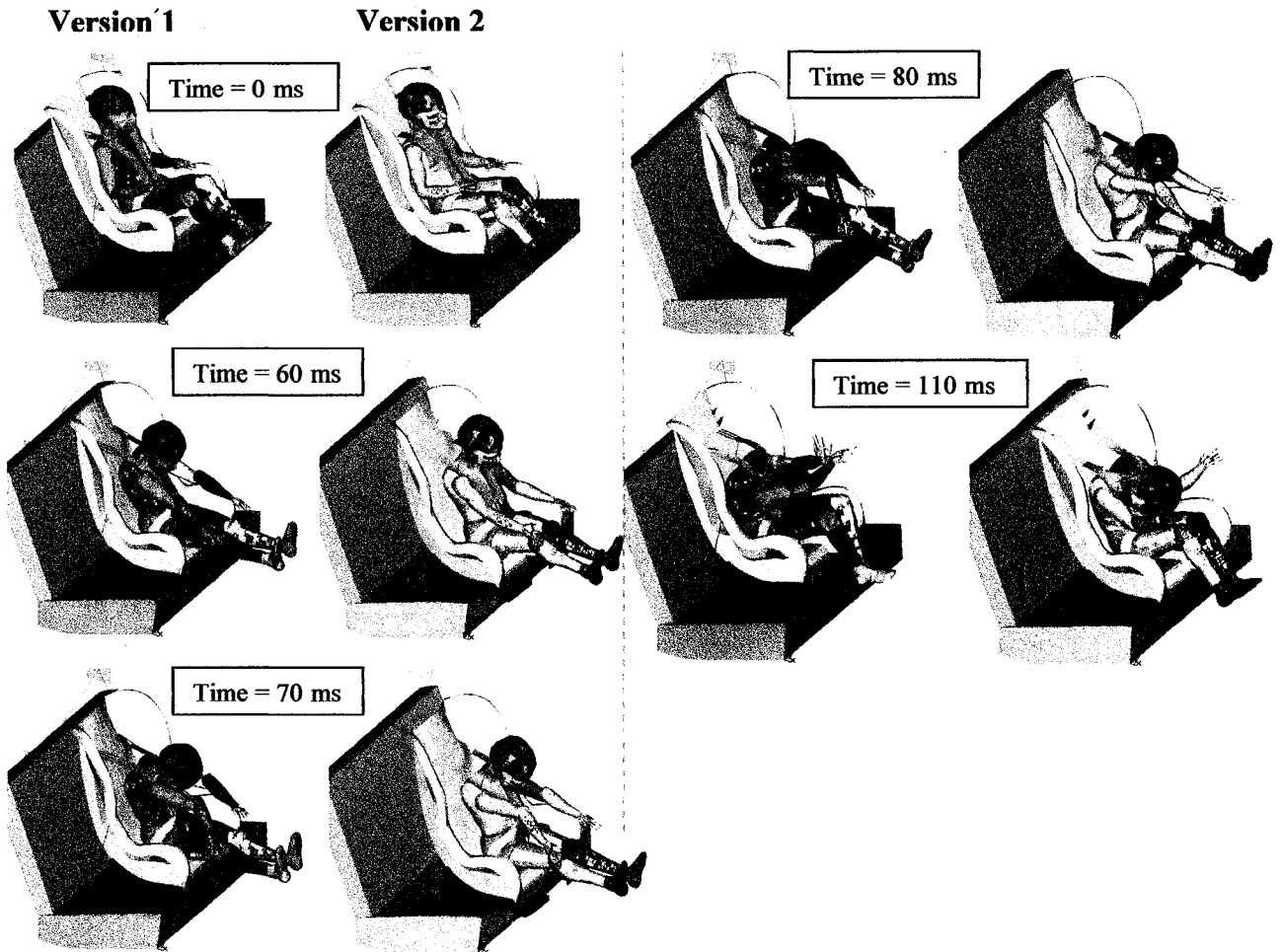


**Figure A.6 Kinematic response comparison of FMVSS 213 simulations of the child model version 1 and version 2.**

- The neck and upper torso of the child model version 1 illustrates more significant deformation at earlier arrival time. At 60 ms it illustrates a significant difference in kinematics between the two versions.
- The head of the child in version 1 first came to in contact with the chest at 72.5 ms, and then the head of the child model in version 2 started to contact with the chest at 82.5 ms.
- The behaviours of the arm and hand also showed large difference between the two versions.
- It was noticed that the scapula of the child in version 1 penetrated through the chest during the simulation.

## Kinematics Comparison (FMVSS 213 CAE Simulations)

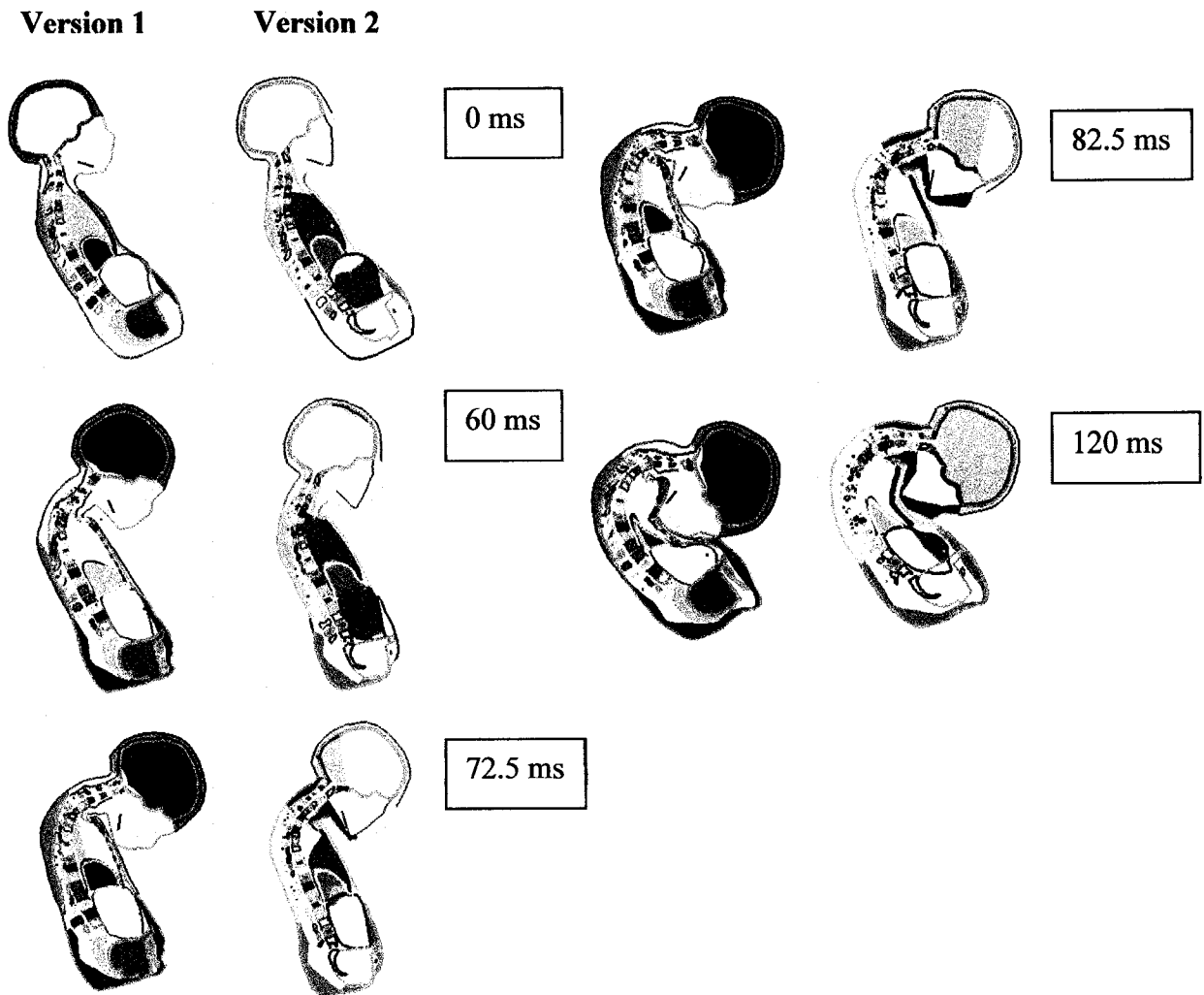
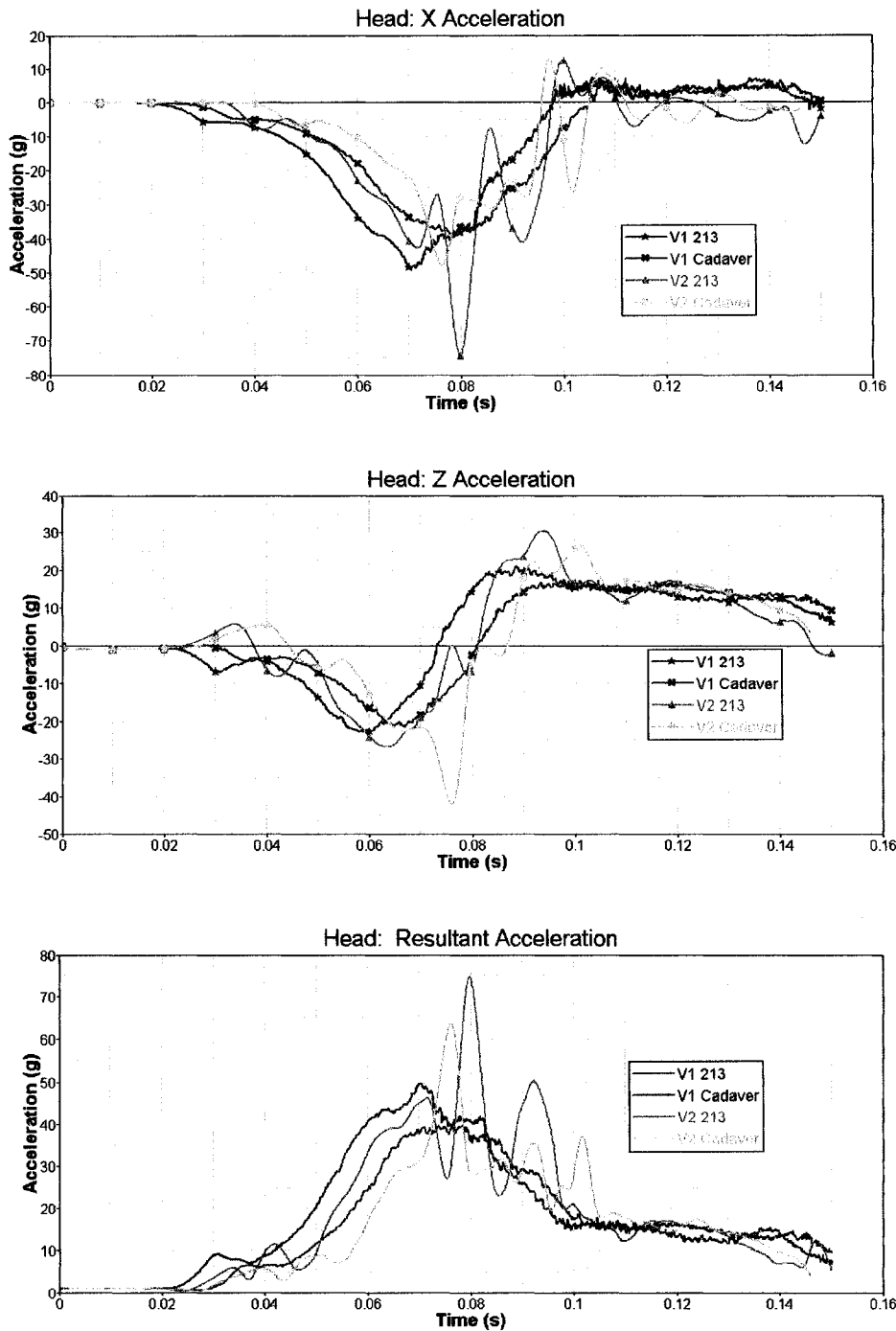


**Figure A.7 Sectional view of kinematic response comparison of FMVSS 213 simulations of the child model version 1 and version 2.**

- The sections of the child model show more clearly the differences between the two models at different time intervals in the simulations. The child model version 1 has more significant and earlier deformation than the version 2.
- The sections show that the head of the child in version 1 came to in contact with the chest at 72.5 ms while the head of the child model in version 2 started to contact with the chest at 82.5 ms. This contact was delayed by 10 milliseconds in the version 2 compared to version1.
- About 120 milliseconds the deformation of the child model reached the maximum.
- During the analysis of the simulation it was found that the child model version 1 had more asymmetric deformation than the version 2.

## Head Acceleration Comparison



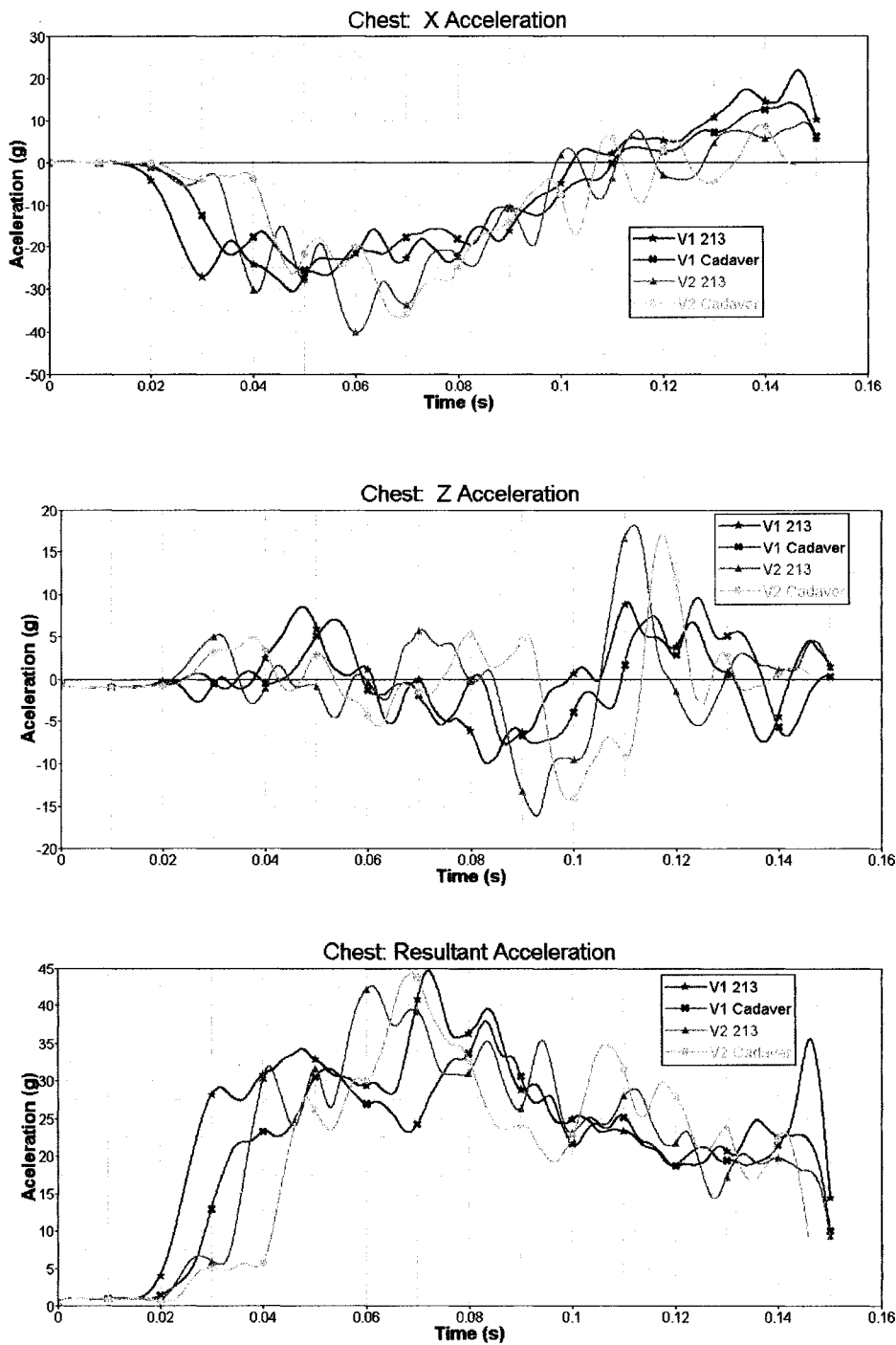
- The head accelerations of child model version 2 are higher than version 1 in both simulation cases using FMVSS 213 sled test and cadaver test acceleration pulses.

- The peak accelerations of the head in the X, Z directions and the peak resultant accelerations from the child model version 2 appear later by 10 ms than version 1 in both simulation cases using FMVSS 213 sled test and cadaver test acceleration pulses.

- The head accelerations from the simulation using cadaver test pulse are lower than using FMVSS 213 sled test pulse.

**Figure A.8 Head acceleration comparison of FMVSS 213 and cadaver sled test simulations of the child model version 1 and version 2.**

## Chest Acceleration Comparison



- The chest accelerations of child model, version 2, are higher than version 1 in both simulation cases using FMVSS 213 sled test and cadaver test acceleration pulses.

- The peak accelerations of the chest in the X, Z direction and the peak resultant accelerations from the child model version 2 appear later by 10 ms than version 1 in both simulation cases using FMVSS 213 sled test and cadaver test acceleration pulses.

- The chest acceleration pulses from the CAE simulation using cadaver test pulse are lower than using sled test pulse.

**Figure A.9 Chest acceleration comparison of FMVSS 213 and cadaver sled test simulations of the child model version 1 and version 2.**

## Neck Section Normal Force Comparison

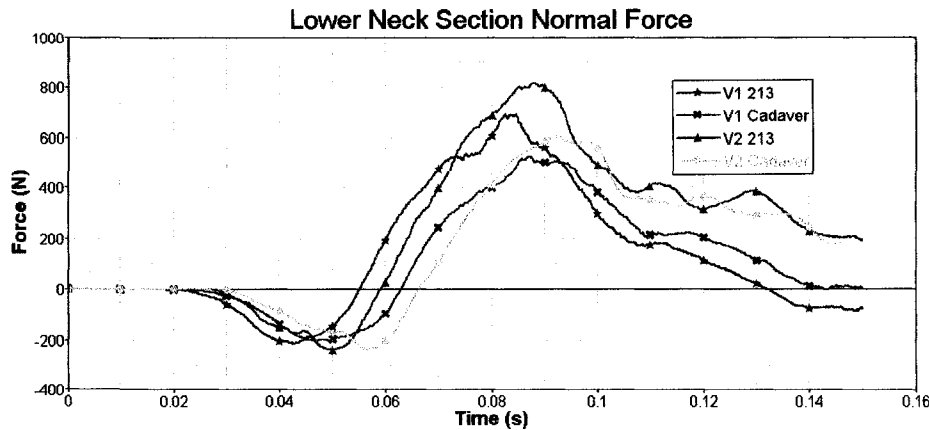


**Figure A.10 Lower neck section force comparison of FMVSS 213 and cadaver sled test simulations of the child model version 1 and version 2.**

Comparison of the lower neck section normal force presented in Figure A.10 illustrates that the maximum values of the neck tensile force from the child model version 2 are higher and commence later than from version 2 in both CAE simulation cases.

## Discussion

The overall comparison of the two version child models shows that the child model version 1 exhibits lower stiffness of the neck and upper torso, and softer pulses of the head and chest than the version 2. The possible causes for these differences are as follows:

- The material properties of the brain and skull changed from Rigid to Isotropic\_Elastic\_Plastic in version 2;
- The significant deformation of the shoulder/arm deformation in version 1;
- The scapula penetrated the chest at shoulder inversion 1;
- Pelvis change in version 2.

The kinematics of the upper extremity has significantly changed in version 2. The following reasons may be responsible for these changes:

- The Head - Arm Contact has been added in version 2 and;
- SEATBELT elements between scapula and rib are new in version 2 (indicated in the original input file, but not yet identified in the model);
- The penetration of the scapula has been eliminated in version 2.

## **APPENDIX B**

### **The Abbreviated Injury Scale**

The Abbreviated Injury Scale (AIS) provides a ranking of the severity of injury. Injuries are ranked on a scale of 1 to 6, with 1 being minor and 6 being an unsurvivable injury. The scale represents the threat to life associated with an injury and is not meant to represent a comprehensive measure of severity. The AIS is not an injury scale, in that the difference between AIS1 and AIS2 is not the same as that between AIS4 and AIS5.

<b>Injury</b>	<b>AIS Score</b>
1	Minor
2	Moderate
3	Serious
4	Severe
5	Critical
6	Unsurvivable

## APPENDIX C

### Strain Energy Distribution of Neck Soft Tissues in the Child Head/Neck

#### Component Model

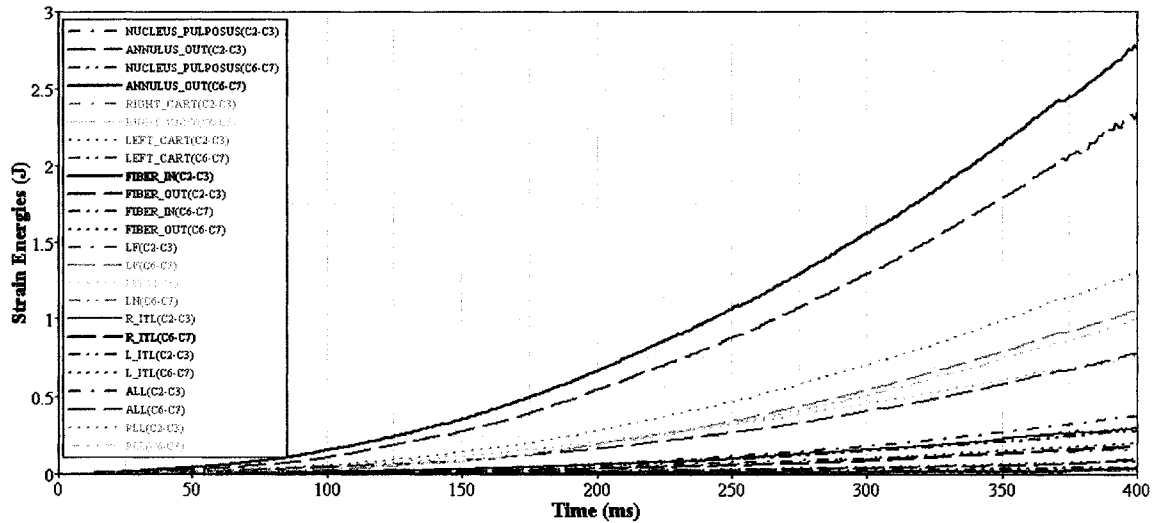


**Figure A. 10 Strain energy distribution of neck soft tissues in the child head/neck component model under tensile loading condition.**

LN: interspinous ligament (ISL);

LF: ligamentum flavum (LF);

ALL: anterior longitudinal ligament

PLL: posterior longitudinal ligament

ANNULUS\_OUT: annulus fibrosus intervertebral discs;

RIGHT\_CART, LEFT CART: facet joints between two adjacent vertebrae;

FIBER\_IN, FIBER\_OUT: on the out skin of two portions of the disc there were seatbelt elements as fiber connecting the adjacent two vertebrae.

## APPENDIX D

### Copyright Permission

#### Copyright Permission from LIPPINCOTT WILLIAMS & WILKINS

**From:** "Johnson, Gwen" <Gwen.Johnson@wolterskluwer.com>  
**Subject:** Copyright Permission Approval  
**Date:** Thu, 31 Jul 2008 08:39:05 -0500  
**To:** <zhangl@uwindsor.ca>

Dear Mr. Zhang,

Permission is granted to reproduce the requested material for use in your academic thesis/dissertation. Permission is granted provided a prominent credit line is placed stating the original source and copyright owner, LIPPINCOTT WILLIAMS & WILKINS.

Sincerely,

*Gwen Johnson*  
*Sen. Permissions Editor*  
*Wolters Kluwer Health*  
*351 W Camden Street*  
*Baltimore, MD 21201*  
*410-528-4416*  
*Gwen.Johnson@wolterskluwer.com*  
*<http://www.lww.com/resources/permissions/journals.html>*

**From:** Zhang Wencheng [mailto:zhangl@uwindsor.ca]  
**Sent:** Thursday, July 24, 2008 3:20 PM  
**To:** Johnson, Gwen  
**Subject:** Seeking Copyright Permission

Dear Ms. Gwen Johnson,

I am writing my thesis , Master of Applied Science degree in Mechanical Engineering at the University of Windsor, Ontario, Canada. Within my thesis I would like to use Figures 1 and 2 and test data of Figures 3 and 4 in the publication "Biomechanical Assessment of the Pediatric Cervical Spine Under Bending and Tensile Loading" in SPINE Vol. 30 No. 24, 2005, pp. e716-e723 as reference. I am requesting your permission to use these figures in my thesis. My thesis would be printed in 5 copies. Two copies would be deposited in the University of Windsor Library. One copy would be deposited in the Mechanical Engineering Department. The other two copies would be given to individuals. I would very appreciate it if

you could respond to this at your earliest convenience.

Thank you very much!



Best regards,

Wencheng Zhang

MASc. Candidate

University of Windsor  
Department of Mechanical, Automotive and Materials  
Engineering  
401 Sunset Avenue, Windsor, Ontario, Canada N9B 3P4 > Tel: +1 (519) 253-3000 ext. 2619  
Email: [zhangl@uwindsor.ca](mailto:zhangl@uwindsor.ca)

### Copyright Permission from SAE

**From:** "Dawn Frenchak" <dawn@sae.org>  
**Subject:** RE: Seeking copyright permission  
**Date:** Wed, 30 Jul 2008 09:12:30 -0400  
**To:** "Zhang Wencheng" <zhangl@uwindsor.ca>

Dear Sir,

Thank you for your e-mail in which you requested permission to use Figure 7 from SAE Paper # 2006-21-0007, Figure 3A and 3B from 2006-01-0253, Table 1 and Figures 2-7 from 2004-01-0319, and Figures 1, 2, and 6 from 2006-01-1141. I understand that these figures and table will be used in your thesis at the University of Windsor.

We request that the following credit line be used for all with the exception of SAE Paper # 2006-21-0007:

"Reprinted with permission from SAE Paper # XXXXXX\* © XXXX\*\* SAE International."

(\*please insert the paper number and \*\*year of publication)

Credit line for 2006-21-0007:

"Reprinted with permission from SAE Paper # 2006-21-0006 © 2006 Convergence Transportation Electronics Association and SAE International."

Permission is for this one-time use only. New requests are required for subsequent editions, for reprints or excerpts, or for other uses of the material.

Thank you for contacting SAE and for your cooperation.

Sincerely,

Dawn Frenchak

Intellectual Property Rights Administrator

SAE Permissions

Phone: 1-724/772-8518

Fax: 1-724/776-3036

**From:** Zhang Wencheng [mailto:[zhangl@uwindsor.ca](mailto:zhangl@uwindsor.ca)]

**Sent:** Tuesday, July 29, 2008 7:04 AM

**To:** copyright

**Cc:** Dawn Frenchak

**Subject:** Seeking copyright permission

**Importance:** High

Dear Sir or Madam,

I am writing my thesis for my Master of Applied Science degree in Mechanical Engineering at the University of Windsor, Ontario, Canada. Within my thesis I would like to use the figures and tables in the publications listed in the attached file. I am requesting your permission to use these figures and table in my thesis. My thesis would be printed in 5 copies. Two copies would be deposited in the University of Windsor Library. One copy would be deposited in the Mechanical Engineering Department. The other two copies would be given to individuals. I would very appreciate it if you could respond to this at your earliest convenience.

Thank you very much!

Best regards,

Wencheng Zhang

MASc. Candidate

University of Windsor

Department of Mechanical, Automoti! ve and Materials  
Engineering

401 Sunset Avenue, Windsor, Ontario, Canada N9B 3P4

Tel: +1 (519) 253-3000 ext. 2619

Email: [zhangl@uwindsor.ca](mailto:zhangl@uwindsor.ca)

## Copyright Permission from American Academy Pediatrics

**From:** "Angela Zade" <AZade@aap.org>  
**Subject:** Permission Agreement  
**Date:** Fri, 20 Jun 2008 12:57:07 -0500  
**To:** <zhangl@uwindsor.ca>

Hi, Wencheng.

Thank you for your request to utilize content from PEDIATRICS. There is no fee associated with your request. We do ask, however, that you please sign, date and return the permissions agreement letter for our records at your earliest convenience. Thank you!

Enjoy the rest of your day,  
Angela

Angela R. Zade  
Permissions & Rights Specialist  
Division of Scholarly Journals & Professional Periodicals  
American Academy of Pediatrics  
141 Northwest Point Blvd.  
Elk Grove Village, IL 60007-1098  
[www.aappublications.org](http://www.aappublications.org)  
Voice: 847-434-4344  
Fax: 847-434-8000  
Email: [azade@aap.org](mailto:azade@aap.org)

See the permissions agreement letter in the next page.



MAILOR FAX TO:	▶	American Academy of Pediatrics
		Attn: Medical Journal Permissions
		141 Northwest Point Blvd.
		Elk Grove Village, IL 60007
		Fax 847-434-8000

Date: 6/19/08  
AAP Fed. ID: 36-2275-597  
Permissions Fee: No Charge

To: Name: Wencheng Zhang  
Title: Student  
Organization: University of Windsor

Email: zhangl@uwindsor.ca  
Phone: Fax:

Address:

Fr: Angela Zade, Division of Scholarly Journals and Professional Periodicals,  
azade@aap.org  
Re: Citation: Dennis R. Durbin, Irene Chen, Rebecca Smith, Michael R. Elliott, and  
Flaura K. Winston  
Effects of Seating Position and Appropriate Restraint Use on the Risk of Injury to  
Children in Motor Vehicle Crashes  
Pediatrics, Mar 2005; 115: e305 - e309  
Reason for Use: Reproduce FIGURE 1 in thesis  
Permissions Fee: NO CHARGE /Permissible Purpose: student courtesy

#### Conditions of Agreement

The conditions of this Agreement are listed below. If the conditions are agreeable with you please sign, date, and return this form to the address or fax number above.

1. The following credit line must appear:  
**Reproduced with permission from «Journal», Vol. «Vol», Page(s) «Pages», Copyright © «Year» by the AAP**
2. The requester guarantees to reprint the materials exactly as originally published. Obvious typographical errors may be corrected. No deletions, alterations, or other changes may be made without the written consent of the American Academy of Pediatrics.
3. Rights granted herein are not exclusive and the American Academy of Pediatrics reserves the right to grant the same permission to others. Permission is granted for only the reproduction media specified on the invoice.
4. Original artwork or copies of articles cannot be supplied, but PDF files may be downloaded from [www.pediatrics.org](http://www.pediatrics.org) or [www.pedsinreview.org](http://www.pedsinreview.org). Quantities of reprints and eprints of *Pediatrics* and *Pediatrics in Review* articles can be obtained by contacting Catherine Lee, Reprint Sales Specialist at Cadmus Communications, by email at [leec@cadmus.com](mailto:leec@cadmus.com) or by phone at 410/691-6274.
5. This permission will not be valid until a signed copy of this Agreement is received by the American Academy of Pediatrics.

6. This permission is granted on a one-time basis only. Future use of this material is subject to the conditions stated herein. *Gratis permissions are not issued for use in materials available for commercial sale, even for educational use.*

Requester Accepts:

\_\_\_\_\_  
Signature

\_\_\_\_\_  
Date

\_\_\_\_\_  
Please Print Name

### **Copyright Permission from American Academy Pediatrics**

ELSEVIER LIMITED LICENSE TERMS AND CONDITIONS

Jul 21, 2008

This is a License Agreement between Wencheng Zhang ("You") and Elsevier Limited ("Elsevier Limited"). The license consists of your order details, the terms and conditions provided by Elsevier Limited, and the payment terms and conditions.

Supplier: Elsevier Limited The Boulevard, Langford Lane Kidlington, Oxford, OX5 1GB, UK

Registered Company Number 1982084

Customer name: Wencheng Zhang

Customer address: 2282 Rankin Ave Windsor, ON N9B 3V8

License Number: 1993880181367

License date: Jul 21, 2008

Licensed content publisher: Elsevier Limited

Licensed content publication: Clinical Biomechanics

Licensed content title: Biomechanics of the cervical spine Part 2. Cervical spine soft tissue responses and biomechanical modeling

Licensed content author: Narayan, Yoganandan | Srirangam, Kumaresan | Frank A., Pintar

Licensed content date: January 2001

Volume number: 16

Issue number: 1

Pages: 27

Type of Use: Thesis / Dissertation

Portion: Figures/table/illustration/abstracts

Portion Quantity: 5

Format: Both print and electronic

You are an author of the Elsevier article: No

Are you translating? No

Purchase order number

Expected publication date: Oct 2008

Elsevier VAT number: GB 494 6272 12

Permissions price: 0.00 USD

Value added tax: 0.0% 0.00 USD

Total: 0.00 USD

## Terms and Conditions

### INTRODUCTION

1. The publisher for this copyrighted material is Elsevier. By clicking "accept" in connection with completing this licensing transaction, you agree that the following terms and conditions apply to this transaction (along with the Billing and Payment terms and conditions established by Copyright Clearance Center, Inc. ("CCC"), at the time that you opened your Rightslink account and that are available at any time at <<http://myaccount.copyright.com>>). GENERAL TERMS
2. Elsevier hereby grants you permission to reproduce the aforementioned material subject to the terms and conditions indicated.
3. Acknowledgement: If any part of the material to be used (for example, figures) has appeared in our publication with credit or acknowledgement to another source, permission must also be sought from that source. If such permission is not obtained then that material may not be included in your publication/copies. Suitable acknowledgement to the source must be made, either as a footnote or in a reference list at the end of your publication, as follows: " Reprinted from Publication title, Vol /edition number, Author(s), Title of article / title of chapter, Pages No., Copyright (Year), with permission from Elsevier [OR APPLICABLE SOCIETY COPYRIGHT OWNER]. " Also Lancet special credit - " Reprinted from The Lancet, Vol. number, Author(s), Title of article, Pages No., Copyright (Year), with permission from Elsevier. "
4. Reproduction of this material is confined to the purpose and/or media for which permission is hereby given.
5. Altering/Modifying Material: Not Permitted. However figures and illustrations may be altered/adapted minimally to serve your work. Any other abbreviations, additions, deletions and/or any other alterations shall be made only with prior written authorization of Elsevier Ltd. (Please contact Elsevier at [permissions@elsevier.com](mailto:permissions@elsevier.com))
6. If the permission fee for the requested use of our material is waived in this instance, please be advised that your future requests for Elsevier materials may attract a fee.
7. Reservation of Rights: Publisher reserves all rights not specifically granted in the combination of (i) the license details provided by you and accepted in the course of this licensing transaction, (ii) these terms and conditions and (iii) CCC's Billing and Payment terms and conditions.
8. License Contingent Upon Payment: While you may exercise the rights licensed immediately upon issuance of the license at the end of the licensing process for the transaction, provided that you have disclosed complete and accurate details of your proposed use, no license is finally effective unless and until full payment is received from you (either by publisher or by CCC) as provided in CCC's Billing and Payment terms and conditions. If full payment is not received on a timely basis, then any license preliminarily granted shall be deemed automatically revoked and shall be void as if never granted. Further, in the event that you breach any of these terms and conditions or any of CCC's Billing and Payment terms and conditions, the license is automatically revoked and shall be void as if never granted. Use of materials as described in a revoked license, as well as any use of the materials beyond the scope of an unrevoked license, may constitute copyright infringement and publisher reserves the right to take any and all action to protect its copyright in the materials.
9. Warranties: Publisher makes no representations or warranties with respect to the licensed material.
10. Indemnity: You hereby indemnify and agree to hold harmless publisher and CCC, and their respective officers, directors, employees and agents, from and against any and all claims arising out of your use of the licensed material other than as specifically authorized pursuant to this license.
11. No Transfer of License: This license is personal to you and may not be sublicensed, assigned, or transferred by you to any other person without publisher's written permission.
12. No Amendment Except in Writing: This license may not be amended except in a writing signed by both parties (or, in the case of publisher, by CCC on publisher's behalf).
13. Objection to Contrary Terms: Publisher hereby objects to any terms contained in any purchase order, acknowledgment, check endorsement or other writing prepared by you, which terms are inconsistent with these terms and conditions or CCC's Billing and Payment terms and conditions. These terms and conditions, together with CCC's Billing and Payment terms and conditions (which are incorporated herein), comprise the entire agreement between you and publisher (and CCC)

concerning this licensing transaction. In the event of any conflict between your obligations established by these terms and conditions and those established by CCC's Billing and Payment terms and conditions, these terms and conditions shall control.

14. Revocation: Elsevier or Copyright Clearance Center may deny the permissions described in this License at their sole discretion, for any reason or no reason, with a full refund payable to you. Notice of such denial will be made using the contact information provided by you. Failure to receive such notice will not alter or invalidate the denial. In no event will Elsevier or Copyright Clearance Center be responsible or liable for any costs, expenses or damage incurred by you as a result of a denial of your permission request, other than a refund of the amount(s) paid by you to Elsevier and/or Copyright Clearance Center for denied permissions.

#### **LIMITED LICENSE**

The following terms and conditions apply to specific license types:

15. Translation: This permission is granted for non-exclusive world English rights only unless your license was granted for translation rights. If you licensed translation rights you may only translate this content into the languages you requested. A professional translator must perform all translations and reproduce the content word for word preserving the integrity of the article. If this license is to re-use 1 or 2 figures then permission is granted for non-exclusive world rights in all languages.

16. Website: The following terms and conditions apply to electronic reserve and author websites: Electronic reserve: If licensed material is to be posted to website, the web site is to be password-protected and made available only to bona fide students registered on a relevant course if: This license was made in connection with a course, This permission is granted for 1 year only. You may obtain a license for future website posting, All content posted to the web site must maintain the copyright information line on the bottom of each image, A hyper-text must be included to the Homepage of the journal from which you are licensing at <http://www.sciencedirect.com/science/journal/xxxxx> or the Elsevier homepage for books at <http://www.elsevier.com> , and Central Storage: This license does not include permission for a scanned version of the material to be stored in a central repository such as that provided by Heron/XanEdu.

17. Author website for journals with the following additional clauses: This permission is granted for 1 year only. You may obtain a license for future website posting, All content posted to the web site must maintain the copyright information line on the bottom of each image, and The permission granted is limited to the personal version of your paper. You are not allowed to download and post the published electronic version of your article (whether PDF or HTML, proof or final version), nor may you scan the printed edition to create an electronic version, A hyper-text must be included to the Homepage of the journal from which you are licensing at <http://www.sciencedirect.com/science/journal/xxxxx> , or the Elsevier homepage for books at <http://www.elsevier.com> and Central Storage: This license does not include permission for a scanned version of the material to be stored in a central repository such as that provided by Heron/XanEdu.

18. Author website for books with the following additional clauses: Authors are permitted to place a brief summary of their work online only. A hyper-text must be included to the Elsevier homepage at <http://www.elsevier.com> This permission is granted for 1 year only. You may obtain a license for future website posting, All content posted to the web site must maintain the copyright information line on the bottom of each image, and The permission granted is limited to the personal version of your paper. You are not allowed to download and post the published electronic version of your article (whether PDF or HTML, proof or final version), nor may you scan the printed edition to create an electronic version, A hyper-text must be included to the Homepage of the journal from which you are licensing at <http://www.sciencedirect.com/science/journal/xxxxx> , or the Elsevier homepage for books at <http://www.elsevier.com> and Central Storage: This license does not include permission for a scanned version of the material to be stored in a central repository such as that provided by Heron/XanEdu.

19. Website (regular and for author): “ A hyper-text must be included to the Homepage of the journal from which you are licensing at <http://www.sciencedirect.com/science/journal/xxxxx>. ”

20. Thesis/Dissertation: If your license is for use in a thesis/dissertation your thesis may be submitted to your institution in either print or electronic form. Should your thesis be published commercially, please reapply for permission. These requirements include permission for the Library and Archives of Canada to supply single copies, on demand, of the complete thesis and include permission for UMI to supply single copies, on demand, of the complete thesis. Should your thesis be published commercially, please reapply for permission. v1.

21. Other conditions: None



## **VITA AUCTORIS**

Wencheng Zhang was born in Shuangcheng, China on September 3, 1960. He graduated from Harbin Institute of Technology (HIT) (former Harbin Architectural and Civil Engineering Institute) in 1982 with a Bachelor degree of Civil Engineering with major in structural engineering. From there, he conducted research, teaching, structural analysis and design in the field of structural engineering in China and Europe until 9 years ago. He has been working in the automobile industry as a CAE engineer since 1999. He is currently a candidate for the Master's degree in Mechanical Engineering at the University of Windsor and hopes to graduate in the fall of 2008.